AD-A100 374 BENDIX CORP BALTIMORE MD COMMUNICATIONS DIV F/6 9/1
TACTICAL MINIATURE CRYSTAL OSCILLATOR.(U)
APR 81 H M GREENHOUSE, R L MCGILL, W FEFEL DAAB07-75-C-1327
UNCLASSIFIED BCD-FR-81-001 DELET-TR-75-1327-F NL

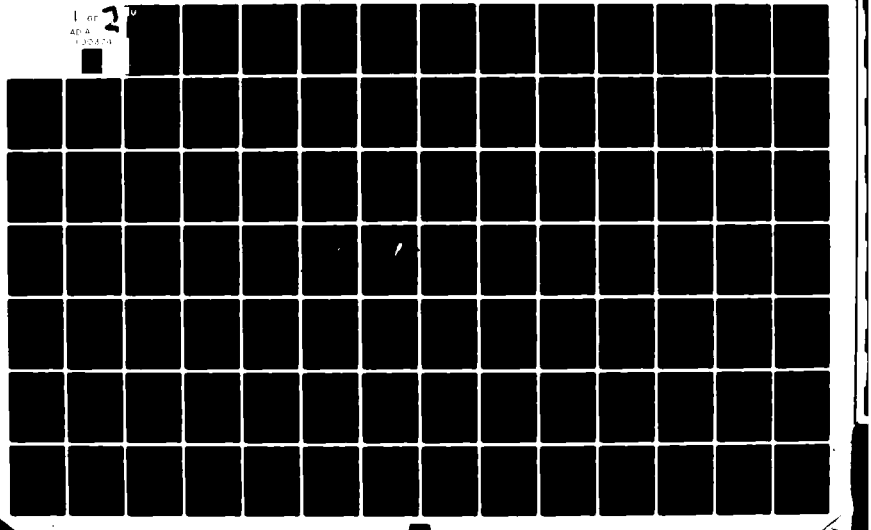

Research and Development Technical Report

DELET-TR-75-1327-F

TACTICAL MINIATURE CRYSTAL OSCILLATOR

H. M. Greenhouse
R. L. McGill
W. Fefel
H. Jackson
D. Brown
R. Bryan
T. Hawkins

THE BENDIX CORPORATION
COMMUNICATIONS DIVISION
East Joppa Road
Baltimore, Maryland 21204

Report No. BCD-FR-81-001

April 1981

Final Report 15 April 1975 – 1 October 1980

PREPARED FOR
ELECTRONICS TECHNOLOGY & DEVICES LABORATORY

ERADCOM

US ARMY ELECTRONICS RESEARCH AND DEVELOPMENT COMMAND
FORT MONMOUTH, NEW JERSEY 07703

NOTICES

Disclaimers

The citation of trade names and names of manufacturers in this report is not to be construed as official Government indorsement or approval of commercial products or services referenced herein.

Disposition

Destroy this report when it is no longer needed. Do not return it to the originator.

UNCLASSIFIED

SECURITY CLASSIFICATION OF THIS PAGE (When Data Entered)

REPORT DOCUMENTATION PAGE	READ INSTRUCTIONS BEFORE COMPLETING FORM
1. REPORT NUMBER: DELET-FR-75-1327-F	2. GOVT ACCESSION NO.: AD-A100374
3. RECIPIENT'S CATALOG NUMBER:	
4. TITLE (and Subtitle): TACTICAL MINIATURE CRYSTAL OSCILLATOR	5. TYPE OF REPORT & PERIOD COVERED: FINAL REPORT 1 Apr 75 - 1 Oct 80
6. PERFORMING ORG. REPORT NUMBER: BCD-FR-81-001	
7. AUTHOR(s): H. M. Greenhouse, R. L. McGill, W. Fefel, H. Jackson, D. Brown, R. Bryan, T. Hawkins	8. CONTRACT OR GRANT NUMBER(s): DAAB07-75-C-1327
9. PERFORMING ORGANIZATION NAME AND ADDRESS: The Bendix Corporation, Bendix Communications Division, E. Joppa Road, Baltimore, Maryland 21204	10. PROGRAM ELEMENT, PROJECT, TASK AREA & WORK UNIT NUMBERS: 672705 11 H94 F2 01
11. CONTROLLING OFFICE NAME AND ADDRESS: Microwave & Signal Processing Devices Division, DELET-MQ-O, US Army Electronics R&D Command, Fort Monmouth, NJ 07703	12. REPORT DATE: April 1981
	13. NUMBER OF PAGES: 144
14. MONITORING AGENCY NAME & ADDRESS (if different from Controlling Office)	15. SECURITY CLASS. (of this report): Unclassified
	15a. DECLASSIFICATION/DOWNGRADING SCHEDULE

16. DISTRIBUTION STATEMENT (of this Report)

Approved for Public Release: Distribution Unlimited

17. DISTRIBUTION STATEMENT (of the abstract entered in Block 20, if different from Report)

18. SUPPLEMENTARY NOTES

19. KEY WORDS (Continue on reverse side if necessary and identify by block number)

TMXO
Oscillator
Quartz Crystal
Temperature Control
Frequency Stability
High Vacuum
Microcircuit

20. ABSTRACT (Continue on reverse side if necessary and identify by block number)

This report describes the further exploratory development of a high performance Tactical Miniature Crystal Oscillator (TMXO). The intended use for this TMXO is as a reference frequency source in advanced tactical communications systems and in time ordered navigational systems. This effort, conducted in 2 phases, was a continuation by the authors of a previous study which defined particular problem areas. The TMXO as configured in this effort is an evacuated enclosure containing a thermal insulating pedestal, a vacuum sealed hybrid microcircuit and a precision quartz crystal unit. Phase I utilized chip and wire

DD FORM 1 JAN 73 1473 EDITION OF 1 NOV 65 IS OBSOLETE

UNCLASSIFIED

SECURITY CLASSIFICATION OF THIS PAGE (When Data Entered)

microelectronic construction and a custom crystal unit in a metallic enclosure approximating the thermal characteristics of the new ceramic flatpack enclosed crystal unit in development. Phase II used thick film technology in conjunction with early developmental ceramic enclosed crystal units. This final report includes all the work of phases I and II.

The TMXO design resulting from this effort provided the baseline approach for the TMXO advanced development program being reported under contract DAAB07-78-C-2990.

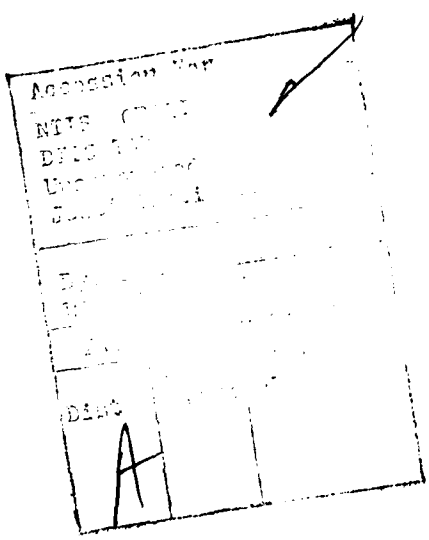

CONTENTS

CONTENTS

CONTENTS

FIGURES

FIGURES

TABLES

1. INTRODUCTION

1.1 Purpose. The objective of this program is the further exploratory development of a Tactical Miniature Crystal Oscillator (TMXO). The present effort is a continuation of research and development conducted by the Bendix Communications Division under contracts DAAB07-71-C-0265 and DAAB07-73-C-0199. This earlier work has been reported in ECOM-0265F and ECOM-0199F.

The tasks to be performed during the present contract fall into two categories. The first contains the unsolved problems remaining from the previous work. This includes excess power aging (because of the inability to maintain a vacuum inside the TMXO) and frequency recovery. The latter is most probably related to the crystal and its package. The severity of this problem is expected to be greatly diminished when a new type ceramic crystal enclosure (presently under development elsewhere) becomes available. The second category consists of new and/or additional performance requirements.

1.2 Performance goals of this contract. The required characteristics of the TMXO are given below:

(a) Size. Volume not to exceed 1 cubic inch.

(b) Input voltage. 12 volts dc, $\pm$5 percent.

(c) Available warmup power. Not to exceed 10.0 watts at any ambient temperature ($-54^{\circ}C$ to $+75^{\circ}C$) during the allowed warmup time (3 minutes).

(d) Operating power. After warmup, the maximum power input to the TMXO shall not exceed 250 milliwatts at any temperature.

(e) Power aging. Aging of the TMXO power consumption shall not exceed 1 percent per month.

(f) Voltage control. The TMXO shall have provision for voltage control, allowing a frequency deviation no less than 1.0×10^{-7} for a dc voltage change from 0 to +10 volts.

(g) Ambient temperature range. The TMXO shall meet all requirements of this specification over the ambient temperature range of $-54^{\circ}C$ to $+75^{\circ}C$.

(h) Frequency adjustment. A control shall be provided so that the output frequency may be conveniently and uncritically adjusted to 5.115 MHz $\pm 1 \times 10^{-10}$ with a minimum range of $\pm 1 \times 10^{-8}$.

(i) Frequency/temperature stability (steady state). The maximum permissible frequency deviation over the temperature range of $-54^{\circ}C$ to $+75^{\circ}C$ shall be $\pm 1 \times 10^{-8}$.

(j) Frequency/temperature stability (transient). The frequency of the TMXO shall not change more than $\pm 1 \times 10^{-8}$ from its initial value when subjected to a positive $10^{\circ}C$ amplitude, at a rate of $1^{\circ}C$/minute, air temperature ramp starting at $-40^{\circ}C$, $-5^{\circ}C$, $+30^{\circ}C$, and $+65^{\circ}C$.

(k) Frequency/load stability. The maximum frequency deviation for a load variation of 50 ohms ± 10 percent, $\pm 20^{\circ}$ phase, shall be $\pm 1 \times 10^{-9}$.

(l) Frequency/voltage stability. The maximum permissible frequency deviation for a supply voltage variation of 12 volts dc +5 percent shall be $\pm 1 \times 10^{-9}$.

(m) Frequency aging. Aging of the TMXO output frequency shall not exceed 2×10^{-10} per week, operating, after a 30-day stabilization period.

(n) Short term stability. The maximum rms frequency deviation shall be $\pm 1 \times 10^{-11}$ for averaging times ranging from 1 second to 20 minutes under conditions of input voltage and ambient temperature controlled to ± 1 millivolt and $\pm 0.1^{\circ}C$, respectively.

(o) Frequency acceleration stability. The maximum frequency change of the TMXO measured during static acceleration shall be less than 5×10^{-10}/g when tested in accordance with Method 513, Procedure II (helicopter category) MIL-STD-810B. Permanent frequency change shall be no greater than $\pm 1 \times 10^{-9}$.

(p) Frequency/vibration stability. The maximum permissible frequency change of the TMXO measured during and following vibration without isolators shall be $\pm 1 \times 10^{-9}$ when tested in accordance with Method 514, curve M, MIL-STD-810B. The frequency deviation represented by the modulation sidebands at the vibration frequency shall not exceed 5×10^{-10} times the peak acceleration level specified for that frequency by curve M.

(q) Frequency/shock stability. The maximum permissible frequency change of the TMXO following a shock of 50 g, 11 milliseconds, shall be $\pm 1 \times 10^{-9}$ wnen tested in accordance with method 213 condition G, MIL-STD-202D.

(r) Frequency/attitude stability. The maximum frequency change of the TMXO for a 90 $\pm 5^{\circ}$ attitude change in any axis shall be less thant $\pm 5 \times 10^{-10}$.

(s) Frequency/altitude stability. The maximum frequency change of the TMXO following an altitude change from sea leavel to 10,000 feet shall be $\pm 1 \times 10^{-9}$.

(t) Stabilization time. Following application of power, the frequency of the TMXO shall be within $\pm 1 \times 10^{-8}$ of final frequency in 3 minutes.

(u) Frequency recovery at -40°C. The output frequency of the TMXO after warmup during each turn-on period for a five-cycle frequency recovery test shall remain within $\pm 3 \times 10^{-9}$ of the frequency measured on the first cycle. Each cycle shall consist of complete frequency stabilization during turn-on, followed by complete thermal stabilization after power is removed.

(v) Output voltage. A minimum of 0.125 volt rms at the 5.115 MHz output frequency shall be available across an external resistive load of 50 ohms.

1.3 General description of the two phase program. The work on the contract was done in two phases. The first phase utilized the chip and wire microelectronic technology, with this circuitry in a gold-plated copper enclosure. The crystal was in a metallic

enclosure, which was thermally designed to approximate match the characteristics of a new ceramic type crystal enclosure.

During the second phase, the thick film technology was used in conjunction with a ceramic enclosure for the microelectronics. The crystal was of a new type in a ceramic enclosure, the result of a parallel development.

The activity and results of phase 1 were reported in ECOM-75-1327-1 (April 1976) and in ECOM-75-1327-2 (June 1977). This first phase ended in June 1976. From October 1977 to February 1979, this program was inactive for lack of the new type crystal. This final report includes all the work of phase 1 and phase 2.

2. ELECTRONIC DESIGN

2.1 General. The electrical schematic, used in the deliverable models, at the end of phase 1, is shown in Figure 1. It is the same as presented in the final report ECOM-0199F with the exception of the values of R27 and the external temperature setting potentiometer. The value of R27 has been changed from an unspecified select-by-test value to (RT1 at 90°C) - 22 kΩ. The potentiometer has been changed from 20 kΩ to 50 kΩ.

These changes were necessary to allow for the resistance tolerance of the thermistor at 90°C and for the ±5°C variation in the upper turn temperature of the crystal. The value of the thermistor at 90°C is 54 kΩ, ±10 percent. The minimum thermistor value due to its tolerance is 49.6 kΩ at 90°C. If the upper turn temperature of the crystal is at 95°C, the minimum thermistor value will be 42 kΩ. The maximum thermistor value will be a +10 percent tolerance thermistor, when the upper turn temperature is +85°C. This value is 73 kΩ. Therefore, allowing for a ±10 percent thermistor tolerance and a ±5°C upper turn temperature tolerance, the thermistor range will be from 42 kΩ to 73 kΩ. The minimum potentiometer value is 73 kΩ -42 kΩ = 31 kΩ. Using a 50 kΩ potentiometer, the near optimum value of R27 = RT - 22 kΩ, measuring RT at 90°C. See Table 1.

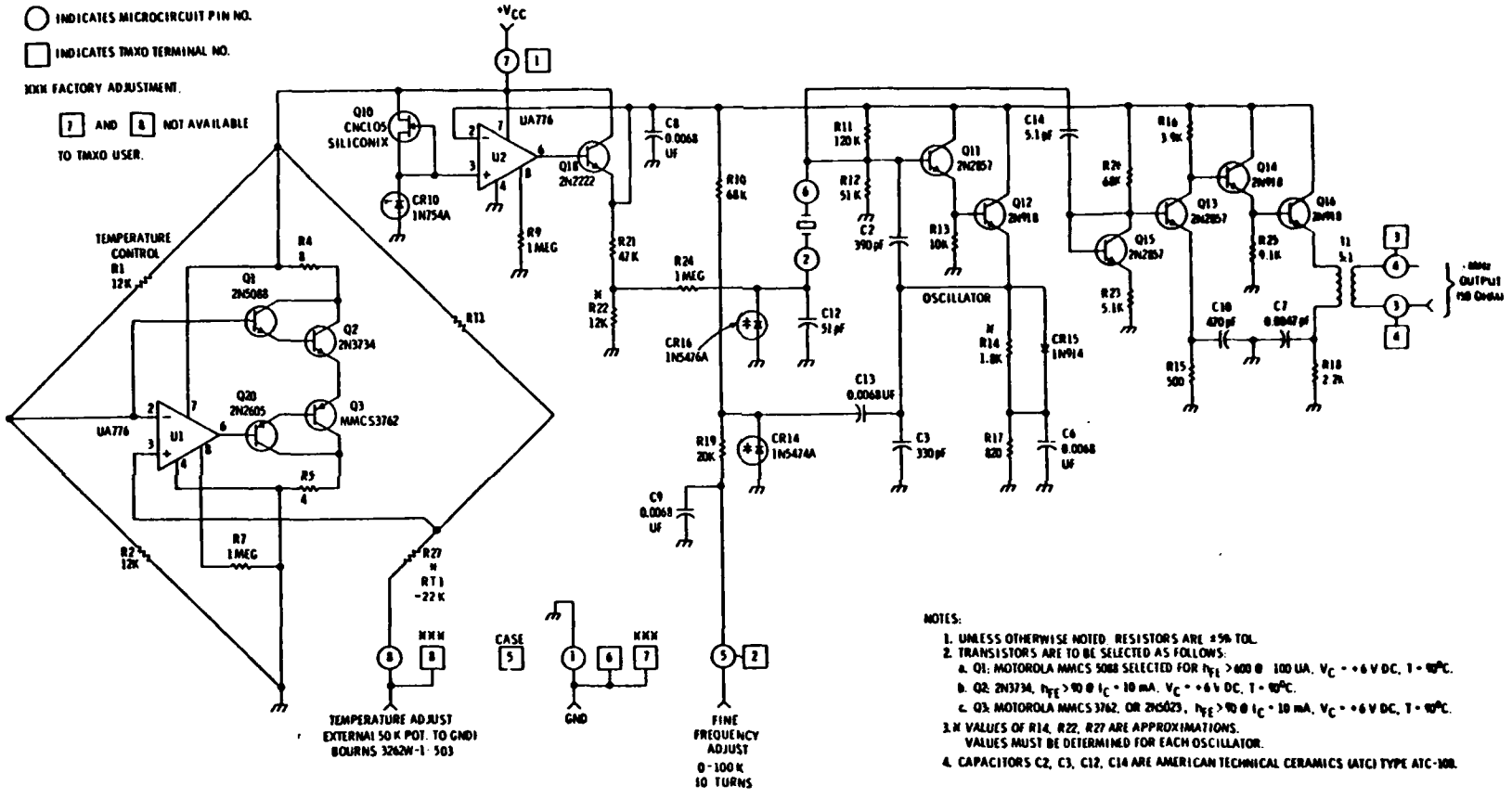

Figure 1. Electrical schematic of TMXO at end of phase 1.

TABLE 1. THE RANGE OF R27 AND POTENTIOMETER

RT at 90°C	R27 (RT-22k)	RT with 85°C X1e	Pot. with 85°C X1e	RT with 95°C X1e	Pot. with 95°C X1e
60 kΩ	38 kΩ	73 kΩ	35 kΩ	51 kΩ	13 kΩ
48 kΩ	26 kΩ	58 kΩ	32 kΩ	42 kΩ	16 kΩ

An up-dated parts list is presented in Figure 2.

To test the microcircuit (without a crystal), a microcircuit test fixture was fabricated. With this fixture, the sealed and unsealed microcircuit was tested in conjunction with a temperature controlled test crystal. This crystal was kept at its upper turn temperature being part of a TMXO configuration with the oscillator disconnected. The crystal leads were brought to two TMXO terminals, where short (2 inch) rigid leads went to the microcircuit under test.

2.2 Voltage controlled fine frequency tuning.

2.2.1 General Considerations. The requirement of a minimum frequency deviation of 1×10^{-7} for an applied control voltage from 0 to 10 V dc could have been met by modifying the present circuitry. This circuit modification would have added a pin to the microcircuit package and a terminal to the TMXO package. The addition of these pins would have decreased the TMXO's performance due to a lower thermal resistance and a more complex mechanical structure. Therefore, it was decided that an effort would be made to utilize the present circuitry and the present fine frequency control terminal. The fine frequency adjustment, without an applied control voltage, was accomplished using a 10-turn 0 to 100 kΩ potentiometer between this terminal and ground. Preliminary experimentation, consisting of applying 0 to 10 V dc to the fine frequency terminal (with the 0 to 100 kΩ

QTY	IDENT	MANUFACTURER	SIZE	DESCRIPTION	PART NO.	NOTES
1			—	PKG COVER. BENDIX No SK1140-100-1		NOTE 5
—			Dia=1	GOLD WIRE		
—	—	EPOTEK	—	EPOXY; INSULATING	H61	NOTE 7,8
—	—	EPOTEK	—	EPOXY, SILVER CONDUCTING	H31	NOTE 6
1	—		—	MICROCIRCUIT PKG. BENDIX No. SK1140-100-2		NOTE 5
—	S-1	KESTER	—	SOLDER 95% Sn-5% Sb SOLIDUS=232°C	995	
1	PtAu	BENDIX	50x50	PLATINUM-GOLD ON CERAMIC, NEAR PIN 2		
2	BeOAu-7,-9	ANY	40x20x12	GOLD ON BeO; UNDER Q15, UNDER Q19.		
1	BeOAu-6	ANY	40x40x12	GOLD ON BeO; UNDER CR16		
1	BeOAu-5	ANY	60x40x12	GOLD ON BeO; UNDER CR14		
2	BeOAu-3,-8	ANY	60x20x12	GOLD ON BeO, UNDER Q18, UNDER Q14 & Q16		
2	BeOAu-2,-4	ANY	50x30x12	GOLD ON BeO; UNDER Q10, UNDER Q11 & Q12		
1	BeOAu-1	BENDIX	110x60x12	GOLD ON BeO, 2 CUT SPACES-5MILS EACH, UNDER Q1,3,9, & RT1 - NOTE 1		
1	BeO-2	ANY	55x55x12	PLAIN BeO; UNDER C14		
1	BeO-1	ANY	110x40x12	PLAIN BeO; UNDER C2		
1	GAuT-5	BENDIX	70x20x6	GOLD TRACK ON GLASS		
3	GAuT-2,3,4	BENDIX	100x20x6	GOLD TRACK ON GLASS; AT PIN 7, PIN 1, NEAR R5.		
1	GAuT-1	BENDIX	75x20x6	GOLD TRACKS ON GLASS, BETWEEN U1 & U2.		
1	G3	BENDIX	50x50x6	PLAIN GLASS, UNDER C13		
1	GAu-6	BENDIX	150x20x6	GOLD ON GLASS; NEAR PIN 8		
2	G1,G2	BENDIX	65x50x6	PLAIN GLASS; UNDER U1 & U2.		
2	GAu-4,-5	BENDIX	100x20x6	GOLD ON GLASS, REG NEAR R12, BETWEEN R21 & R22		
3	GAu-1,-2,-3	BENDIX	20x20x6	GOLD ON GLASS, NEAR U2, ON C2, ON C9		
1	R23	BENDIX	27x16	THIN FILM RESISTOR 5.1KΩ±5%		
1	R100	BENDIX	34x16	THIN FILM RESISTOR 22.5KΩ±5%		
1	R27	BENDIX	40x16	THIN FILM RESISTOR (RT1 AT 90°C=10KΩ)		NOTE 4
1	R25	BENDIX	21x16	THIN FILM RESISTOR 9.1KΩ±5%		
1	R22	BENDIX		THIN FILM RESISTOR; VALUE TO BE DETERMINED		NOTE 3
1	R21	BENDIX	60x16	THIN FILM RESISTOR 47KΩ±5%		
1	R19	BENDIX	34x16	THIN FILM RESISTOR 20KΩ±5%		
1	R18	BENDIX	20x18	THIN FILM RESISTOR 2.2KΩ±5%		
1	R17	BENDIX	20x26	THIN FILM RESISTOR 620Ω±5%		
1	R16	BENDIX	27x16	THIN FILM RESISTOR 3.9KΩ±5%		
1	R15	BENDIX	20x22	THIN FILM RESISTOR 500Ω±5%		
1	R14C	BENDIX	27x16	THIN FILM RESISTOR 4KΩ±5%		
1	R14B	BENDIX	21x16	THIN FILM RESISTOR 3KΩ±5%		
1	R14A	BENDIX	20x18	THIN FILM RESISTOR 2KΩ±5%		
1	R13	BENDIX	21x16	THIN FILM RESISTOR 10KΩ±5%		
1	R12	BENDIX	60x16	THIN FILM RESISTOR 51KΩ±5%		
1	R11	BENDIX	50x60	THICK FILM RESISTOR 120KΩ±5%		
2	R10,26	BENDIX	60x16	THIN FILM RESISTOR 68KΩ±5%		
3	R7,9,24	BENDIX	50x50	THICK FILM RESISTOR 1MEG±10%		
3	R5A,5B,5C	BENDIX	50x50	THICK FILM RESISTOR 12Ω±10%		
3	R4A,4B,4C	BENDIX	50x50	THICK FILM RESISTOR 24Ω±10%		
2	R1,R2	BENDIX	27x16	THIN FILM RESISTOR 12KΩ±5%		
1	C14	AMER. TECH. CER.	55CADE	CAPACITOR, 5.1 pf ±.25pf	ATC-100A5R1-C-C	NOTE 8
1	C12	AMER. TECH. CER	55Cube	CAPACITOR, 51 pf ±10%	ATC-100A510FC	
1	C10	ANY	60x40x40	CAPACITOR CHIP, 470 pf ±10%, K1200		
1	C7	ANY	60x60x40	CAPACITOR CHIP, .0047 mf ±10%, K1200		
4	C6,8,9,13	ANY	50x50x30	CAPACITOR CHIP .0068 mf ±20%, K1200		NOTE 8 (C13)
1	C3	AMER. TECH CER.	110 CUBE	CAPACITOR, 330 pf ±10%	ATC-100B331KC	
1	C2	AMER. TECH. CER.	110 Cube	CAPACITOR, 390 pf. ±5%	ATC-100B391JC	NOTE 8
1	T1	BENDIX (WOUND)		TRANSFORMER 5:1, 60 TURNS PRI., 12 TURNS SEC.		NOTE 2,7
1	RT1	NAT. LEAD	30x30	THERMISTOR CHIP, BENDIX No → 0032655-0701		
1	CR16	MOT.	40x40	VARACTOR DIODE CHIP	1N5476A	
1	CR15	ANY	15x15	DIODE CHIP	1N914	
1	CR14	MOT.	37x37	VARACTOR DIODE CHIP	1N5474A	
1	CR10	MOT.	25x25	ZENER DIODE CHIP	1N754A	
2	U1,U2	FAIR.	50x65	OP. AMP. CHIP	μA776	
1	Q20	NAT. OR OTHER	18x18	TRANSISTOR CHIP	2N2605	
1	Q18	NAT. OR OTHER	18x18	TRANSISTOR CHIP	2N2222	
3	Q12,14,16	NAT. OR OTHER	15x15	TRANSISTOR CHIP	2N918	
3	Q11,13,15	NAT OR MOT.	15x15	TRANSISTOR CHIP	2N2857	
1	Q10	SILICONIX	30x30	FET, CURRENT LIMITING CHIP	CNCL05	
1	Q3	MOT.	29x20	TRANSISTOR CHIP	MMCS 3762	NOTE 1
1	Q2	NAT. OR MOT.	33x27	TRANSISTOR CHIP	2N3734	NOTE 1
1	Q1	NAT. OR MOT.	18X18	TRANSISTOR CHIP	2N5088	
QTY REQD	CODE IDENT NO.	PART OR IDENTIFYING NUMBER	SIZE (MILS)	NOMENCLATURE OR DESCRIPTION	SPECIFICATION	NOTES & REF DESIGNATIONS
-0501				PARTS LIST		

...AT NO.	NOTES
...1	NOTE 5
H61	NOTE 7,8
H31	NOTE 6
·8	NOTE 6
995	
PIN 2	
Q13.	
...Q14 & Q16	
& Q12	
, UNDER Q1,2,3,	...RT1. ADD 1
...1, NEAR R5.	
U1 & U2.	
...TWEEN R21 & R22	
..., ON C9	
	NOTE 4
... DETERMINED	NOTE 3
...C-100A5R1-C-C	NOTE 8
...C-100A510FC	
	NOTE 8 (C13)
...C-100B331KC	
...C-100B391JC	NOTE 8
..., 12 TURNS SEC.	NOTE 2,7
...32655-0701	
...N 5476A	
...N 914	
...N5474A	
...N 754A	
...A776	
...N 2605	
...N 2222	
...N 918	
...N 2857	
...NCL05	
...MCS 3762	NOTE 1
...N 3734	NOTE 1
...N 5088	
SPECIFICATION	NOTES & REF DESIGNATIONS

NOTE 1:

SELECT Q2 AND Q3, EACH TO HAVE h_{11} >90; AT I_c = 10mA. +6 VOLTS AND AT 90°C. EUTECTICALLY BOND Q2 AND Q3 TO B.OAu-1.

NOTE 2:

TRANSFORMER WOUND ON FERITE TOROID. IND. GEN. Q1 MATERIAL, SHAPE CF-120; 155 O.D. 88 ID, 55 H (mils), K=L/N² = 0.018. WIRE, ESSEX No. 38 SINGLE CLAD POLLYTHERMOLEX 200.

NOTE 3: PRELIMINARY WIRING FOR DETERMINING THE VALUE OF R22. WIRE AS ON RIGHT, LEAVING THE WIRE BETWEEN R22 AND GAu-5 OUT. DO NOT SEAL. R22 IS ±0.5%

NOTE 4:

MAKE R27 = RT1-22kΩ. USE MEASURED VALUE OF RT1 AT 90°C.

NOTE 5:

ORIENTATION OF COVER TO PKG. IS SPECIFIC. ORIENT AS BELOW:

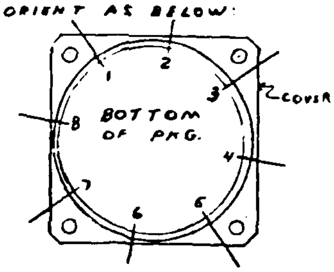

SOLDER PKG TO COVER USING SOLDER S-1.

NOTE 6:

PUT ALL PARTS (EXCEPT Q2, Q3, T1, C2, C13 & C14) DOWN WITH EPOXY H31.

NOTE 7:

SECURE T1 IN PLACE WITH EPOXY H-61.

NOTE 8:

PUT C2, C13 AND C14 DOWN WITH H61

NOTE 9:

SELECT Q1 TO HAVE h_{11} >600, AT I_c = 100μA. +6 VOLTS AND AT 90°C.

Figure 2. Parts list of TMXO at end of phase 1.

potentiometer removed) yielded the following results. The magnitude of the frequency deviation and its absolute value was a function of the 0 to 10 V dc power supply impedance. To optimize the frequency deviation and the absolute frequency (relative to the 0 to 100 kΩ adjustment), a theoretical investigation was initiated, followed by an experimental verification.

2.2.2 Theoretical investigation. Consider the present frequency adjust network:

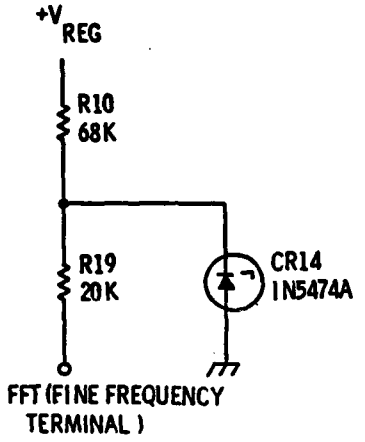

If: C_2 and C3 are the π network feedback capacitors
C_4 is the π network crystal series capacitor
C_T is the crystal load capacitance
h and k are defined by $C_3 = hC_2 = kC_4$

An expression for frequency variation as a function of C3, the variation of CR14 capacitance, is:

$$\frac{\delta f}{f} = \frac{-C_1 \, \delta C_3}{2C_T^2 (1 + h + k)^2} = 3.4 \times 10^4 \, \delta C_3$$

For $\delta C3 = .44$ pF (change in CR14 capacitance for a resistance change of 100 kΩ to 0 Ω at the fine frequency terminal) $\delta f/f \approx 1.5$ PPM $= \pm 0.75 \times 10^{-6}$. This is an optimum adjustment

range for adjustability to center frequency and for subsequent fine frequency adjustment sensitivity.

(a) Assume that an external voltage control e_s is applied through resistor R_S to the fine frequency terminal and that Δe_s = 10 volts.

(b) Assume also that a resistor R_G is returned to ground from the fine frequency terminal.

(c) Assume that $R_S + R_G$ = 100 kΩ.

An equivalent network for the voltage change at the cathode of CR14 be derived as follows:

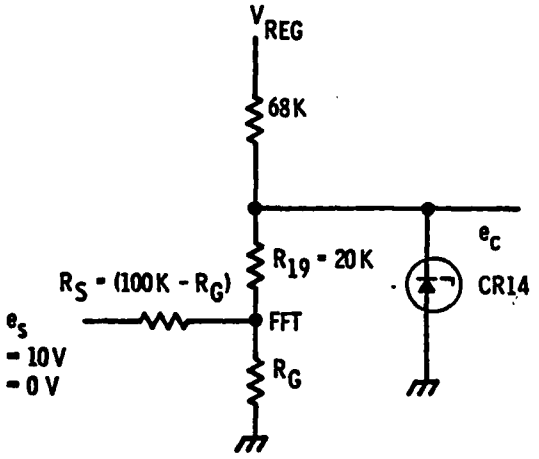

This can be reduced by Thevenin's Theorem to:

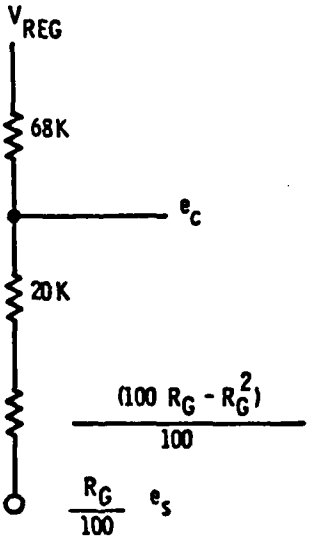

Assuming V_{REG} = 6 volts, the value of e_c (the bias on CR14) can be calculated for a given value of e_s and R_G. To optimize the range of fine frequency adjustment, e_c was calculated for e_s = 10 volts and e_s = 0 V, for values of R_G from 0 Ω to 100 kΩ. The result of these calculations are shown in Figure 3. This situation can be realized by the potentiometer arrangement of network B. In a similar manner, the value of e_c for R_{ext} = 0 Ω, and 100 kΩ was calculated using network A. The curve indicates that for the two adjustments to yield the same center frequency when set at mid range, R_G must equal 20 kΩ. The fine frequency variation as a function of R_{ext} and e_s was calculated assuming V_{REG} = 6 V and R_c = 20 kΩ (Figure 4). Note the near linearity of the voltage adjustment curve.

2.2.3 Experimental verification. To verify the above theoretical analysis, an experiment was conducted to determine the values of R_G and R_S, and the true characteristic of the ΔF/Fo - voltage curve. The values of these resistors were selected so that 5 volts gave the midpoint of the frequency swing. The results of the experiment are shown in Figure 5. The electrical arrangement is shown as network B. R_S was determined to be 85 kΩ, and R_G 15 kΩ. Two curves are plotted in this figure: (1) $\Delta F/F_o$ versus ohms (for the 0-100 k potentiometer) and (2) $\Delta F/F_o$ versus voltage (for the 0-10 V dc). The abscissae have been chosen so that the center of the frequency swing using the potentiometer (22.5 kΩ) or the voltage (5 volts) coincides with F_o. At this center point, the potentiometer gives a $\Delta F/F_o$ of $\pm 8.5 \times 10^{-7}$, and the voltage gives a $\Delta F/F_o$ of $\pm 3 \times 10^{-7}$. The voltage curve is almost perfectly linear, departing only slightly for values below 3 volts. The slope of the $\Delta F/F_o$ - voltage curve is 5.8×10^{-8} per volt, or 5.8×10^{-11} per mV. Therefore, for a voltage supply stable to ±1 mV and a setability to ±1 mV, the frequency can be set to $\pm 5.8 \times 10^{-11}$ with a stability of $\pm 5.8 \times 10^{-11}$.

The above stability and setability are not quite as good as when using a 10-turn potentiometer. The slope of ΔF/F versus

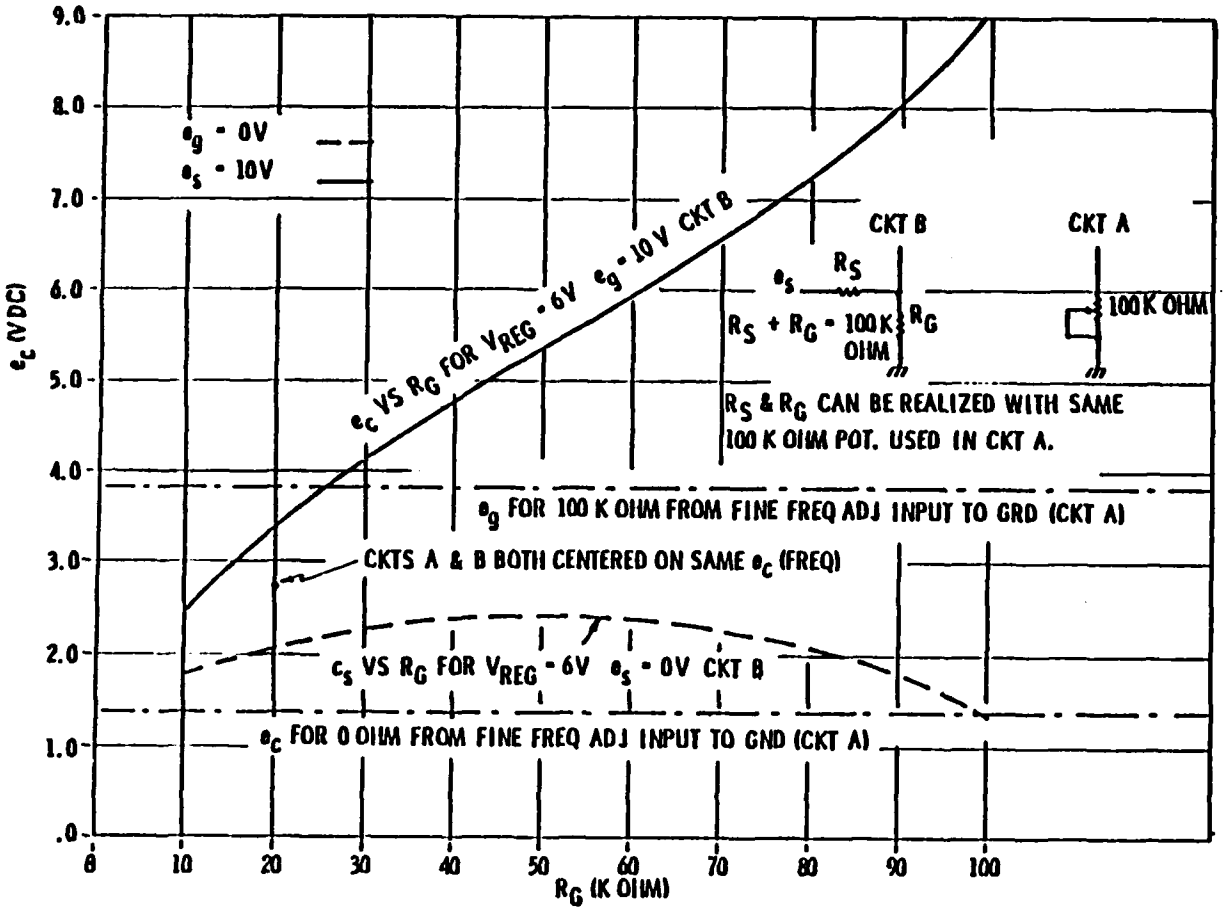

Figure 3. Varactor bias voltage versus R_G.

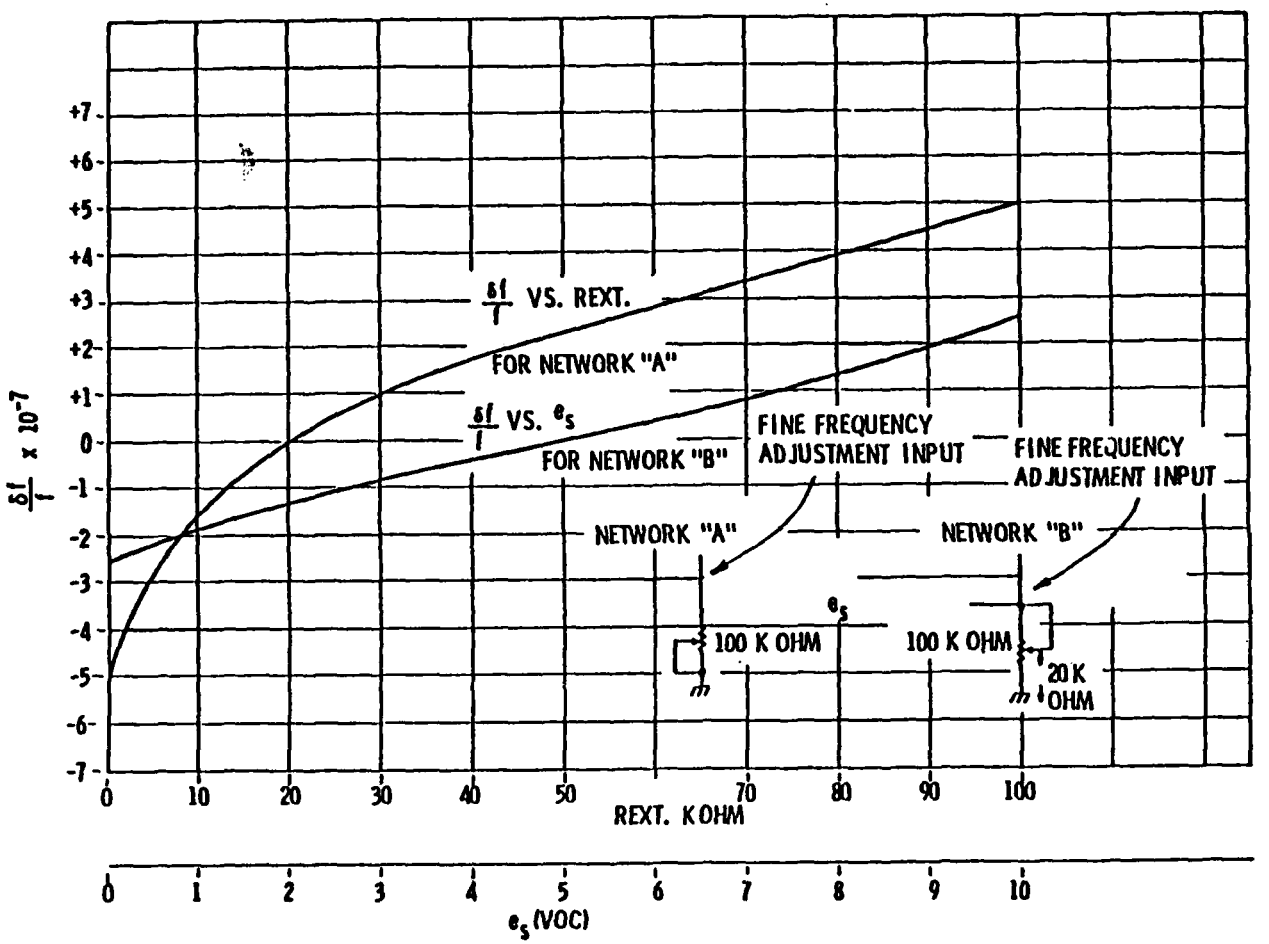

Figure 4. Theoretical fine frequency adjustment characteristics.

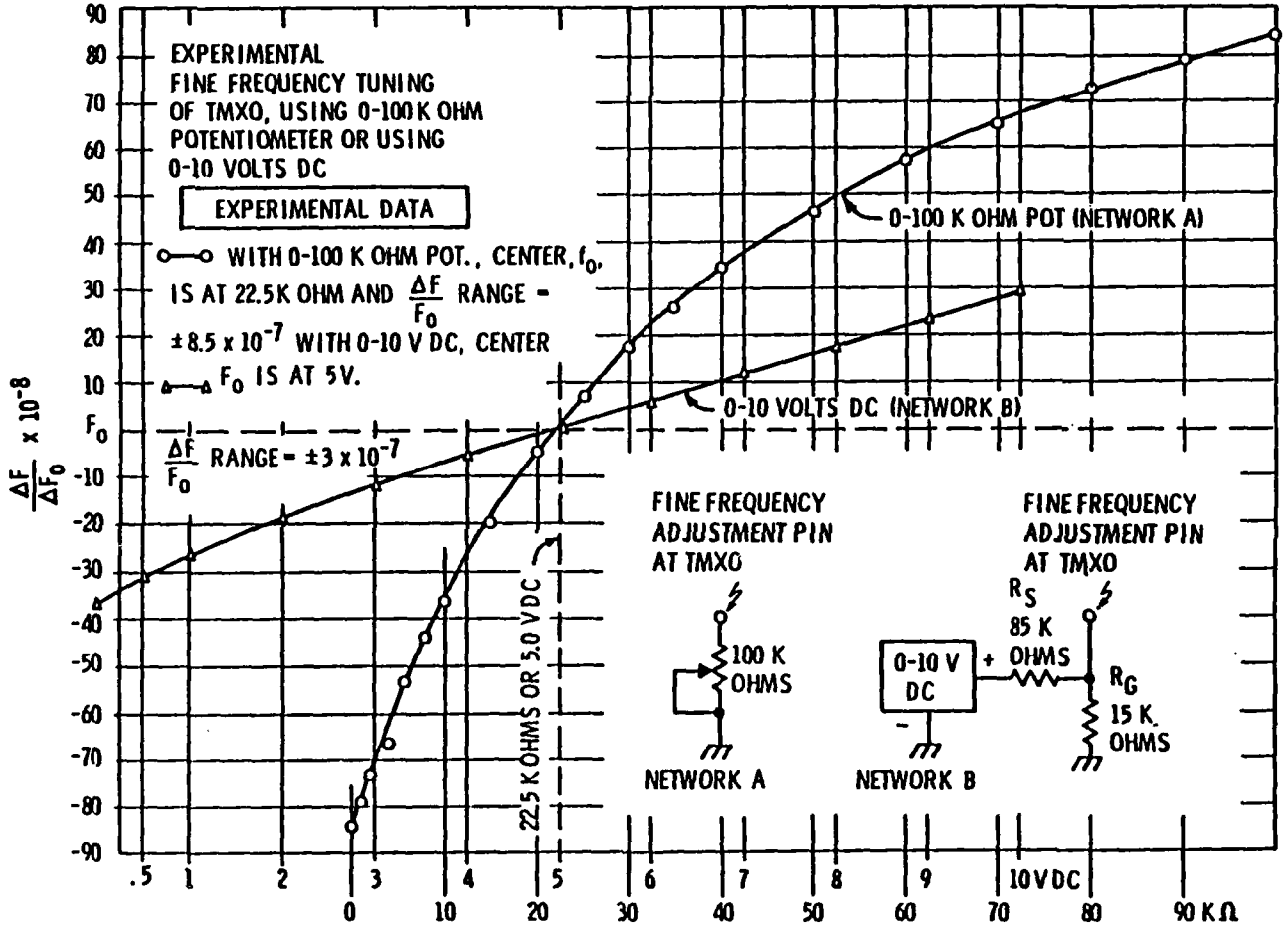

Figure 5. Experimental fine frequency tuning.

ohms at the 22.5 kΩ point is $1.8 \times 10^{-9}/k\Omega$. Using a 3/4-inch diameter clock reading 10-turn potentiometer, the resetability is ±20 Ω. This corresponds to a frequency resetability of $\pm 3.6 \times 10^{-11}$. The stability of the potentiometer is at least 10 times better, giving a frequency stability better than $\pm 3.6 \times 10^{-12}$.

The electrical schematic of the TMXO models delivered at the end of phase 1 is shown in Figure 1. A parts list corresponding to this schematic is given in Figure 2.

2.3 Circuit design changes during phase 2.

2.3.1 Temperature control circuit modifications. The temperature control circuit as it existed at the end of phase 1 was sensitive to popcorn noise in the operational amplifier. Although the amplitude of the popcorn noise was small (10-20 mV), it could produce significant fluctuations in heater current. This fluctuating heater current produces corresponding fluctuations in the temperature of the oscillator components and thus degrades the stability of the oscillator.

A new circuit has been evaluated which was designed to be relatively insensitive to the popcorn noise. This was accomplished by reducing the transconductance of the heater transistor through the use of current feedback. The new circuit is shown in Figure 6. It was constructed in a TO-8 can with a thermal resistance of approximately 500°C/W. As in the previous circuit, the error voltage is developed across a thermistor bridge consisting of resistors R1, R2, RT1, and R5. This voltage is applied to the input of operational amplifier U1. The output of U1 is applied to emitter follower Q1, which drives the heater transistor Q2 through the zener diode CR1. Resistor R4, in the emitter circuit of Q2, functions to limit the maximum current of the heater and provides the degeneration (current feedback) which eliminates the degrading effects of the popcorn noise.

Testing of the new circuit verified that the heater current fluctuations due to the popcorn noise were eliminated (at least to the extent that the fluctuations could be observed with a

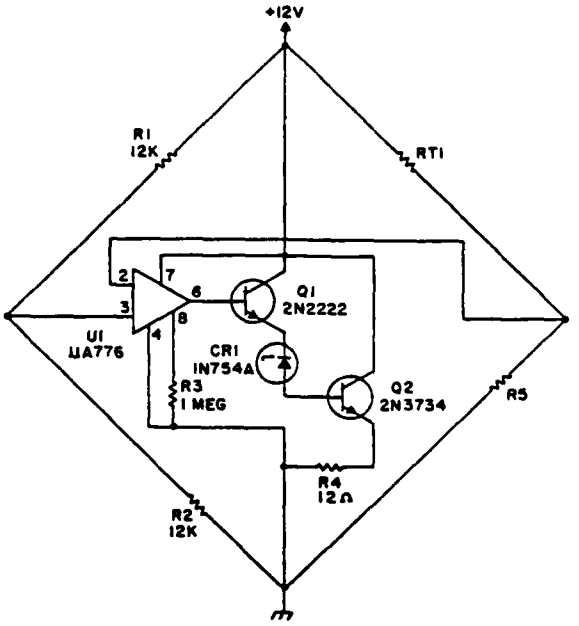

Fgure 6. New temperature control circuit.

current probe and oscilloscope). However, as was the case with previous circuits, this circuit demonstrated a low frequency relaxation oscillation.

Since it was anticipated that the oscillations will cause power supply problems in some applications of the TMXO, an analysis of the total circuit, inluding the thermal elements, was undertaken to determine if the oscillations could be eliminated. Using the standard techniques of control circuit theory, the feedback loop was opened, and measurements were taken to determine the gain and phase characteristics as a function of frequency. As expected, the data indicated that the conditions necessary to produce the oscillations were, in fact, present.

With the use of the gain and phase data from the open loop measurements, an RC phase correction network was designed and added to the circuit. This network consisted of a series resistor and capacitor between pin 6 and pin 2 of the operational amplifier. The value of the resistor was 82 k, and the value of the capacitor was 1 µF. With the addition of the phase correction elements, the circuit exhibited no oscillation and showed no other instability or effects of popcorn noise.

2.3.2 Short term stability. An effort was made to identify potential noise sources and to modify the circuit to minimize the effect of power supply regulator noise. The primary source of noise in the regulator is "microplasma" noise from the zener diode. This noise can be minimized to some extent by proper selection of the zener type.

In evaluating the existing regulator circuit, it was determined that the zener noise was being amplified in the higher frequency region due to a peaked frequency response of the regulator circuit. The frequency response peak occurs at approximately 600 kHz and has a gain at the peak of about three. Circuit modifications to eliminate this peak were studied.

The major effect of the regulator noise is to produce bias fluctuations in the varactor diode used for coarse frequency adjustment. It appeared feasible to eliminate this varactor altogether and substitute a multitap ceramic chip capacitor which has a range of 2 to 57 pF in 0.5 pF steps. It was felt that with the elimination of the coarse control varactor, selection of a low noise zener, and improvement in the regulator frequency response, power supply regulator noise would no longer be a major contribution to short term oscillator noise.

Another source of oscillator frequency variation was the thermal modulation caused by the oscillating heater circuit. This modulation had not been identified previously due to the relatively long integration time used in variance measurements. However, it is easily detected by frequency analysis of the output phase. This thermal modulation would be eliminated with the improved heater circuit which does not produce thermal cycling.

An effort was also made to determine if improvements in stability could be obtained by modification of the oscillator circuit itself. From a practical point of view, this question was much more difficult because of the precision required in making measurements and the necessity for eliminating extraneous effects.

Several methods of evaluating the phase noise were attempted. The most satisfactory method involved phase locking the oscillator under test to a standard reference oscillator and monitoring the oscillator voltage control line. The control line voltage is then amplified and applied to the vertical axis of an x-y plotter. An example of this type of recording is shown in Figure 7. The test setup is easily calibrated by first locking the oscillator under test to a frequency synthesizer which can be modulated with a known deviation and modulation frequency.

In the plots of Figure 7, it is not known how much, if any, of the short term variations are due to the reference oscillator. The general slope of the curves is due to temperature drift of the laboratory oven used to control the temperature of the test oscillator.

2.3.3 Third overtone oscillator circuit. The most straightforward approach to adapting the oscillator circuit for third overtone operation was to add an inductor in parallel with the feedback capacitor located between the transistor base and emitter. This inductor resonates with the parallel capacitor at a frequency below the operating frequency and above the fundamental resonance frequency of the crystal.

A circuit containing the inductor was breadboarded and tested with the third overtone crystals which were furnished GFE. If this circuit is used, it will be necessary to finish the crystals with a loading capacity since the circuit does not operate at series resonance. A load of 50 pF is about the maximum that could be used and still accommodate the $\pm$5 ppm finishing tolerance.

2.3.4 Buffer redesign. One of the objectives of phase 2 was to improve the stability of the oscillator with respect to load variations. To this end, several output amplifier circuit configurations were studied. One configuration containing a field effect transistor (2N4416) was breadboarded and evaluated. With this buffer circuit, no frequency changes with respect to the

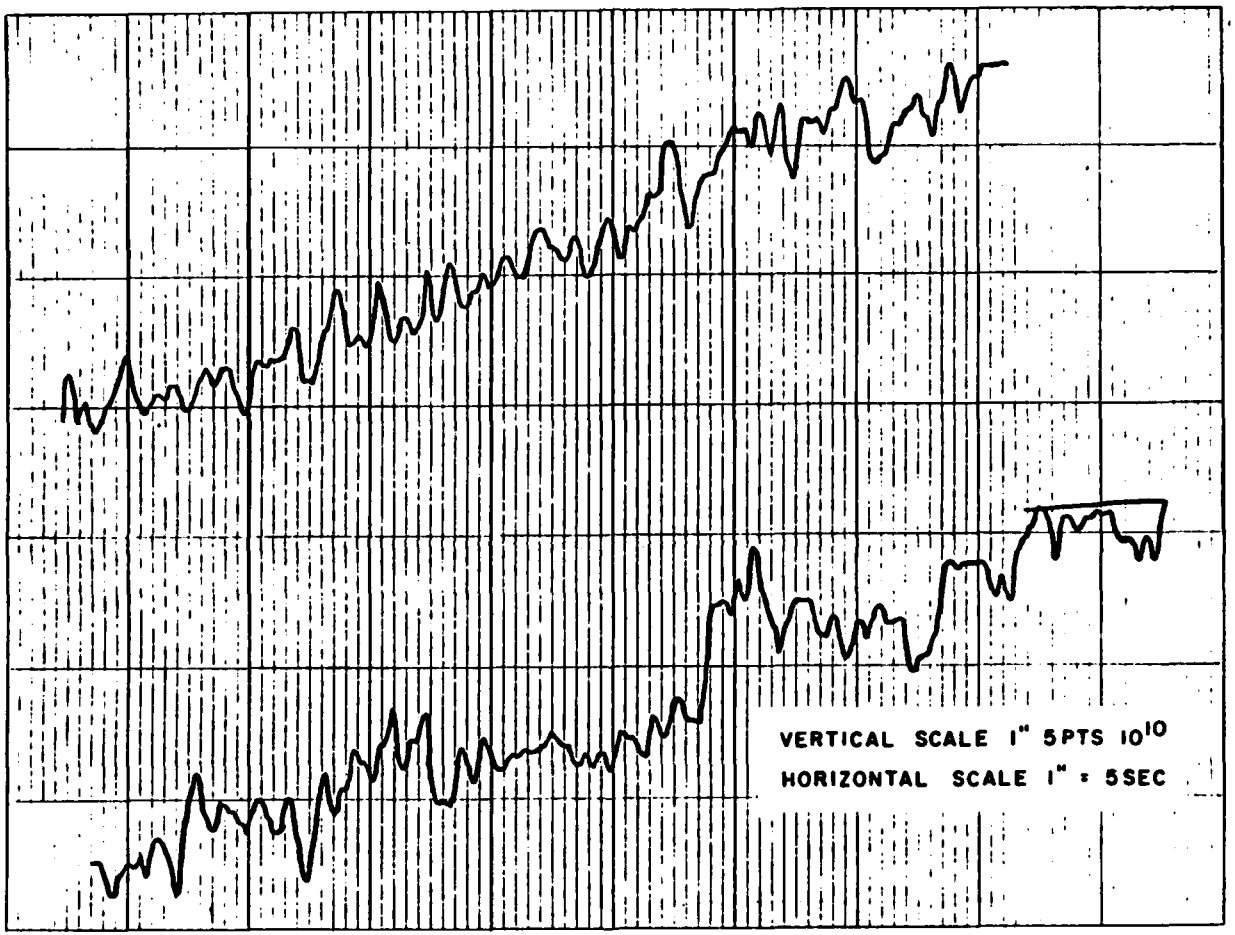

Figure 7. Recording of short term frequency variations.

specified load limits could be measured. When the 2N4416 was incorporated into an actual TMXO, the frequency/load stability was only slightly improved. The cause for the difference in performance between the breadboard and the actual TMXO was the difference in the common impedance in these two physical configurations. In the final circuit (see Figure 8), a bipolar buffer was used because of its equal isolation performance and because of its lower power consumption.

2.3.5 Heater electronics. A microcircuit version of the redesigned temperature controller was fabricated. The circuit was essentially the same as that shown in Figure 6 except for the addition of the phase compensation network and a change of resistor R4 to 6 ohms. The assembly included a 5 MHz fundamental crystal mounted in a TO-8 enclosure which was attached to the temperature control circuit package.

It was intended that the crystal contained in this assembly would be used for evaluation of various oscillator circuit configurations. However, the short term stability achieved with the new temperature controller was less than expected (approximately 3 parts in 10^{11} rms). Significant fluctuations in the heater supply current were also observed.

It was at first thought that the fluctuation in the heater current was due to noise in one of the active devices. However, replacement of the active devices with devices known to have low excess noise did not improve circuit performance. Finally, the entire circuit was disconnected and an external circuit was connected through unused leads in the microcircuit package. With this arrangement, the noisy component was quickly isolated and was found to be the thermistor. Further investigation showed that the thermistor noise was due to the epoxy cement used to bond the thermistor to the BeO substrate (see pparagraph 4.2.2).

2.3.6 Schematic revision. The third overtone schematic had C5 in series with L1. Any variation of C5 would affect the phase

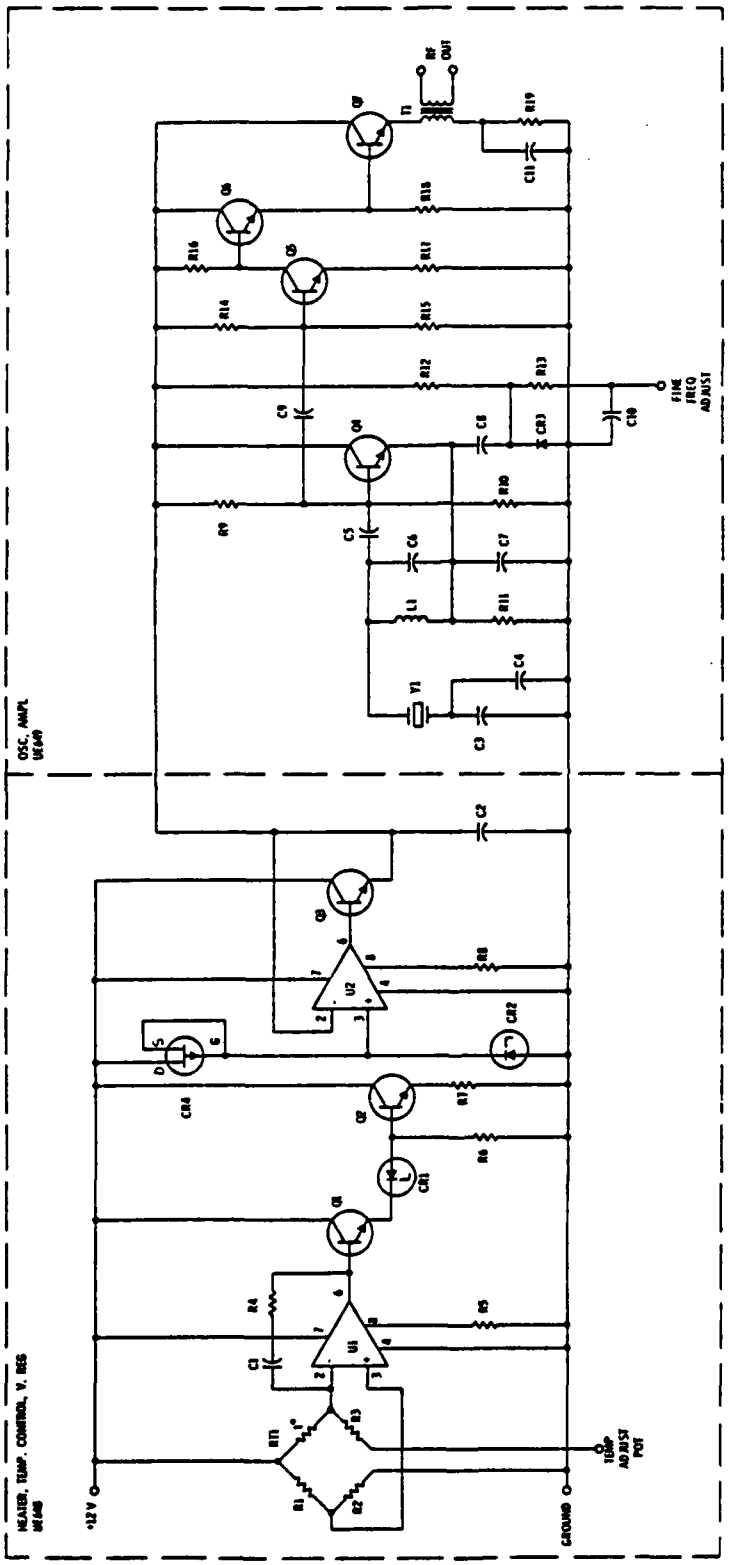

Figure 8. Electrical schematic of TMXO at end of phase 2.

of the crystal current flowing through L1 and hence the oscillator frequency. To minimize the effect which C5 had on the third overtone frequency, C5 has been moved from being in series with L1 to a series position between the crystal and the base of Q4 (see Figure 8). For nonovertone crystals, a short will replace C5.

The circuit was assembled and tested. The heater and temperature controller worked properly, but the voltage regulator did not. The fault was with CR4, Motorola's FET INC5283. The source and drain on this FET are not interchangeable. The schematic calls for the drain to be shorted to the gate. The device has a built-in short from source to gate. The problem was rectified by reversing the S and D on the schematic, and changing the wiring in the circuit accordingly. The revised schematic and parts list at the end of phase 2 is shown in Figure 8 and Table 2.

TABLE 2. PARTS LIST FOR SCHEMATIC AT END OF PHASE 2

Ident	Description	Vendor
U1, U2	776, LOW POWER OP. AMP.	FAIR
Q1, Q3	2N2222A	FAIR. NAT. MOT. TI.
Q2	2N3734	MOT. NAT.
CR1	MZC5.1A5, 5.1 V ZENER ±5%	MOT.
CR2	MZC8.2A5, 8.2 V ZENER ±5%	MOT.
CR4	INC5283, FET	MOT.
C1	1.0 µF ±20%, TANT, 10 W V DC @ 85°C VENDOR NO. 194D105X0010A4	SPRAGUE
C2	.0068 µF, BX	ANY
RT1	THERMISTOR 44C85400	MID. W. COMP.
R1, R2	50 KILOHMS ±5%	
R3	RT1 @ 89°C -22 KILOHMS ±5%	
R4	82 KILOHMS ±5%	
R5, R8	1 MEGOHM ±5%	
R6	470 OHMS ±5%	
R7	6.0 OHMS ±10%	

TABLE 2. PARTS LIST FOR SCHEMATIC AT END OF PHASE 2 (CONT)

Ident	Description	Vendor
Q4, Q5	2N2857	MOT.
Q6, Q7	2N918	NAT. FAIR
CR3	INC5146A OR INC5142A*	MOT.
C3	180 pF-360 pF OR 100 pF-180 pF* ** IN 30 pF STEPS, ±2% S.B.T.	A.T.C. (100)
C4	TAPPED NPO CAPACITOR 2 pF TO 57 pF IN 0.5 pF STEPS, TYPE VC2A S.B.T	VITRAMON
C5*	1000 pF ±2%	A.T.C. (100)
C6	620 pF OR 470 pF OR 300 pF ±2%	A.T.C. (100)
C7	180 pF OR 82 pF ** ±2%	A.T.C. (100)
C8	220 pF ±5% NPO	ANY
C9,C10	.001 µF ±5% BX	ANY
C11	.91 µF ±5% BX	ANY
L1*	1.6 µH, I.G. CORE CF-118-Q1	BENDIX
T1	60 PRI.: 12 SEC., I.G. CORE CF-120-Q1	
R9	22 KILOHMS ±5%	
R10	100 KILOHMS ±5%	
R11	40 KILOHMS - 80 KILOHMS ±5% S.B.T.	
R12	420 KILOHMS ±5%	
R13	150 KILOHMS ±5%	
R14	120 KILOHMS ±5%	
R15	27 KILOHMS ±5%	
R16	2.2 KILOHMS ±5%	
R17	560 OHMS ±5%	
R18	9.1 KILOHMS ±5%	
R19	2.2 KILOHMS ±5%	
Y1	CRYSTAL S.B.T.	

* FOR THIRD OVERTONE, 10 MHz ** FOR FUNDAMENTAL, 10 MHz

2.4 The effect of circuit components on frequency stability. The value of several components in the oscillator has an effect on the frequency. A change in these component values due to aging, thermal retrace, or other (unknown) factors will cause a change in frequency. The following analysis covers these sensitive components. The network below has the following stability equations (see ECOM-0265-F, pg. 14).

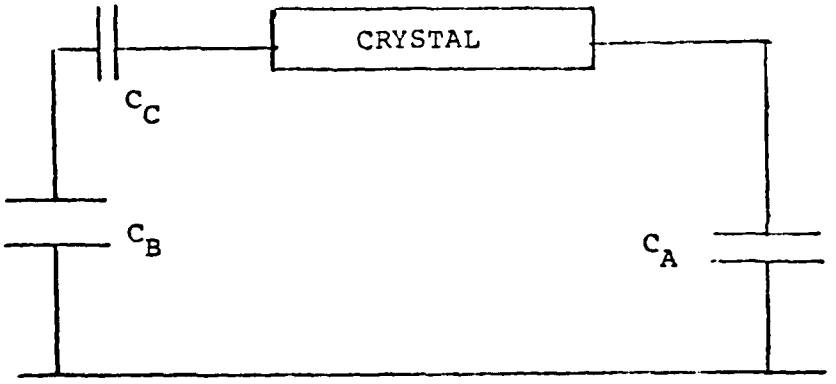

$$C_B = hC_A = kC_C$$

$$C_T = C_X + C_o$$

$$\frac{\delta F(C_x)}{F} = \frac{-C_1 h^2 C_x}{2C_T^2} \text{ ; for a change in CX}$$

$$\frac{\delta F(C_A)}{F} = \frac{-C_1 h^2 \delta C_A}{2C_T^2 (1+h+k)^2}$$

$$\frac{\delta F(C_B)}{F} = \frac{-C_1 \delta C_B}{2C_T^2 (1+h+k)^2}$$

$$\frac{\delta F(C_C)}{F} = \frac{-C_1 k^2 \delta C_C}{2C_T^2 (1+h+k)^2}$$

Referring to the electrical schematic of Figure 8 and for the 5 MHz fundamental mode, C5 and L1 are absent, then:

C_B = C7 with C8 in series with CR3, both in shunt; = C7' = 214 pF (34 pF due to CR3 and C8)

C_C = C6 with Q4 base-emitter capacitance (C_{b-e}) in shunt; = C6' = 620 pF (C_{BE} = 2 pF max)

C_A = C3 in parallel with C4 = C3' = 240 pF
C3 = 210 pF, C4 = 30 pF

$C_T = C_x + C_o$

$$\frac{1}{C_x} = \frac{1}{C7'} + \frac{1}{C6'} + \frac{1}{C3'}$$

CX = 95.6

C_0 = crystal shunt capacitance = 3.3 pF

CT = 95.6 + 3.3 = 98.9 pF

$h = C_B/C_A$ = C7'/C3/ = 214/210 = 1.02

$k = C_B/C_C$ = C7'/C6' = 214/620 = .345

h^2 = 1.04

k^2 = .119

$(1+h+k)^2 = (1+1.02 + .345)^2 = 5.59$

C1 = 10^{-14} farads

Effect of change in C7' on frequency:

$$\frac{\delta F(C7')}{F} = \frac{-C_1 h^2 \ \delta C7'}{2C_T{}^2 (1+h+k)^2}$$

$$\delta C7' = \frac{\delta F(C7')}{F} \times \frac{2C_T{}^2 (1+h+k)^2}{-C_1 h^2}$$

$$\frac{2C_T{}^2 (1+h+k)^2}{-C_1} = \frac{2(100 \times 10^{-12})^2 \ (5.59)}{-10^{-14} \times 1.04}$$

$$= -1.1 \times 10^{-5}$$

for a $\frac{\delta F}{F} = 1 \times 10^{-9}$

$$\delta C7' = 10^{-9} \times \frac{-1.1 \ 10^{-5}}{1.04} = -1.05 \times 10^{-14} \text{ farads}$$

$$\%C7' = \frac{1.05 \times 10^{-14}}{214 \times 10^{-12}} \times 100 = 9.8 \times 10^{-3} = -0.005$$

for a $\frac{\delta F}{F} = 1 \times 10^{-8}$ $\quad \delta C7' = 0.05\%$

for a $\frac{\delta F}{F} = 1 \times 10^{-7}$ $\quad \delta C7' = 0.5\%$

Effect of change in C6' on frequency:

$$\frac{\delta F(C6')}{F} = \frac{-C1 \ \delta C6'}{2C_T{}^2 \ (1+h+k)^2}$$

for a $\frac{\delta F}{F} = 1 \times 10^{-9}$

$$\delta C6' = 10^{-9} \times 2.2 \times 10^{-5} = 1.1 \times 10^{-14} \text{ farads}$$

$$\%\delta C6' = \frac{-1.1 \times 10^{-14} \times 100}{620 \quad 10^{-12}} = 0.0017$$

for $\frac{\delta F}{F} = 1 \times 10^{-8}$, $\delta C6' = 0.017\%$

for $\frac{\delta F}{F} = 1 \times 10^{-7}$, $\delta C6' = 0.17\%$

Effect of change in C3' on frequency:

$$\frac{\delta F(C3')}{F} = \frac{-C_1 k^2 \ \delta C3'}{2C_T^{\ 2} \ (1+h+k)^2}$$

for $\frac{\delta F}{F} = 1 \times 10^{-9}$

$$\delta C3' = \frac{10^{-9} \times -2.2 \times 10^{-5}}{.119} = -18.5 \times 10^{-14} \text{ farads}$$

$$\%\delta C3' = \frac{-18.5 \times 10^{-14} \times 100}{240 \times 10^{-12}} = 0.077$$

for $\frac{\delta F}{F} = 1 \times 10^{-8}$, $\delta C3' = 0.77\%$

for $\frac{\delta F}{F} = 1 \times 10^{-7}$, $\delta C3' = 7.7\%$

Effect of change in Q4 base-emitter capacitance C_{b-e} on frequency.

The maximum value of C_{b-e} is 2 pF, and is in parallel with C6 (620 pF).

for a $\frac{\delta F}{F} = 1 \times 10^{-9}$, $\delta C6'$ if -2.2×10^{-14} farads.

$$\%\delta C_{b-e} = \frac{-2.2 \times 10^{-14} \times 100}{2 \times 10^{-12}} = 1.1$$

for a $\frac{\delta F}{F} = 1 \times 10^{-8}$, $\delta C_{b-e} = 11\%$

for a $\frac{\delta F}{F} = 1 \times 10^{-7}$, $\delta C_{b-e} = 110\%$

The effect of a change C6 is the same as C6'.
The effect of a change in C3 is

$$\text{for } \frac{\delta F}{F} = 1 \times 10^{-9},\ \delta C3' = -18.5 \times 10^{-14} \text{ farads.}$$

$$\%\delta C3 = \frac{-18.5 \times 10^{-14} \times 100}{210 \times 10^{-12}} = 0.088\%$$

$$\text{for } \frac{\delta F}{F} = 1 \times 10^{-8},\ \%\delta C3 = 0.88\%$$

$$\text{for } \frac{\delta F}{F} = 1 \times 10^{-7},\ \%\delta C3 = 8.8\%$$

The effect of a change in C4 is

$$\text{for } \frac{\delta F}{F} = 1 \times 10^{-9},\ \delta C3' = -18.5 \times 10^{-14} \text{ farads.}$$

$$\%\delta C4 = \frac{-18.5 \times 10^{-14} \times 100}{30 \times 10^{-12}} = 0.62\%$$

$$\text{for } \frac{\delta F}{F} = 1 \times 10^{-8},\ \delta C4 = 6.2\%$$

$$\text{for } \frac{\delta F}{F} = 1 \times 10^{-7},\ \delta C4 = 62\%$$

The effect of a change in C7 is

$$\text{for } \frac{\delta F}{F} = 1 \times 10^{-9},\ \delta C7' = -2.1 \times 10^{-14}$$

$$\%\delta C7 = \frac{2.1 \times 10^{-14} \times 100}{130 \times 10^{-12}} = 0.012$$

$$\text{for } \frac{\delta F}{F} = 1 \times 10^{-8},\ \delta C7 = 0.12\%$$

$$\text{for } \frac{\delta F}{F} = 1 \times 10^{-7},\ \delta C7 = 1.2\%$$

The effect of a change in CR3 in series with C8 is

$$C8 \text{ is } \frac{\delta C7'}{34 \text{ pF}}$$

$$\text{for } \frac{\delta F}{F} = 1 \times 10^{-9}, \ \%\delta(CR3/C8) = \frac{2.1 \times 10^{-14} \times 100}{34 \times 10^{-12}} = 0.062$$

$$\text{for } \frac{\delta F}{F} = 1 \times 10^{-8}, \ \delta(CR3/C8) = 0.62\%$$

$$\text{for } \frac{\delta F}{F} = 1 \times 10^{-7}, \ \delta(CR3/C8) = 6.2\%$$

The effect of a change in C8 is

$$\text{for } \frac{\delta F}{F} = 1 \times 10^{-9}, \ \delta C8 = 0.062\% \times \frac{220}{34} = 0.40\%$$

$$\text{for } \frac{\delta F}{F} = 1 \times 10^{-8}, \ \delta C8 = 4.0\%$$

$$\text{for } \frac{\delta F}{F} = -1 \times 10^{-7}, \ \delta C8 = 40\%$$

The effect of a change in CR3 (40 pF) is

$$\text{for } \frac{\delta F}{F} = 1 \times 10^{-9}, \ \delta CR3 = 0.062 \times \frac{40}{34} = 0.073\%$$

$$\text{for } \frac{\delta F}{F} = 1 \times 10^{-8}, \ \delta CR3 = 0.73\%$$

$$\text{for } \frac{\delta F}{F} = 1 \times 10^{-7}, \ \delta CR3 = 7.3\%$$

The sensitivity of CR3 is 1% C per 0.2 volt

$$\text{for } \frac{\delta F}{F} = 1 \times 10^{-9},\ \Delta V = \frac{0.2\ V}{1\%} \times 0.073\% = 14.6\ mV$$

$$\text{for } \frac{\delta F}{F} = 1 \times 10^{-8},\ \Delta V = 146\ mV$$

$$\text{for } \frac{\delta F}{F} = 1 \times 10^{-7},\ \Delta V = 1.46\ V$$

The sensitivity of frequency to component variations was recalculated for a 30 pF crystal load, and for a 50 pF load. For a 30 pF load, C3 will not be used; C4 will be 50 pF.

With the 30 pF load, the frequency will be 2.8 times more sensitive to component variation than with the 50 pF load. This is true for both the fundamental and the third overtone. A change in C4 causes the following frequency change.

For the fundamental:
0.0018% change C4 gives $\Delta F/F = 10^{-9}$

For the third overtone:
0.005% change in C4 gives $\Delta F/F = 10^{-9}$

The effects of component changes on the 5 MHz fundamental, the 10 MHz fundamental and the 10 MHz third overtone have been calculated. The results of these calculations are presented in Tables 3, 4, and 5.

2.5 Performance of early developmental ceramic enclosed crystals.

2.5.1 Serial numbers tested. The four back filled units having serial numbers 157, 161, 162 and 163, and two older crystals (not back filled) having number 90 and 91 have been investigated in a preliminary manner.

TABLE 3. CHANGE IN COMPONENT TO CAUSE $\Delta F/F$, 5 MHz FUNDAMENTAL, C_T = 100 pF

COMPONENT	$\Delta F/F=1x10^{-9}$	$\Delta F/F=1x10^{-8}$	$\Delta F/F=1x10^{-7}$
C3 (210 pF)	.01%	.1%	1.0%
C4 (30 pF)	.07%	.7%	7.0%
C6 (620 pF)	.03%	.3%	3.0%
Cb-e OF Q4 (2 pF max)	9%	90%	900%
C7 (180 pF)	0.012%	0.12%	1.2%
C8 (220 pF)	0.4%	4%	40%
C OF CR3 (40 pF)	0.073%	0.73%	7.3%
ΔV ON CR3	14.6 mV	146 mV	1.46 V
R12	0.07%	0.7%	7%
R13	0.17%	1.7%	17%

TABLE 4. CHANGE IN COMPONENT TO CAUSE $\Delta F/F$, 10 MHz FUNDAMENTAL, C_T = 50 pF

COMPONENT	$\Delta F/F=10^{-9}$	$\Delta F/F=10^{-8}$	$\Delta F/F=10^{-7}$
C3 (140 pF)	.009%	.09%	.9%
C4 (30 pF)	.04%	.4%	4.0%
C6 (300 pF)	.01%	.1%	1.0%
$Q4_{b-e}$ (2 pF)	2%	20%	200%
C7 (82 pF)	.005%	.05%	.05%
C8 (220 pF)	.47%	4.7%	47%
C of CR3 (15 pF)	.03%	.3%	3%
ΔV on CR3	6 mV	60 mV	600 mV

TABLE 5. CHANGE IN COMPONENT TO CAUSE ΔF/F, 10 MHz, THIRD O.T., C_T = 50 pF

COMPONENT	$\Delta F/F=10^{-9}$	$\Delta F/F=10^{-8}$	$\Delta F/F=10^{-7}$
C3 (140 pF)	.024%	.24%	2.4%
C4 (30 pF)	.11%	1.1%	11%
C6 (470 pF)	.023%	.23%	2.3%
$Q4_{b-e}$ (2 pF)	5.5%	55%	550%
C7 (82 pF)	.01%	.1%	1.0%
C8 (220 pF)	.47%	4.7%	47%
C of CR3 (15 pF)	.03%	.3%	3.0%
V on CR3	6 mV	60 mV	600 mV
C5	over 1000%	---	---
L1	.065%	.65%	6.5%

2.5.2 CI measurements. All but serial number 91 were measured on the CI meter with a 100 pF load. The spread was small between them; average values are RS = 6 Ω; C1 = 0.0105 pF.

2.5.3 Stability as a function of drive level. The following chart shows stabilities consistent with earlier work:

Crystal Number	RMS ΔF/F	Drive Level (μA)	Sampling Time (seconds)
90	$7x10^{-11}$	35	1
90	$2x10^{-11}$	100	1
90	$5x10^{-11}$	100	0.1
90	$2x10^{-11}$	100	10
90	$7x10^{-12}$	700	1
90	$2.8x10^{-11}$	700	0.1
90	$8x10^{-12}$	700	10

Crystal Number	RMS ΔF/F	Drive Level (μA)	Sampling Time (seconds)
157	$6x10^{-11}$	35	1
157	7x10-10	35	0.1
161	$8x10^{-11}$	35	1
161	$3x10^{-11}$	100	1

All above were measured in a Bendix test oscillator. Stabilities were also measured in other oscillators, e.g., in the FTS commercial oscillator.

Crystal Number	RMS ΔF/F	Drive Level (μA)	Sampling Time (seconds)
90	$3.5x10^{-11}$	300	1
90	$3x10^{-10}$	300	0.1
90	$1.3x10^{-11}$	300	10

In the no reactance type oscillator.

161	$2.5x10^{-11}$	75	1
161	$4.5x10^{-12}$	75	10

2.5.4 Retrace studies. Crystal number 161 has been measured for retrace in the no reactance test circuits at an ambient of $-40^{o}C$; the oscillator and crystal oven were raised to $+90^{o}C$. Three on-off cycles (taking 3 days) gave a ΔF/F of $\pm 2 \times 10\text{-}9$.

2.5.5 General stability. After operating for 1 month at 35 μA, crystal number 157 became 1 to 2 magnitudes more noisy. Electrrical connections external to the crystal were remade with no improvement. Crystal number 157 was definitely noisy due to a problem inside its enclosure.

After operating crystal number 162 for 3 days, the oscillator output with crystal dropped to about one-half. Using another

crystal in the test oscillator, the output was again normal. Remeasuring crystal number 2 in the CI meter reproduced the original values.

Crystal number 163 was 2 orders of magnitude noisier than the other crystals when first measured. Crystal number 163 remains this noisy.

2.5.6 Short term (1 second) noise measurements. The Allan Variance for 1 second time intervals was measured for two ceramic enclosed crystals supplied by ECOM. The variance was measured on the beat frequency resulting from the test crystal and a more stable reference oscillator. The data are presented in Table 6.

TABLE 6. ALLAN VARIANCE, 1 SECOND INTERVAL

Crystal Under Test	Ref. Oscillator	Total Variance	Test Crystal Variance
H.P. Computing Counter No. 1	H.P. Computing Counter No. 2	5×10^{-12}	3.5×10^{-12}
Ceramic Crystal No. 90	H.P. Computing Counter No. 2	3.6×10^{-11}	3.58×10^{-11}
Ceramic Crystal No. 91	H.P. Computing Counter No. 2	8.1×10^{-11}	8.1×10^{-11}
Philips, Glass Evacuated	H.P. Computing Counter No. 2	1.5×10^{-11}	1.46×10^{-11}

The absolute measurement error has not been determined. The variance as a function of the number of pairs has also not been investigated. However, the relative values are believed to be correct.

2.5.7 Long term stability. The long term stability of two crystals in their temperature-controlled test oscillators was measured. The ovens controlling the temperature for both types were similar. The first series of measurements was made with the ceramic packaged ECOM crystal number 90 (under vacuum), in a circuit similar to that in the present TMXO design. The crystal drive current was about 1 mA.

The same crystal was also put in a test oscillator where the drive current had been reduced to about 50 microamperes. The other type of crystal studied was a 5 MHz, third overtone in a glass envelope, supplied by ECOM. This crystal was in an oscillator driving the crystal at about 50 microamperes. Aging curves are shown in Figure 9. The aging of ceramic crystal number 90 was 5×10^{-9} per day at both the 1 milliampere and 50 microamperes drive currents.

2.5.8 Low frequency perturbations. The low frequency perturbations have been measured for these two crystals: the 5.115 MHz ceramic driven at 1 milliampere, and the third overtone glass driven at 50 microamperes. Figure 10 shows the curves for the 5.115 MHz ceramic crystal. The upper curve shows the frequency variation with time, the frequency being a 10-second average. The bottom curve uses the same data, but displays it in the form of its Fourier transform. That is, the amplitude of the signal is plotted as a function of frequency deviation from the center frequency; i.e., the perturbation frequency.

Figure 11 shows the same kind of information, but for the third overtone crystal.

Figure 12 represents the cmposite spectra of the oscillator/ crystals plotted in Figures 2 and 3. In Figure 4 is included additional data to that shown in those two previous figures. The difference in slopes is again due to the different aging.

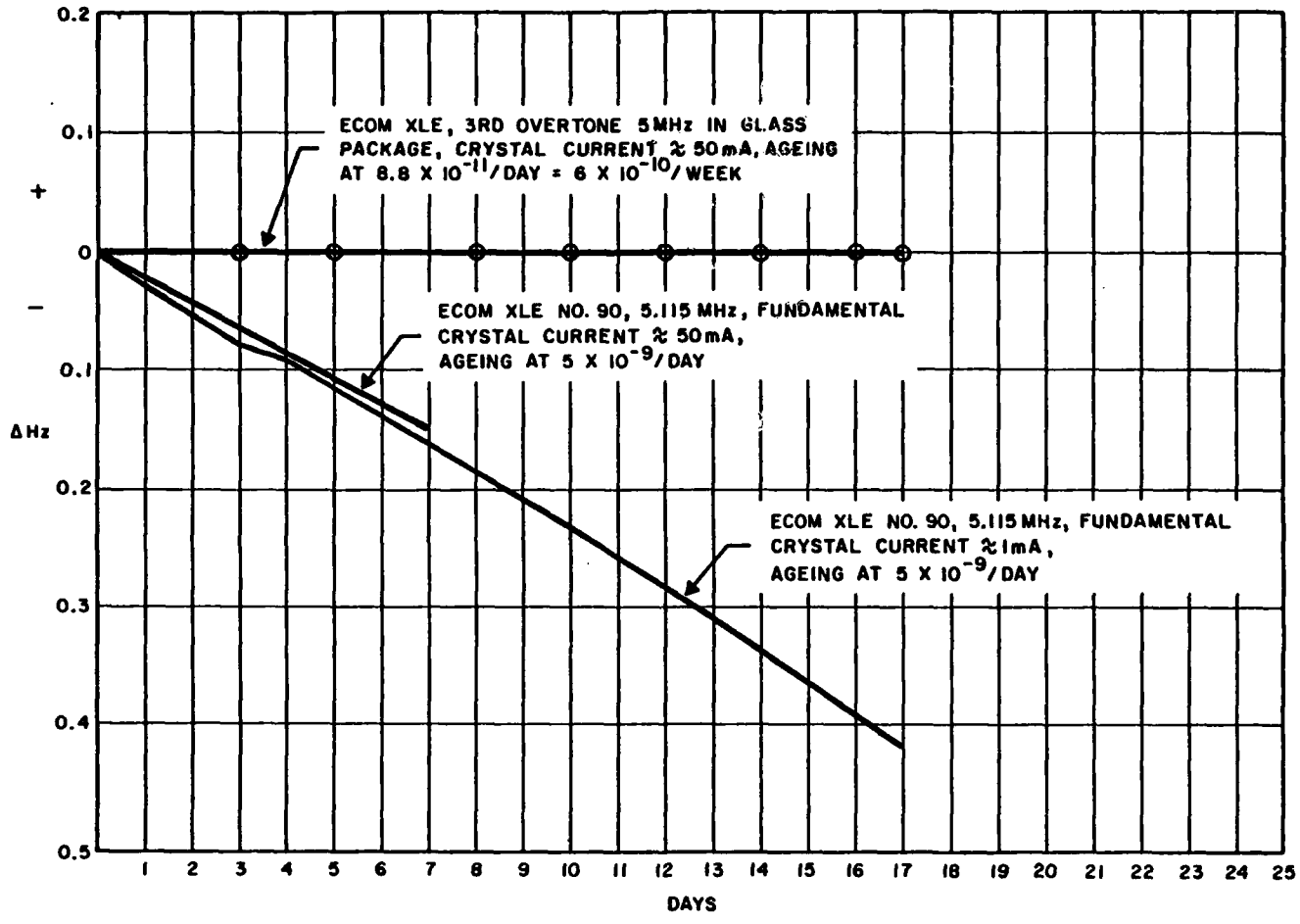

Figure 9. Aging of crystals in oven-controlled test oscillators.

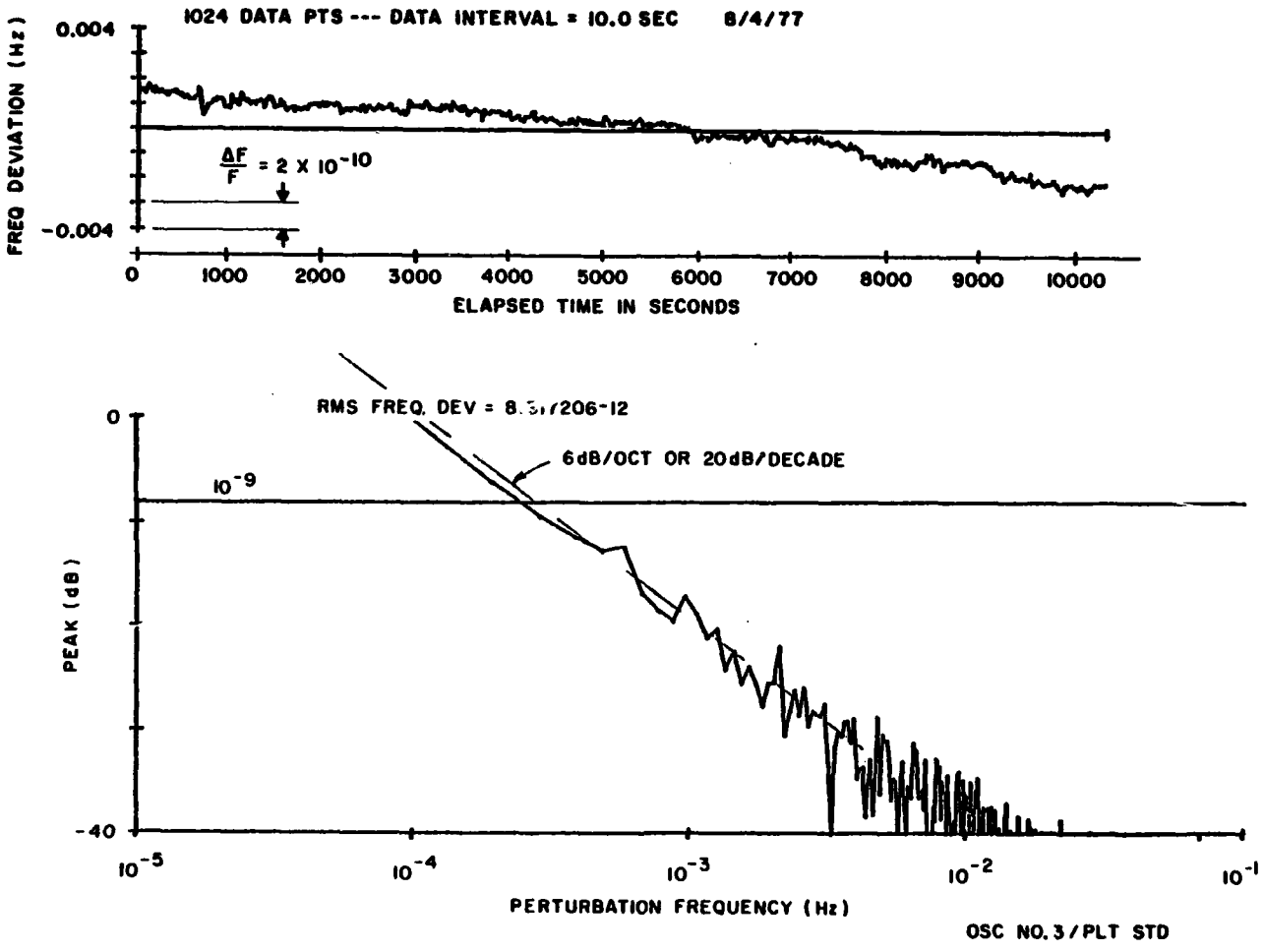

Figure 10. Frequency perturbations for crystal number 90.

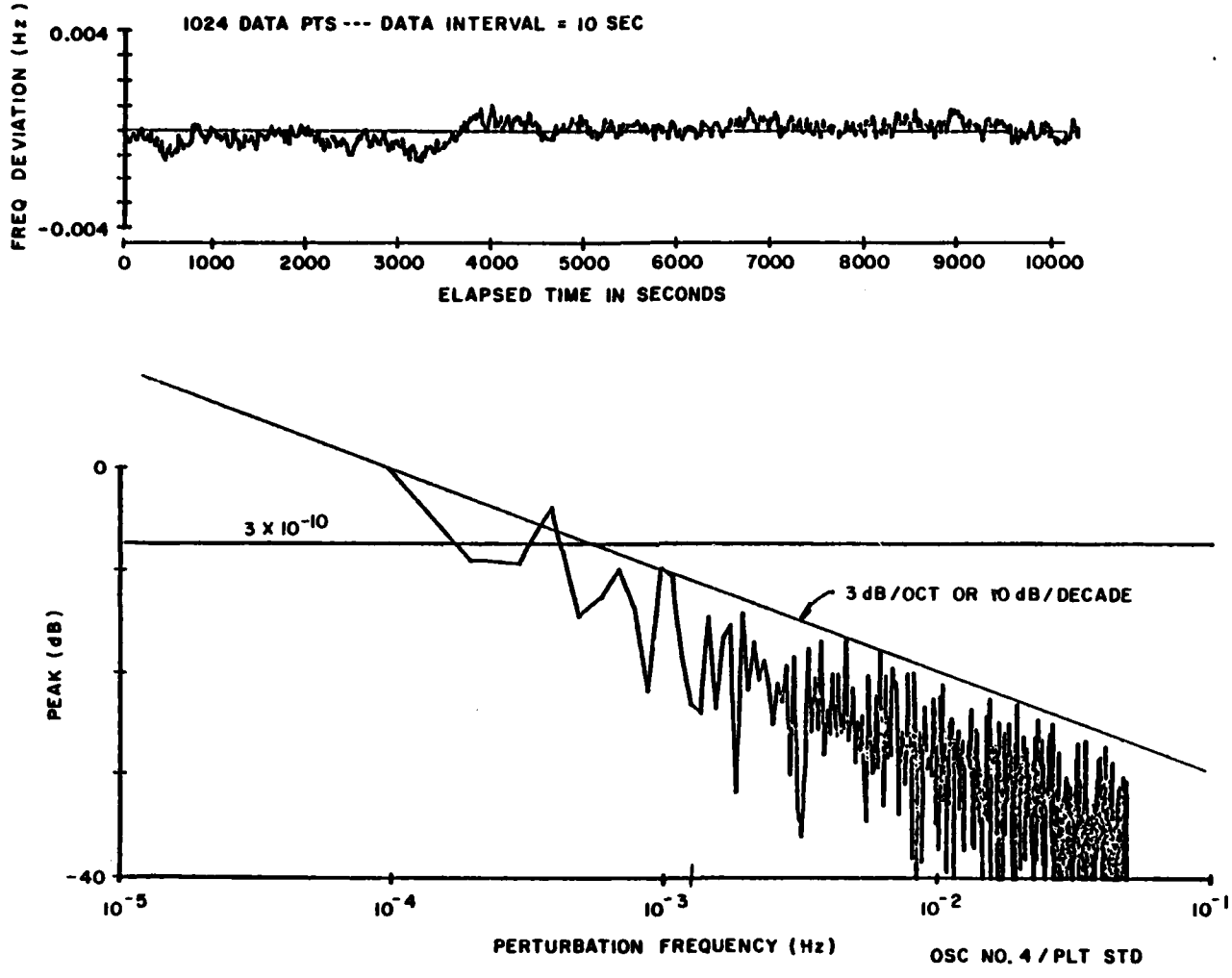

Figure 11. Frequency perturbations for third O.T. crystal.

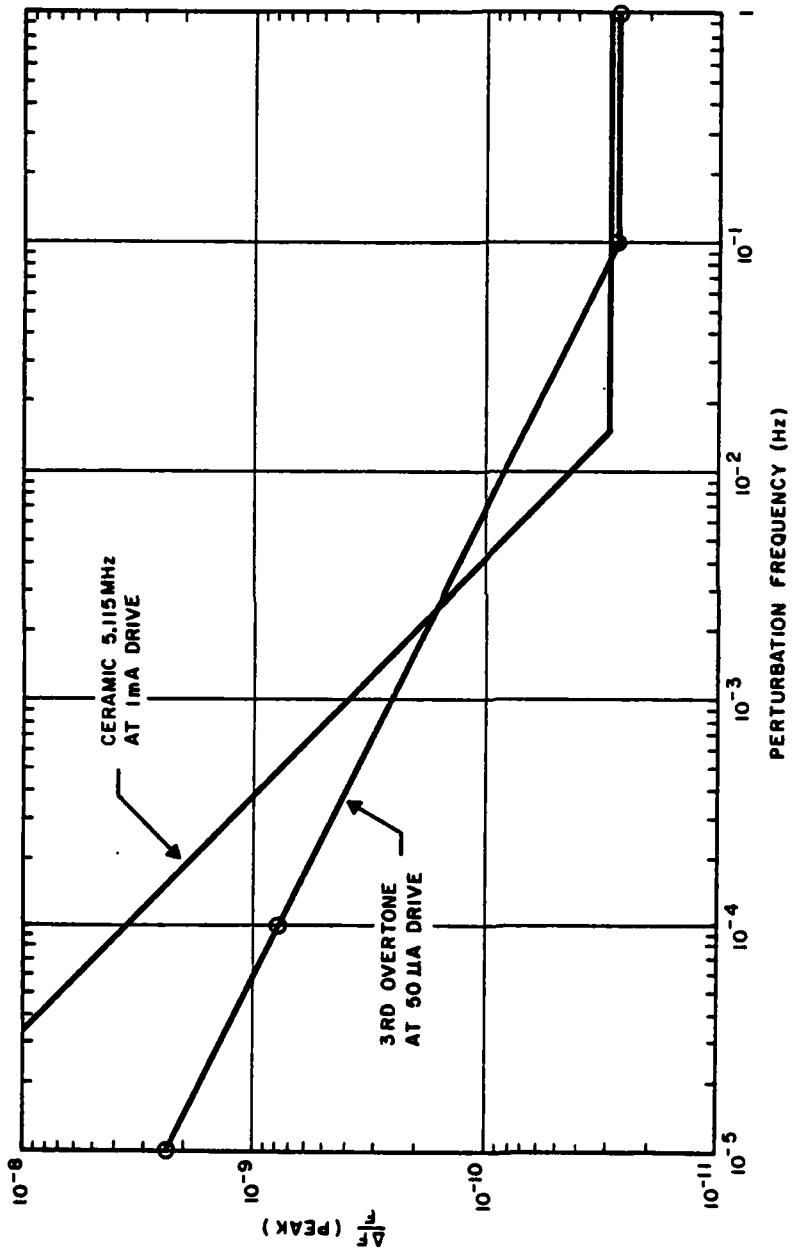

Figure 12. Frequency deviation versus perturbation frequency.

3. THERMAL DESIGN

3.1 General. The general thermal design of the TMXO in this program is nearly the same as that reported in ECOM-0199F. In that report, the thermal equivalent circuit is presented as well as the various heat losses and temperature drops. This detailed presentation is not repeated here. Two mechanical changes, which result in minor thermal changes, have been implemented. These are discussed below.

3.2 Location of the crystal enclosure. All models prior to phase 2 had been fabricated with the crystal enclosure attached to the pedestal and the microcircuit package above the crystal enclosure. This arrangement evolved from the earliest models where there was no microcircuit package, the microelectronics being located on the crystal enclosure. A detailed thermal analysis was made to determine whether the crystal enclosure would be thermally more uniform, above or below the microcircuit package. The thermal radiation from the sides of the microcircuit and crystal enclosures is independent of their location. Also, independent of their location is the heat loss through the wire connections. At $-40^{\circ}C$, this independent heat loss has an equivalent thermal resistance of $2090^{\circ}C/W$. The equivalent thermal resistance due to radiation from the top surface, for either enclosure, is $13,300^{\circ}C/W$. The thermal resistance through the pedestal is $1,838^{\circ}C/W$. Therefore, locating the crystal enclosure above the microcircuit package would decrease the thermal difference between the top and bottom of the crystal enclosure. The crystal enclosure, in this new location, no longer required mounting facilities to the pedestal. This also made the incorporation of a ceramic crystal enclosure much easier.

3.3 The crystal enclosure design. For thermal reasons, previous crystals were mounted in gold-plated copper enclosures. During phase 1, the crystal enclosure was redesigned to:

(a) Be large enough to accept a fifth overtone resonator (F_5 = 5.115 MHz).

(b) Have the same thermal characteristics as a specific alumina crystal enclosure.

Alumina, having a much higher thermal resistance than copper, dictated the use of a material other than copper for the new enclosure. This new material would also require good machinable and sealing properties. After considering the thermal and mechanical characteristics of many materials, nickel was selected. Table 7 gives some pertinent characteristics for three types of crystal enclosures: the previously used gold-plated copper type, the future alumina ceramic type, and the nickel type used in this program.

TABLE 7. CHARACTERISTICS OF CRYSTAL ENCLOSURES

	Old copper enclosures	Alumina* enclosures	Nickel enclosure
Outside Diameter	0.632 inch	0.788 inch	0.792 inch
Inside Diameter	0.592 inch	0.668 inch	0.692 inch
Outside Height	0.210 inch	0.120 inch	0.200 inch
Inside Height	0.150 inch	0.060 inch	0.140 inch
Thermal Resistance (top to bottom)	0.47°C/W	0.69°C/W	0.66°C/W
Thermal Capacity	0.38 Cal/°C	0.53 Cal/°C	0.51 Cal/°C

* The alumina enclosure is not cylindrical. Dimensions are approximately equal to an equivalent cylinder.

3.4 Microcircuit to TMXO header connections. The electrical connections from the microcircuit to the TMXO case header are made with wire welded at the ends. The wire should be selected so as to conduct minimum heat flow, compatible with the electrical current it must carry. The figure of merit for such an application is

$$\frac{\rho(T)}{\rho(E)}$$

where $\rho(T)$ is the thermal resistivity
$\rho(E)$ is the electrical resistivity

Table 8 presents the pertinent data for some materials.

TABLE 8. THERMAL/ELECTRICAL RESISTIVITIES

Material	$\rho(E)$	$\rho(T)$	$\rho(T)/\rho(E)$
Gold	1.21	134	111
Nickel	4	448	112
Karma	67	3030	45
Nichrome	56	3030	54
Chromax	50	3030	61
Michrome V	54	3500	65
Nilvar	42	3500	83
Kovar	25	2275	91
Silver	0.82	94	114
Tantalum	7	729	104
Palladium	5.5	554	101

where $\rho(E)$ is in ohms circular mil/inch
$\rho(T)$ is in mils degree C/watt

Palladium wire, 3 mil diameter, has been chosen for the following microcircuit/header connections: the RF outputs, the fine frequency control, and the leads to the temperature setting potentiometer. The electrical resistance of a 1 inch long wire is

$$\rho(E) = \frac{5.5 \text{ ohms circular mils}}{\text{inch}} \times \frac{1 \text{ inch}}{9 \text{ circular mils}}$$

$$\rho(E) = 61 \text{ ohms.}$$

The thermal resistance of this wire is 78,375°C/watt.

Nickel wire, 10 mil diameter, has been selected for the ground, +12 volts, the connections between microcircuit halves, and the connections to the crystal. The electrical resistance of a 1 inch long wire is

$\rho(E) = 4/100 = 0.04$ ohm.

The wires connecting the microcircuit halves and to the crystal will be about 0.2 inch long and have a resistance of 0.008 ohm. The thermal resistance of the 1 inch long, 10 mil diameter nickel wire is 44,563°C/W.

4. MICROELECTRONIC DESIGN

4.1 For phase 1. A new microcircuit layout was required for the new microcircuit package. Some minor changes were made to simplify the fabrication and enhance the reliability. The layout is shown in Figure 13.

4.2 For phase 2.

4.2.1 Connecting the transformer leads. During the sealing of the microcircuit package, a temperature of about 300°C is reached. Therefore, the transformer leads cannot be soldered. One possible solution to this problem is to thermocompression bond the transformer lead. The transformer lead is a number 38 wire. The insulation was stripped from some of this wire, and it was then gold-plated. Attempts to bond this wire by thermocompression means were unsuccessful. The condition of gold plating on the wire may not have been suitable.

Another approach to the problem was to weld the number 38 copper wire to a gold-plated kovar tab. Thermocompression bonds can then be made to the tab, and/or the tab could be epoxied in place. The welding was successful using a parallel gap welder.

4.2.2 High temperature epoxies. Four epoxies were evaluated for mechanical adhesion. Two of these were also evaluated electrically. The four epoxies were:

(a) EPOTEK H61 (insulating)
(b) EPOTEK H31 (silver conducting)
(c) ABLEBOND 71-1 (silver conducting)
(d) ABLEBOND 71-2 (insulating)

The adhesion tests showed that with the exception of H61, the epoxies had strong adhesion after 1 hour at 270°C + 1 hour at 300°C, or 1 hour and 40 minutes at 300°C.

The electrical evaluation was carried out on transistors. The beta and VCE SAT were measured before and after a thermal treatment of 1 hour and 40 minutes at 300°C in air. Data are presented below:

EPOXY H31

Transistor number	Beta before	Beta after	$V_{CE\ SAT}$ before (volts)	$V_{CE\ SAT}$ after (volts)
1	190	188	0.05	0.06
2	180	180	0.035	0.11
3	152	150	0.06	0.06
4	190	188	0.05	0.06
5	180	175	0.05	0.06
6	150	166	0.05	0.13
7	160	166	0.05	0.06
8	150	150	0.05	0.95
9	165	170	0.05	0.07
10	125	133	0.06	0.07

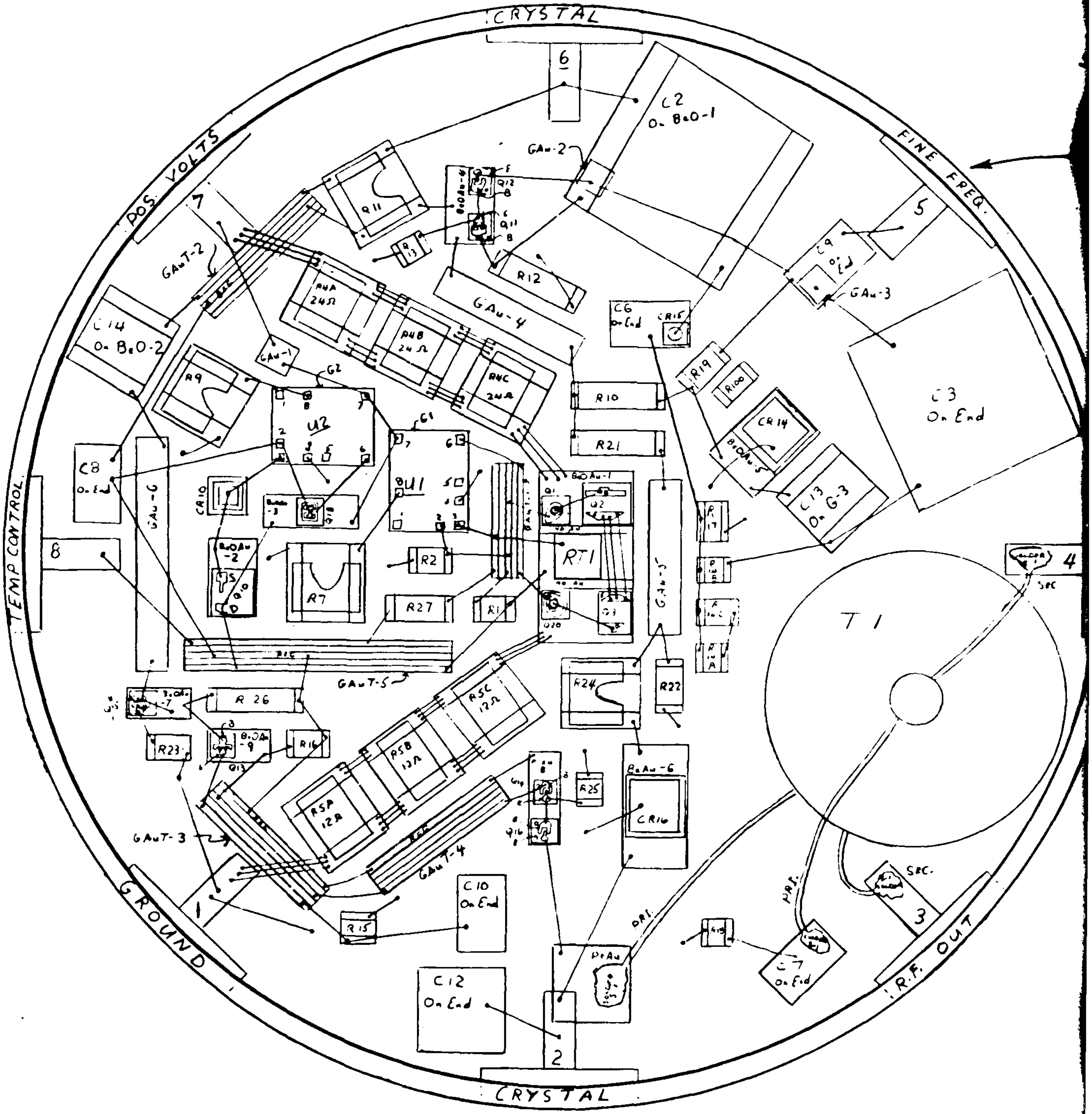

CRYSTAL
C2
On BeO-1
GAu-2
FINE FREQ.
POS. VOLTS
Q11
Q12
Q11
Q13
R12
GAu-4
C9 On End
5
GAu-3
7
GAuT-2
R4A 24Ω
R4B 24Ω
R4C 24Ω
C14
On BeO-2
GAu-1
R9
C6 On End
CR15
R19
R100
R10
R21
C3
On End
CR14
BeOAu-5
C13 On G-3
U2
U1
C8
On End
GAu-6
CR10
BeOAu-1
Q1
Q2
RT1
GAu-5
TEMP CONTROL
8
BeOAu-2
Q10
R7
R2
R27
R1
Q20
4
SEC
T1
GAuT-5
R24
R22
R 26
Q15
BeOAu-7
R23
BeOAu-9
Q13
R16
R5C 12Ω
R5B 12Ω
R5A 12Ω
R25
Q16
BeAu-6
CR16
GAuT-3
GAuT-4
GROUND
1
C10
On End
R15
SEC.
3
PRI.
C7
On End
R.F. OUT
PtAu
C12
On End
2
CRYSTAL

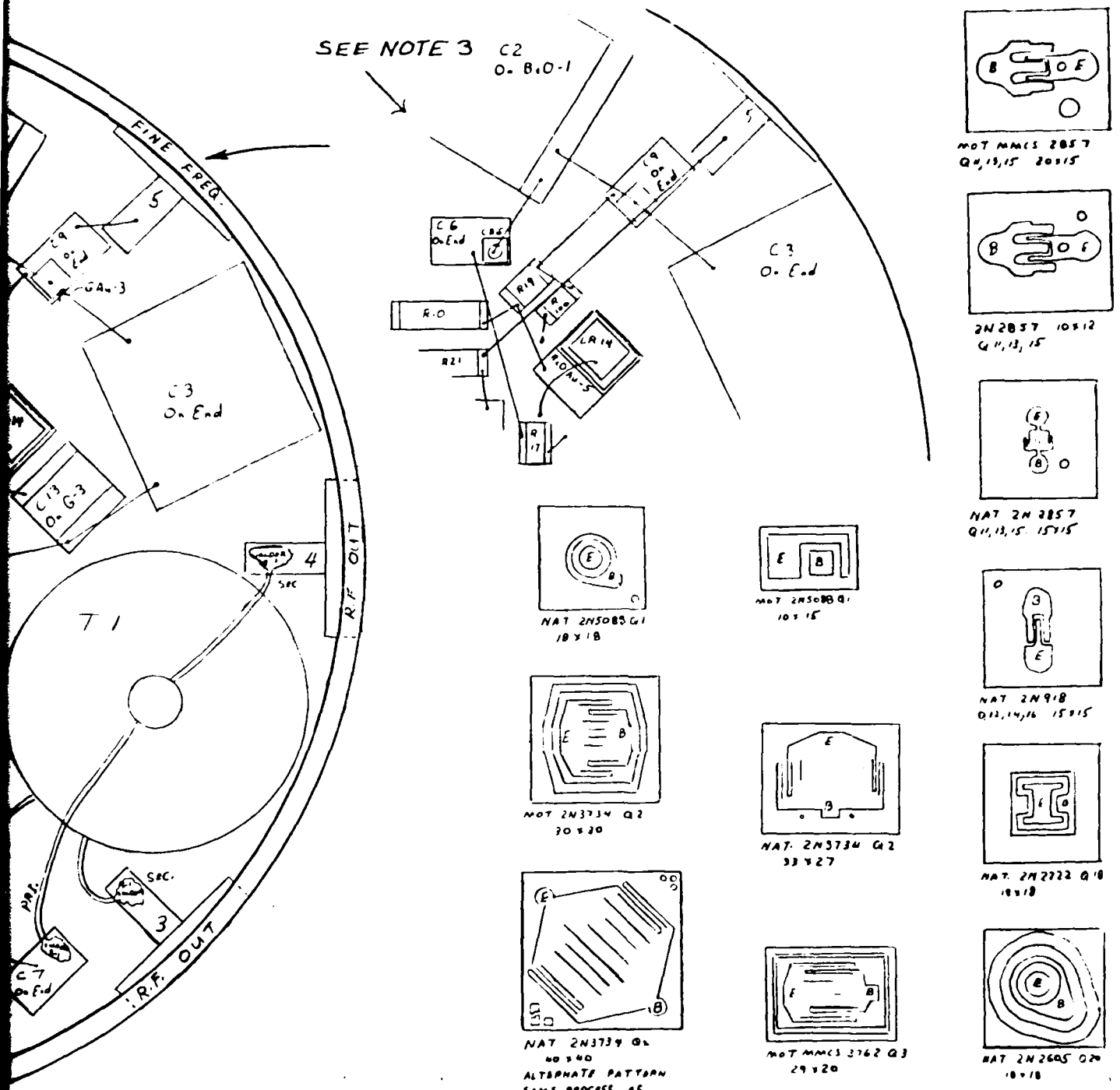

Figure 13. Microelectronic layout for phase 1 (sheet 1 of 2).

1.7

QTY	IDENT	MANUFACTURER	SIZE	DESCRIPTION	PART NO.	NOTES
1			—	PKG COVER. BENDIX No. SK1190-100-1		NOTE 5
—			DIA .001	GOLD WIRE		
—	—	EPOTEK	—	EPOXY; INSULATING	H61	NOTE 7,8
—	—	EPOTEK	—	EPOXY, SILVER CONDUCTING	H31	NOTE 6
1	—		—	MICROCIRCUIT PKG. BENDIX No. SK1100-100-2		NOTE 6
—	S-1	KESTER	—	SOLDER 95% Sn-5% Sb SOLIDUS 232°C	995	
1	PtAu	BENDIX	50x50	PLATINUM-GOLD ON CERAMIC, NEAR PIN 2		
2	BeOAu-7,-9	ANY	[illegible]	GOLD ON BeO; UNDER Q15, UNDER Q13.		
1	BeOAu-6	ANY	[illegible]	GOLD ON BeO; UNDER CR16		
1	BeOAu-8	ANY	[illegible]	GOLD ON BeO; UNDER CR14		
2	BeOAu-3,-8	ANY	[illegible]	GOLD ON BeO; UNDER Q18, UNDER Q14 & Q16.		
2	BeOAu-2,-4	ANY	[illegible]	GOLD ON BeO; UNDER Q10, UNDER Q11 & Q12		
1	BeOAu-1	BENDIX	[illegible]	GOLD ON BeO, 2 CUT SPACES-SAME EACH, UNDER Q1,2,3,	[illegible]	
1	BeO-2	ANY	[illegible]	PLAIN BeO; UNDER C14		
1	BeO-1	ANY	[illegible]	PLAIN BeO, UNDER C2		
1	GAuT-5	BENDIX	[illegible]	GOLD TRACK ON GLASS		
3	GAuT-2,3,4	BENDIX	[illegible]	GOLD TRACK ON GLASS, AT PIN 7, PIN 1, NEAR R5		
1	GAuT-1	BENDIX	[illegible]	GOLD TRACKS ON GLASS. BETWEEN U1 & U2.		
1	G3	BENDIX	[illegible]	PLAIN GLASS UNDER C13		
1	GAu-6	BENDIX	[illegible]	GOLD ON GLASS; NEAR PIN 8		
2	G1, G2	BENDIX	[illegible]	PLAIN GLASS; UNDER U1 & U2.		
2	GAu-4,-5	BENDIX	[illegible]	GOLD ON GLASS, REG NEAR R12, BETWEEN R21 & R22		
3	GAu-1,-2,-3	BENDIX	[illegible]	GOLD ON GLASS, NEAR U2, ON C2, ON C9		
1	R23	BENDIX	27x16	THIN FILM RESISTOR 5.1KΩ ±5%		
1	R100	BENDIX	30x16	THIN FILM RESISTOR 22.5KΩ ±5%		
1	R27	BENDIX	40x16	THIN FILM RESISTOR (RT1 AT 90°C-22KΩ)		NOTE 4
1	R25	BENDIX	21x16	THIN FILM RESISTOR 9.1KΩ ±5%		
1	R22	BENDIX		THIN FILM RESISTOR; VALUE TO BE DETERMINED		NOTE 3
1	R21	BENDIX	60x16	THIN FILM RESISTOR 47KΩ ±5%		
1	R19	BENDIX	30x16	THIN FILM RESISTOR 20KΩ ±5%		
1	R18	BENDIX	20x18	THIN FILM RESISTOR 2.2KΩ ±5%		
1	R17	BENDIX	20x26	THIN FILM RESISTOR 620Ω ±5%		
1	R16	BENDIX	27x16	THIN FILM RESISTOR 3.9KΩ ±5%		
1	R15	BENDIX	20x22	THIN FILM RESISTOR 500Ω ±1%		
1	R14C	BENDIX	27x16	THIN FILM RESISTOR 4KΩ ±5%		
1	R14B	BENDIX	21x16	THIN FILM RESISTOR 3KΩ ±5%		
1	R14A	BENDIX	20x18	THIN FILM RESISTOR 2KΩ ±5%		
1	R13	BENDIX	21x16	THIN FILM RESISTOR 10KΩ ±5%		
1	R12	BENDIX	60x16	THIN FILM RESISTOR 51KΩ ±5%		
1	R11	BENDIX	50x60	THICK FILM RESISTOR 120KΩ ±5%		
2	R10, 26	BENDIX	60x16	THIN FILM RESISTOR 68KΩ ±5%		
3	R 7, 9, 24	BENDIX	50x50	THICK FILM RESISTOR 1MEG ±10%		
3	R5A, 5B, 5C	BENDIX	50x50	THICK FILM RESISTOR 12Ω ±10%		
3	R4A, 4B, 4C	BENDIX	50x50	THICK FILM RESISTOR 24Ω ±10%		
2	R1, R2	BENDIX	27x16	THIN FILM RESISTOR 12KΩ ±5%		
1	C14	AMER. TECH CER.	55 CUBE	CAPACITOR 5.1 pf ±.25 pf	ATC-100A5R1-C-C	NOTE 8
1	C12	AMER. TECH. CER.	55 CUBE	CAPACITOR 51 pf ±10%	ATC-100A510FC	
1	C10	ANY	[illegible]	CAPACITOR CHIP 470 pf ±10%, K1200		
1	C7	ANY	[illegible]	CAPACITOR CHIP, .0047 μf ±10%, K1200		
4	C6, 8, 9, 13	ANY	[illegible]	CAPACITOR CHIP .0068 μf ±20%, K1200		NOTE 8 (C13)
1	C3	AMER. TECH CER.	110 CUBE	CAPACITOR 330 pf ±10%	ATC-100B331KC	
1	C2	AMER. TECH. CER.	110 CUBE	CAPACITOR, 390 pf. ±5%	ATC-100B391JC	NOTE 8
1	T1	BENDIX (WOUND)		TRANSFORMER 5:1, 60 TURNS PRI. 12 TURNS SEC.		NOTE 2,7
1	RT1	NAT. LEAD	30x30	THERMISTOR CHIP, BENDIX No. →	0032655-0701	
1	CR16	MOT.	40x00	VARACTOR DIODE CHIP	1N5476A	
1	CR15	ANY	15x15	DIODE CHIP	1N914	
1	CR14	MOT.	37x37	VARACTOR DIODE CHIP	1N5474A	
1	CR10	MOT.	25x25	ZENER DIODE CHIP	1N754A	
2	U1, U2	FAIR.	50x65	OP. AMP. CHIP	μA776	
1	Q20	NAT. OR OTHER	18x18	TRANSISTOR CHIP	2N2605	
1	Q18	NAT. OR OTHER	18x18	TRANSISTOR CHIP	2N2222	
3	Q12, 14, 16	NAT. OR OTHER	15x15	TRANSISTOR CHIP	2N918	
3	Q11, 13, 15	NAT OR MOT.	15x15	TRANSISTOR CHIP	2N2857	
1	Q10	SILICONIX	30x30	FET, CURRENT LIMITING CHIP	CNCL05	
1	Q3	MOT.	29x20	TRANSISTOR CHIP	MMCS 3762	NOTE 1
1	Q2	NAT. OR MOT.	33x27	TRANSISTOR CHIP	2N3734	NOTE 1
1	Q1	NAT. OR MOT.	18x18	TRANSISTOR CHIP	2N5088	
QTY REQD	CODE IDENT NO.	PART OR IDENTIFYING NUMBER	SIZE (MILS)	NOMENCLATURE OR DESCRIPTION	SPECIFICATION	NOTES & REF DESIGNATIONS
-0501				PARTS LIST		

...TION	PART NO.	NOTES
BENDIX No. SK1100-100-1		NOTE 5
...ATING	H61	NOTE 7,8
...R CONDUCTING	H31	NOTE 6
...G. BENDIX No. SK1100-100-2		NOTE 5
...-5% Sb SOLIDUS 232°C	995	
... ON CERAMIC, NEAR PIN 2		
...; UNDER Q15, UNDER Q13.		
UNDER CR16		
...: UNDER CR14		
...; UNDER Q18, UNDER Q14 & Q16.		
UNDER Q10, UNDER Q11 & Q12		
CUT SPACERS-5MILS EACH, UNDER Q1,2,3, & RT1.		NOTE 1
UNDER C14		
UNDER C2		
... GLASS		
... GLASS; AT PIN 7, PIN 1, NEAR R5.		
...ON GLASS, BETWEEN U1 & U2.		
UNDER C13		
...S; NEAR PIN 8		
UNDER U1 & U2.		
...SS; REG NEAR R12,	BETWEEN R21 & R22	
...SS; NEAR U2, ON	C2, ON C9	
...SISTOR 51KΩ ± 5%		
...SISTOR 22.5KΩ ± 5%		
...TOR (RT1 AT 90°C - 22KΩ)		NOTE 4
...ESISTOR 9.1KΩ ± 5%		
...SISTOR; VALUE TO	BE DETERMINED	NOTE 3
...RESISTOR 47KΩ ± 5%		
...RESISTOR 20KΩ ± 5%		
...RESISTOR 2.2KΩ ± 5%		
...SISTOR 620Ω ± 5%		
...RESISTOR 3.9KΩ ± 5%		
...RESISTOR 500Ω ± 1%		
...SISTOR 4KΩ ± 5%		
...SISTOR 3KΩ ± 5%		
...SISTOR 2KΩ ± 5%		
...SISTOR 10KΩ ± 5%		
...SISTOR 51KΩ ± 5%		
...RESISTOR 120KΩ ± 5%		
...ISTOR 68KΩ ± 5%		
...RESISTOR 1MEG ± 10%		
...RESISTOR 12Ω ± 10%		
...RESISTOR 24Ω ± 10%		
...SISTOR 12KΩ ± 5%		
...1 pf ± .25 pf	ATC-100A5R1-C-C	NOTE 8
...51 pf ± 10%	ATC-100A510 KC	
...HIP, 470 pf ± 10%, K1200		
...HIP, .0047 µf ± 10%, K1200		
...HIP .0068 µf ± 20%, K1200		NOTE 8 (C13)
... 330 pf ± 10%	ATC-100B331KC	
...390 pf. ± 5%	ATC-100B391JC	NOTE 8
...ER 5:1, 60 TURNS PRI. 12 TURNS SEC.		NOTE 2,7
...CHIP, BENDIX No. → 9032655-0701		
... DIODE CHIP	1N 5476A	
...HIP	1N 914	
... DIODE CHIP	1N5474 A	
...ODE CHIP	1N 754A	
... CHIP	µA 776	
...R CHIP	2N 2605	
...R CHIP	2N 2222	
...R CHIP	2N 918	
...R CHIP	2N 2857	
...NT LIMITING CHIP	CNCL05	
... CHIP	MMCS 3762	NOTE 1
...R CHIP	2N 3734	NOTE 1
...R CHIP	2N 5088	
...ENCLATURE OR DESCRIPTION	SPECIFICATION	NOTES & REF DESIGNATIONS
... LIST		

NOTE 1:
SELECT Q2 AND Q3, EACH TO HAVE $h_{FE} > 90$; AT I_C = 10mA. +6VOLTS AND AT 90°C. EUTECTICALLY BOND Q2 AND Q3 TO B-OAu-1.

NOTE 2:
TRANSFORMER WOUND ON FERITE TOROID. IND. GEN. Q1 MATERIAL, SHAPE CF-120, 155 O.D, 88 I.D, 55 H. (mils), $K = L/N^2$ = 0.C.8. WIRE, ESSEX No. 38 SINGLE CLAD POLY THERMOLEX 200.

NOTE 3: PRELIMINARY WIRING FOR DETERMINING THE VALUE OF R22. WIRE AS ON RIGHT, LEAVING THE WIRE BETWEEN R22 AND GAu-5 OUT. DO NOT SEAL. R22 IS ±0.5%

NOTE 4:
MAKE R27 = RT1-22KΩ. USE MEASURED VALUE OF RT1 AT 90°C.

NOTE 5:
ORIENTATION OF COVER TO PKG. IS SPECIFIC. ORIENT AS BELOW:

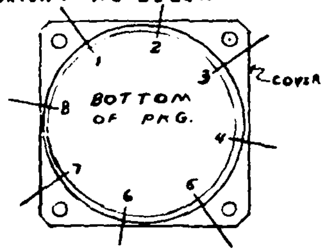

SOLDER PKG TO COVER USING SOLDER S-1.

NOTE 6:
PUT ALL PARTS (EXCEPT Q2, Q3, T1, C2, C13 & C14) DOWN WITH EPOXY H31.

NOTE 7:
SECURE T1 IN PLACE WITH EPOXY H-61.

NOTE 8:
PUT C2, C13 AND C14 DOWN WITH H61

NOTE 9:
SELECT Q1 TO HAVE $h_{FE} > 600$, AT I_C = 100µA. +6VOLTS AND AT 90°C.

Figure 13. Microelectronic layout for phase 1 (sheet 2 of 2).

EPOXY ABLEBOND 71-1

Transistor number	Beta before	Beta after	$V_{CE\ SAT}$ before (volts)	$V_{CE\ SAT}$ after (volts)
1	150	180	0.05	0.05
2	155	153	0.05	0.05
3	181	180	0.06	0.06
4	175	180	0.05	0.05
5	180	180	0.05	0.06
6	175	175	0.05	0.06
7	143	150	0.06	0.06
8	180	166	0.06	0.06
9	175	166	0.06	0.07
10	180	180	0.05	0.06

The degradation of $V_{CE\ SAT}$ is due to an increase in the electrical resistance of the epoxy. The data show that epoxy H31 would not be acceptable. Ablebond 71-1 remains unchanged, and it was used in an experimental model. All betas remain essentially unchanged, as expected.

The polyimide, Ablebond 71-1, conducting epoxy was found to be a noise source when used to attach the thermistor. Epo-Tek H31 was evaluated for noise and found to be unacceptable. Ablebond 20-1 was evaluated and found to be about 2 orders of magnitude better than the other epoxies. Its high temperature strength was evaluated and was found to be acceptable. The high temperature electrical characteristics of this epoxy is not as good as the Ablebond 71-1. Fortunately, this deficiency is not relevant to the TMXO, that is, the TMXO contains no epoxy connections which must be a very low resistance.

The epoxies selected for use were:

(a) Conductive epoxy: Ablebond 20-1
(b) Insulating epoxy: Ablebond 71-2

4.2.3 Stability of thick film resistors to high temperatures. A sample of thick film resistors screened onto a test substrate using DuPont 1400 series resistive inks with gold terminations were measured. They were remeasured after subsequent heat treatments in air. The data are presented in Table 9 and show that untrimmed resistors of the 1400 series inks can be reheated in air for 1-1/2 hours at 600°C with less than a 20 percent change; 1 hour at 500°C in air causes only a few percent change. Ceramic frames may be attached to substrates, having these types of resistors, without harm to the resistors, if the attachment temperature is less than 600°C.

TABLE 9. STABILITY OF THICK FILM RESISTORS

Ckt. No.	R No.	RESISTANCE IN OHMS As Fired	1 Hr at 400°C	1 Hr at 400° + 1 Hr at 500°C	1 Hr at 400°C +1 at 500°C +1-1/2 Hr at 600°C
1	1	21.0 k	21.0 k	20.4 k	22.3 k
2	1	21.6 k	21.7 k	20.8 k	23.4 k
3	1	19.4 k	19.4 k	18.7 k	22.2 k
4	1	17.4 k	17.4 k	16.8 k	20.9 k
5	1	19.3 k	19.4 k	18.6 k	24.1 k
6	1	20.1 k	20.2 k	19.5 k	26.1 k
1	2	1.20 k	1.20 k	1.91 k	1.20 k
2	2	1.48 k	1.50 k	1.46 k	1.48 k
3	2	1.04 k	1.10 k	1.03 k	1.07 k
4	2	1.10 k	1.10 k	1.10 k	1.15 k
5	2	1.21 k	1.21 k	1.21 k	1.30 k
6	2	1.11 k	1.11 k	1.12 k	1.20 k
1	3	185 k	187 k	185 k	190 k
2	3	185 k	187 k	123 k	133 k
3	3	143 k	144 k	142 k	162 k

TABLE 9. STABILITY OF THICK FILM RESISTORS (CONT)

Ckt. No.	R No.	RESISTANCE IN OHMS As Fired	1 Hr at 400°C	1 Hr at 400° + 1 Hr at 500°C	1 Hr at 400°C +1 at 500°C +1-1/2 Hr at 600°C
4	3	116 k	117 k	113 k	133 k
5	3	126 k	127 k	122 k	151 k
6	3	159 k	161 k	159 k	192 k
1	4	5.43 k	5.44 k	5.37 k	5.60 k
2	4	3.91 k	3.93 k	3.86 k	4.04 k
3	4	5.46 k	5.47 k	5.36 k	5.93 k
4	4	6.20 k	6.20 k	6.05 k	6.87 k
5	4	5.91 k	5.93 k	5.82 k	6.92 k
6	4	5.71 k	5.75 k	5.66 k	6.91 k
1	5	143 k	144 k	142 k	150 k
2	5	172 k	173 k	169 k	178 k
3	5	160 k	161 k	159 k	177 k
4	5	178 k	180 k	173 k	194 k
5	5	172 k	175 k	168 k	195 k
6	5	171 k	173 k	167 k	206 k
1	6	322 k	224 k	323 k	324 k
2	6	350 k	353 k	349 k	369 k
3	6	321 k	324 k	319 k	356 k
4	6	405 k	408 k	398 k	448 k
5	6	349 k	351 k	343 k	409 k
6	6	319 k	322 k	312 k	394 k
1	7	6.05 k	6.07 k	6.05 k	6.37 k
2	7	8.22 k	8.25 k	8.10 k	8.40 k
3	7	5.35 k	5.36 k	5.26 k	5.72 k
4	7	5.36 k	5.38 k	5.17 k	5.70 k
5	7	6.23 k	6.25 k	6.12 k	6.94 k
6	7	5.85 k	5.86 k	5.66 k	6.72 k

TABLE 9. STABILITY OF THICK FILM RESISTORS (CONT)

Ckt. No.	R No.	RESISTANCE IN OHMS As Fired	1 Hr at 400°C	1 Hr at 400° + 1 Hr at 500°C	1 Hr at 400°C +1 at 500°C +1-1/2 Hr at 600°C
1	8	64.6	64.7	64.5	64.3
2	8	72.0	72.1	71.8	71.7
3	8	60.0	60.0	57.9	60.2
4	8	74.0	74.1	73.4	74.2
5	8	72.8	72.9	72.4	73.9
6	8	56.7	56.8	56.2	57.5
1	9	34.6 k	34.8 k	34.6 k	39.0 k
2	9	28.0 k	28.0 k	27.5 k	30.6 k
3	9	29.3 k	29.5 k	28.8 k	33.2 k
4	9	31.1 k	31.2 k	30.3 k	37.0 k
5	9	26.5 k	26.5 k	25.6 k	32.7 k
6	9	32.5 k	32.7 k	31.7 k	41.4 k
1	10	51.2 M	51.7 M	51.6 M	52.0 M
2	10	46.0 M	46.5 M	46.0 M	45.0 M
3	10	43.4 M	44.0 M	43.3 M	43.5 M
4	10	44.5 M	45.3 M	44.2 M	45.5 M
5	10	44.4 M	45.0 M	44.0 M	46.4 M
6	10	52.6 M	53.7 M	52.2 M	55.5 M
1	11	19.8 k	19.8 k	19.8 k	21.0 k
2	11	19.3 k	19.4 k	19.1 k	20.0 k
3	11	19.1 k	19.2 k	18.8 k	20.3 k
4	11	18.4 k	18.5 k	18.1 k	20.1 k
5	11	18.0 k	18.0 k	17.8 k	20.6 k
6	11	18.6 k	18.6 k	18.5 k	22.1 k

TABLE 9. STABILITY OF THICK FILM RESISTORS (CONT)

Ckt. No.	R No.	RESISTANCE IN OHMS As Fired	1 Hr at 400°C	1 Hr at 400° + 1 Hr at 500°C	1 Hr at 400°C +1 at 500°C +1-1/2 Hr at 600°C
1	12	1.34 k	1.34 k	1.3 k	1.40 k
2	12	1.02 k	1.04 k	1.03 k	1.03 k
3	12	1.30 k	1.30 k	1.30 k	1.33 k
4	12	1.30 k	1.30 k	1.30 k	1.33 k
5	12	1.27 k	1.27 k	1.25 k	1.30 k
6	12	1.47 k	1.48 k	1.46 k	1.52 k
1	13	13.6 k	13.7 k	13.6 k	14.3 k
2	13	14.2 k	14.2 k	14.0 k	14.7 k
3	13	14.3 k	14.4 k	14.1 k	15.1 k
4	13	14.3 k	14.3 k	14.0 k	15.3 k
5	13	13.1 k	13.2 k	12.7 k	14.1 k
6	13	13.1 k	13.1 k	12.9 k	15.1 k
1	14	62.2	62.3	61.1	62.0
2	14	57.7	57.7	57.5	57.0
3	14	59.1	59.0	59.0	59.0
4	14	67.0	67.1	66.8	67.0
5	14	59.5	59.6	59.0	59.0
6	14	57.8	57.9	57.7	59.0

4.2.4 Substrates for microcircuit covers. Blank octagonal 96 percent alumina substrates, 0.020 inch thick, were employed. There are four laser scribed octagons on one substrate (see Figure 14). After thick film printing, these octagons become the microcircuit covers.

4.2.5 Thick film layout. The part of the TMXO circuit comprising the heater, heater control, and voltage regulator has

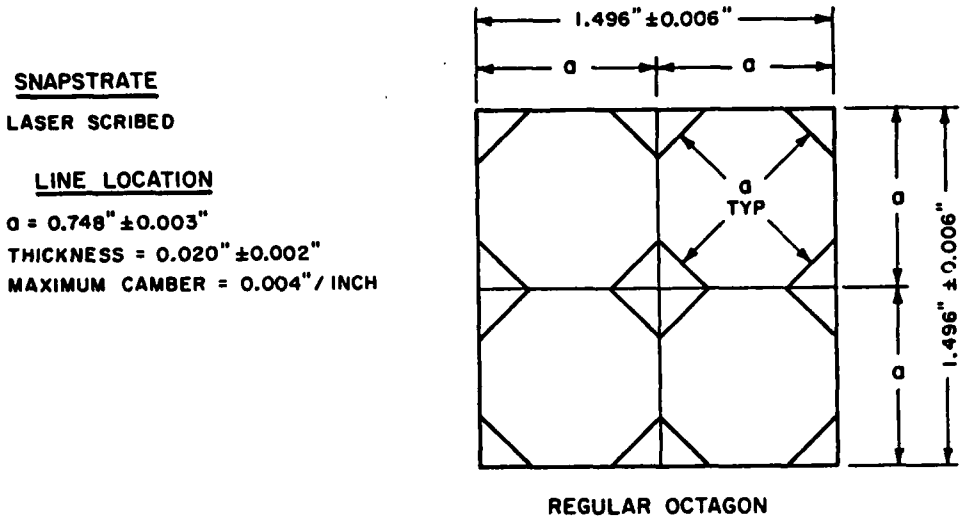

Figure 14. Octagonal substrate/snapstrate.

been laid out in a thick film hybrid topology. This half of the TMXO circuit has two inputs, +12 volts and ground, and two outputs, +7 volts and a terminal to the temperature control potentiometer. The layout of the temperature controller/voltage regulator substrate is shown in Figure 15. The oscillator/amplifier layout is shown in Figure 16.

5. MECHANICAL DESIGN

5.1 For phase 1.

5.1.1 General configuration. The TMXO package consists of a stainless steel cylinder having a square mounting flange. The cylinder diameter as well as the sides of the square flange is 1.25 inches. The unit is slightly over 1 inch high, excluding the electrical terminals which protrude from the bottom (flange side). A drawing of the package can be seen in Figure 17.

The package was sealed under vacuum with solder having composition of 70 percent tin, 18 percent lead, and 12 percent indium. This has a eutectic temperature of 162°C.

Q1,Q3 FAIR.

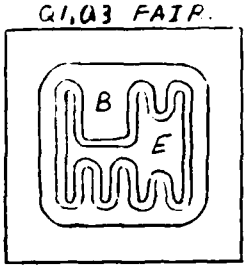

Q1,Q3 NAT.

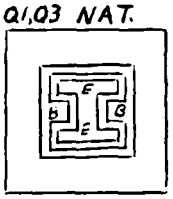

T.I.
Q1,Q3

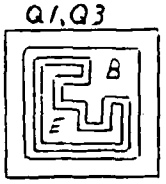

Q1,Q3 MOT.

Q2 NAT.

27x33

Q2, MOT.

24x24

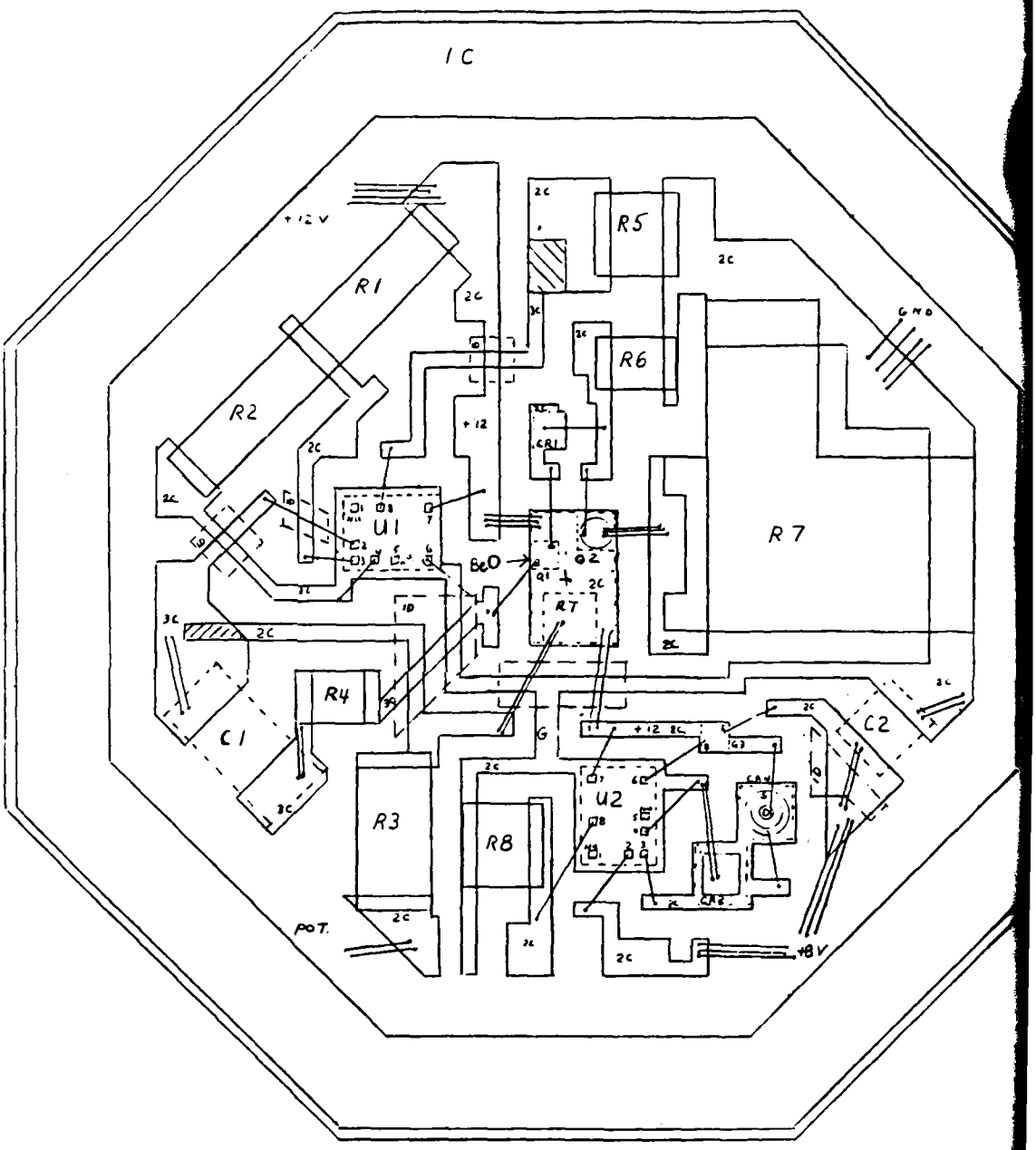

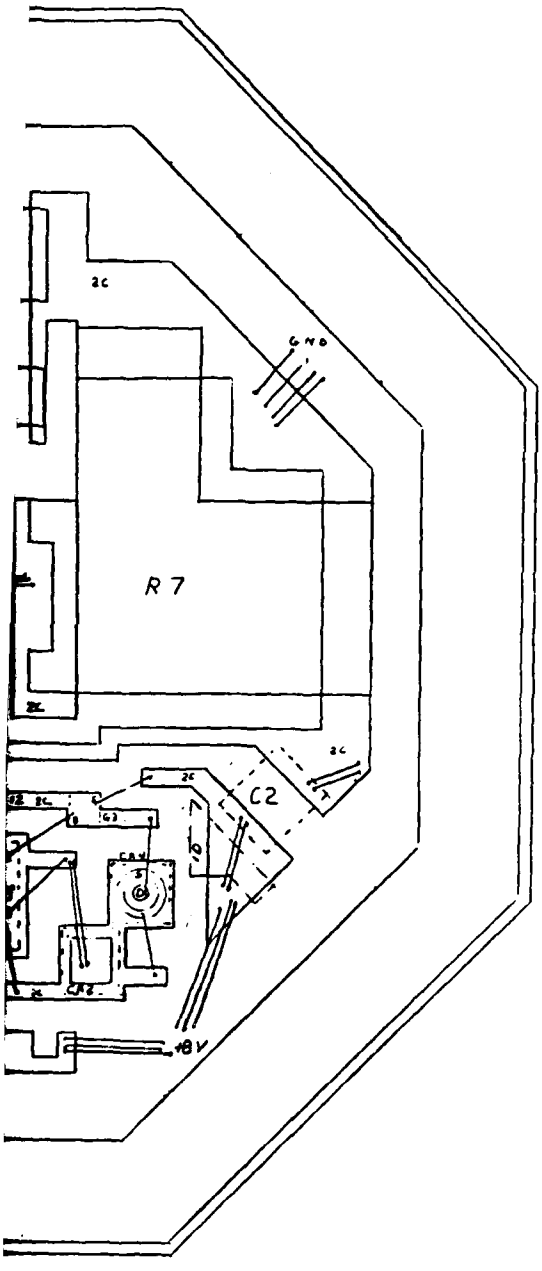

COMPONENT	TYPE	MAX SIZE	VENDOR
U1, U2	μA776	55 × 70	FAIR.
Q1, Q3	2N2222A	20 × 20	FAIR.
Q2	2N3734	25 × 25	MOT.
CR1	MZC5.1A5	25 × 25	MOT.
CR2	MZC8.2A5	25 × 25	MOT.
CR4	1NC5283	40 × 40	MOT.
C1	1.μF (TA.)	110 × 60	SPRAGUE
C2	.0068 μF	60 × 50	ANY
RT	44C65400	33 × 33	MIDW. COM.
BeO	—	60 × 90 × 15	—

COMPONENT	DESIGN	INK	Ω/□	PRINT	L	W
R1, R2	50KΩ	1441	10K	30KΩ	105	35
R3	RT-22KΩ	1441	10K	17KΩ	85	50
R4	82KΩ	1441/1451 = 1/3	50K	50KΩ	40	40
R5, R8	1MΩ	9678	1MEG	640KΩ	35	50
R6	470Ω	1421/1431 : 1/1	300	300Ω	35	35
R7	6.0Ω	9314/1011 : 1/4	8	4.5Ω	—	—
1C	—	[illegible]	<.003	—	—	—
2C, 3C	—	9260 (AU)	<.01	—	—	—
1D	—	9429	—	—	—	—

ALL RESISTORS ARE ± 5 %, EXCEPT R7, WHICH IS ± 10 %.

NOTES:

1. EUTECTICALLY BOND Q2 TO GOLD PLATED BeO.
2. ATTACH ALL CHIPS, EXCEPT Q2, WITH ABLEBOND 20-1.
3. PRINT IC ON BACK OF SUBSTRATE.
4. WIRE IS .001 "D. GOLD.
5. N.U = NOT USED.

Figure 15. Layout of temperature controller/voltage regulator.

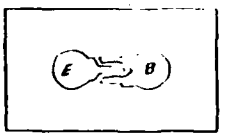

Q6, Q7
T.I.

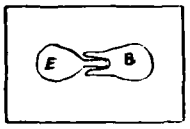

Q6, Q7
FAIRCHILD

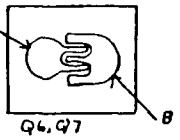

Q6, Q7
MOTOROLA

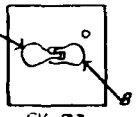

Q6, Q7
NATIONAL

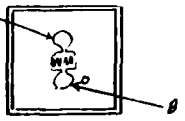

Q4, Q5
NATIONAL

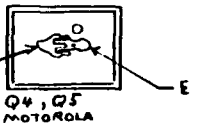

Q4, Q5
MOTOROLA

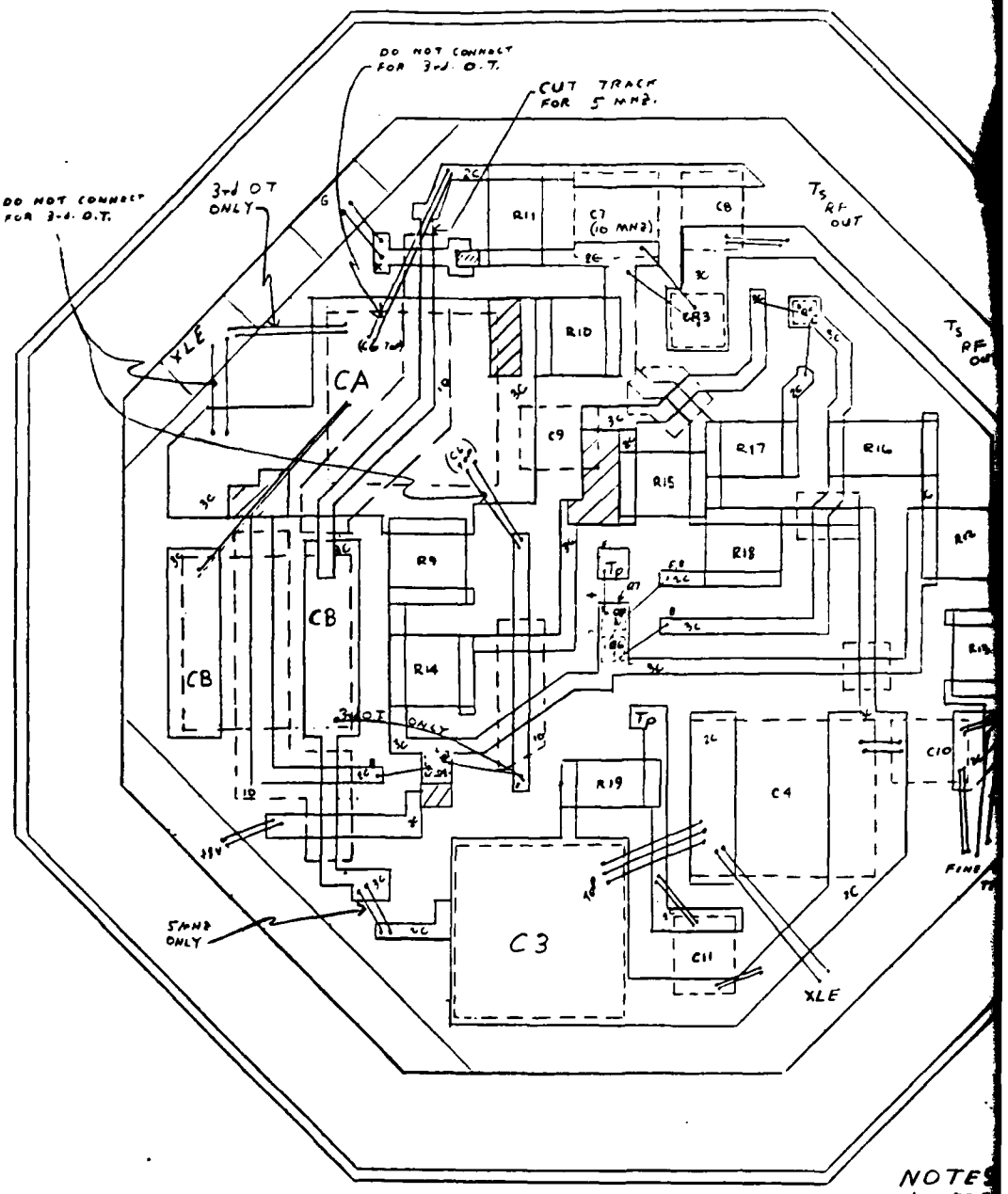

NOTES
1. FOR
2. FOR
3. FOR
4. ATT
5. WI
6. ATT
7. CONN
SEC

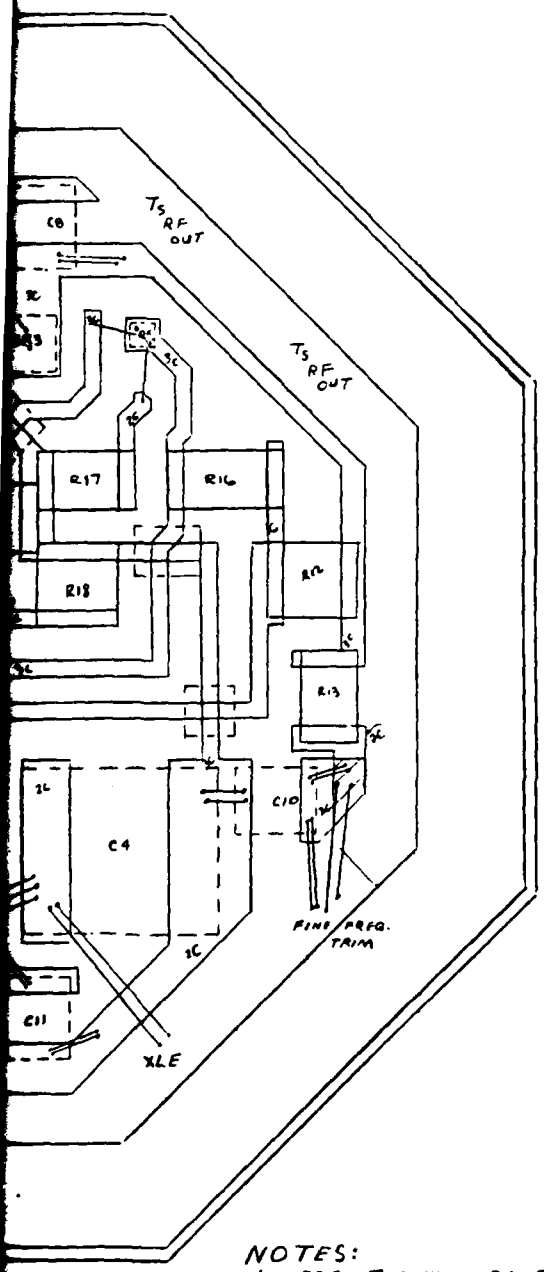

COMPONENT	TYPE	MAX SIZE	VENDOR
Q4, Q5	2N2857	20 X 20	MOT.
Q6, Q7	2N918	20 X 20	NAT., FAIR
CR3	INC5176A INC5182A*	40 X 40	MOT.
C3, S.B.T.	180-360 PF 100-180PF*	120x120 x120	ATC (100)
C4, TAPPED .2PF STEPS	2-57 PF VC2A	110x125	VITRAMON
C5 *±2%	1000 PF	120x120x120	ATC (100)
C6 ±2%	620 PF 470 PF* 300 PF**	120 x120 x 120	ATC (100)
C7 ±2%	180 PF 82 PF**	120x120x120 60x60x60	ATC (100)
C8 ±5%	220 PF	55 x45	ANY (NPO)
C9, C10 ±5%	.001μF	55 x45	ANY (BX)
C11 ±5%	.01μF	55 x45	ANY (BX)
L1*	1.6μH		BENDIX
T1	I.C. CORE CF-120-Q1, 60 PRI. 2 SEC.		BENDIX

* FOR 10 MHZ 3rd. O.T. ONLY

** FOR 10 MHZ FUNDEMENTAL ONLY

COMPONENT	DESIGN	INK	Ω/□	PRINT	L	W
R9	22KΩ	~~1441~~ 1431	20K	14KΩ	35	50
R10	100KΩ	1451	100K	70KΩ	35	50
R11 S.B.T.	40K-80KΩ	~~1441~~ 1451	20K	26KΩ	45	35
R12	420KΩ	~~1421~~ 1441	300K	262KΩ	35	40
R13	150KΩ	1451	100K	100KΩ	35	35
R14	120KΩ	1451	100K	78KΩ	35	45
R15	27KΩ	~~1441~~ 1451	20K	17KΩ	35	40
R16	2.2KΩ	1431	1K	1.4KΩ	50	35
R17	560Ω	~~1421~~ 1431	300	342Ω	40	35
R18	9.1KΩ	1441	10K	6KΩ	30	50
R19	2.2KΩ	1431	1K	1.5KΩ	45	30
1C	—	PT 994 # 1130 (DYNAMIC) PASTES	<.003	—	—	—
2C, 3C	—	9260	<.01	—	—	—
1D	—	9429	—	—	—	—

ALL RESISTORS ARE ±5%

NOTES:
1. FOR 5 MHZ, CA=C6=620 PF., CB=C7=180 PF
2. FOR 10 MHZ FUND., CA=C6=300 PF, CB= NOT USED
3. FOR 10 MHZ. 3rd. O.T., CA=C5=1000 PF, CB=C6=470 PF.
4. ATTACH ALL CAPACITORS AND ALL SEMICONDUTORS WITH ABLEBOND 20-1.
5. WIRE IS .001" D. GOLD.
6. ATTACH L1 AND T1 IN PLACE WITH ABLEBOND 71-2.
7. CONNECT PRIMARY OF T1 TO THE T_P PADS, THE SECONDARY TO T_1 TERMINALS.

Figure 16. Layout of oscillator/ amplifier.

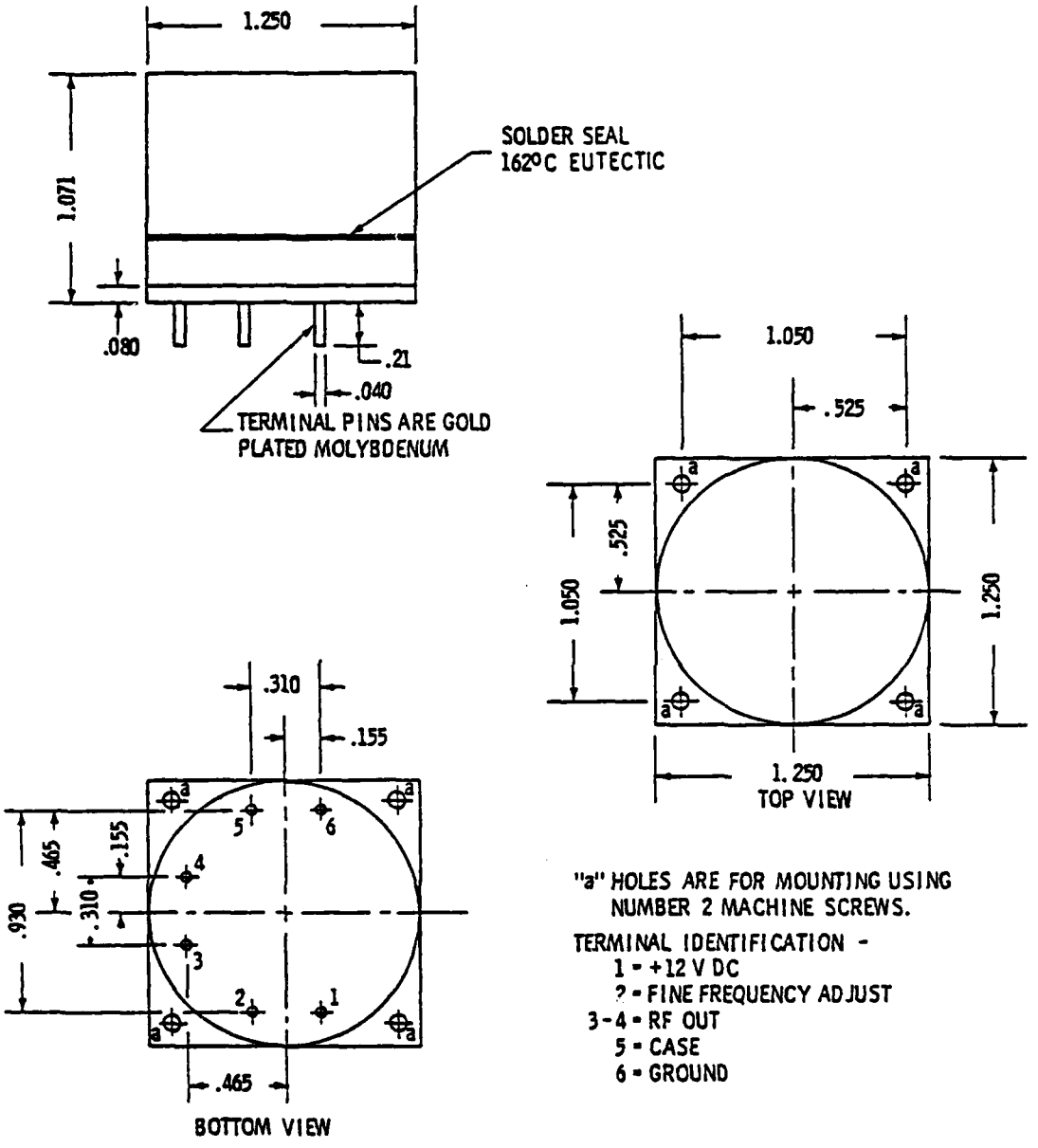

Figure 17. TMXO package outline.

5.1.2 TMXO header and cover design. The previous header had a threaded outside diameter onto which was screwed the cover. The vacuum-tight seal was made by compressing a copper gasket. Although this seal did not leak, the high torque required for gasket compression caused serious difficulties. The torque transferred a stress to the header, deforming the stainless steel flange, resulting in an air leak at one or more of the terminals. In addition to this problem, the two terminals located in the header recess (not accessible to the user) were of the glass/metal type, limiting maximum outgassing temperature to 230°C. The header is shown in Figure 18.

The header was redesigned, replacing the glass/metal terminals with the ceramic/metal type. The sealing means was changed from a gasket to a solder seal around the circumference. The cover was redesigned for the solder seal (see Figure 19).

The header and the cover are made out of 302 or 304 stainless steel. Although 303 stainless is easier to machine, it contains greater amounts of high vapor pressure elements which could produce some outgassing difficulties.

5.1.3 Crystal and crystal mount. The quartz crystal is an AT-cut, natural quartz with an upper turn temperature of 89°C $\pm$5°C. It is highly polished, plano- convex, having a frequency of 5.115 MHz $\pm$5 PPM into 100 pF at the upper turn temperature. The crystals were supplied by the vendor without any metallization. We deposited chromium-gold bonding pads and bonded the crystal to nickel-plated stainless steel clips by electroplating a low stress nickel. The crystal was then mounted in the nickel ring enclosure by welding a 0.010 inch nickel wire between the clips and the enclosure terminals. The details of this configuration are shown in Figures 20 and 21. The mounted crystals were returned to the crystal vendor for electrode deposition to frequency. We then completed the enclosure and sealed the unit in an atmosphere of 10 to 100 torr of nitrogen.

5.1.4 Sealing the crystal enclosure. The crystal enclosure consists of a ring and two cover plates, all made out of nickel.

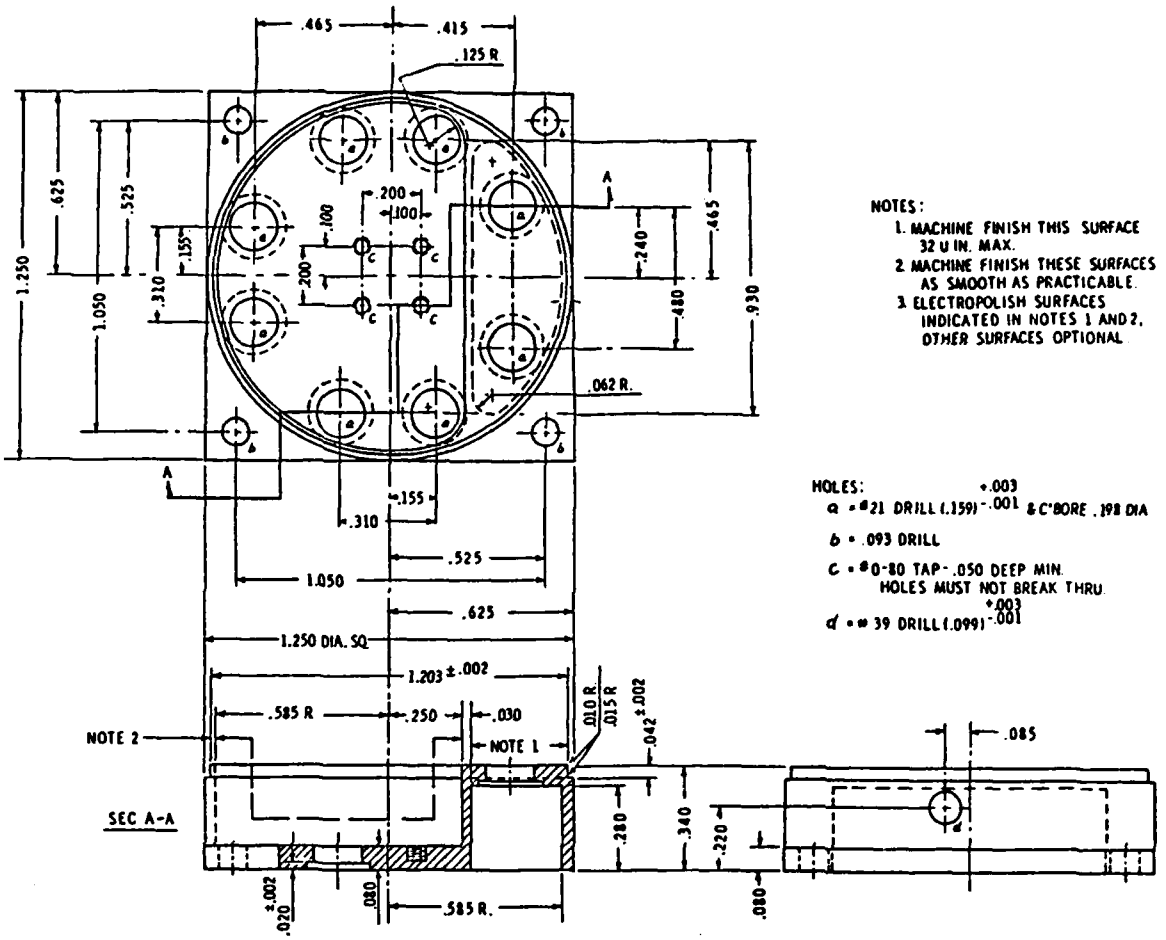

Figure 18. Machined header of TMXO.

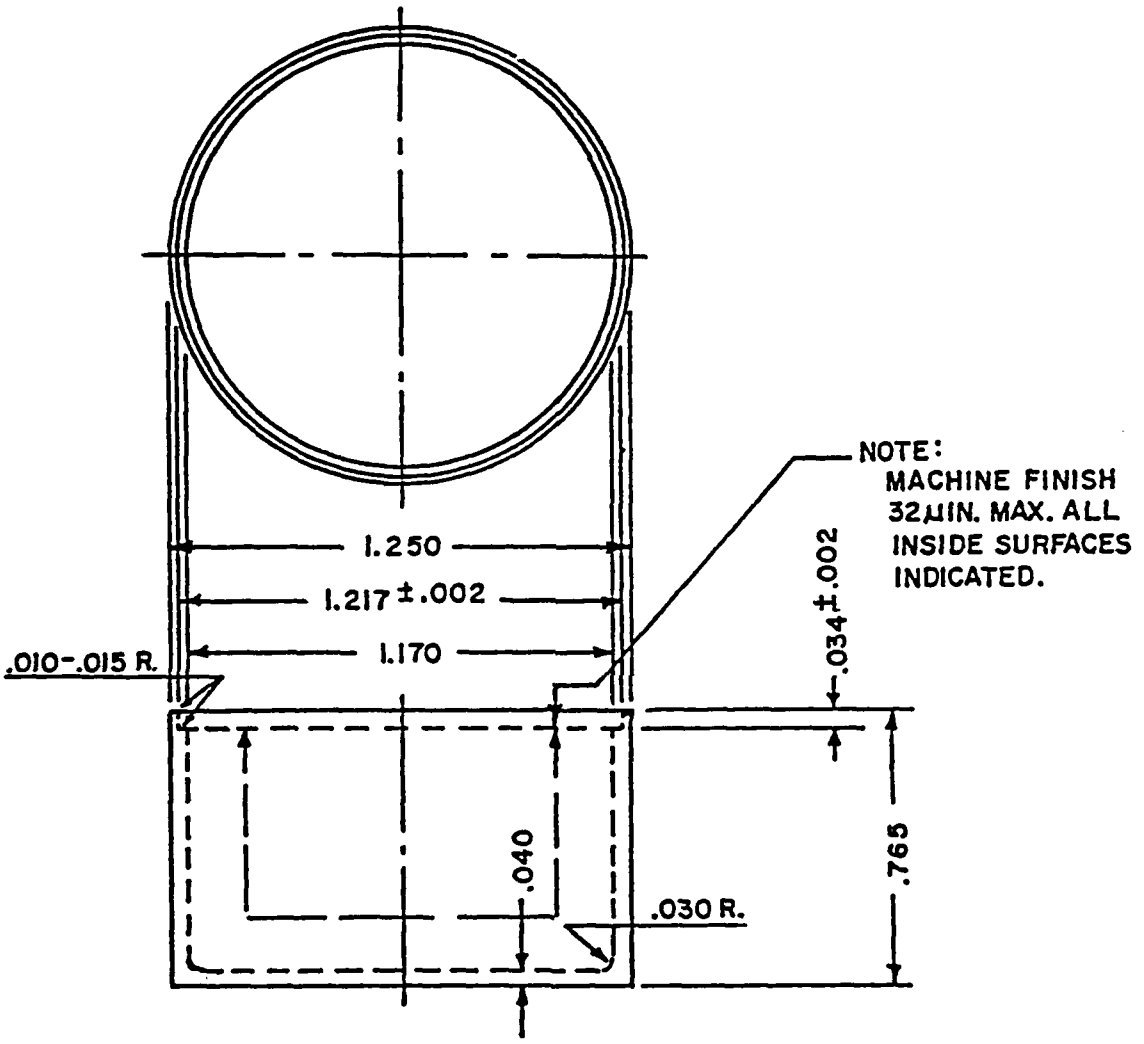

Figure 19. Cover of TMXO.

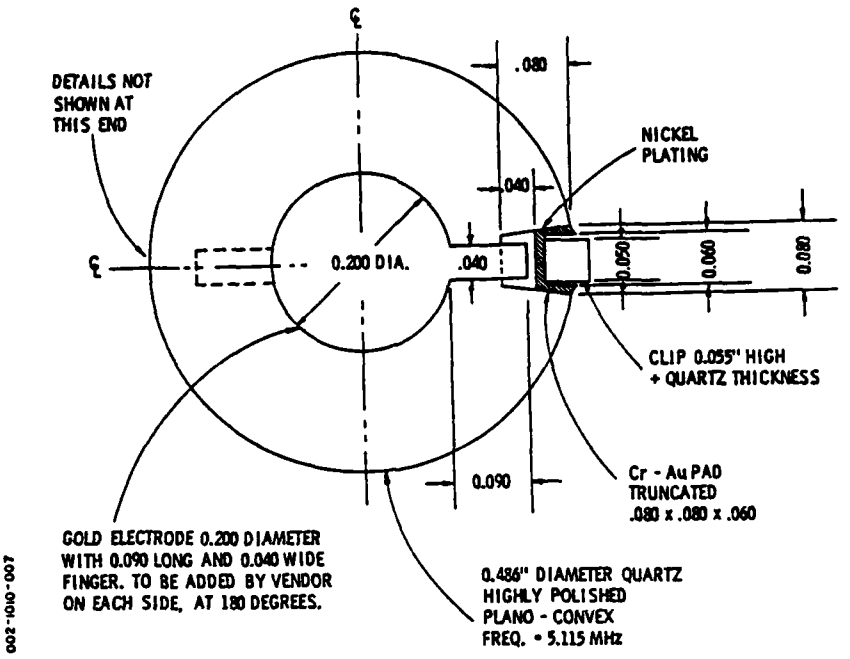

Figure 20. Bonding pads and electrode configuration on crystal.

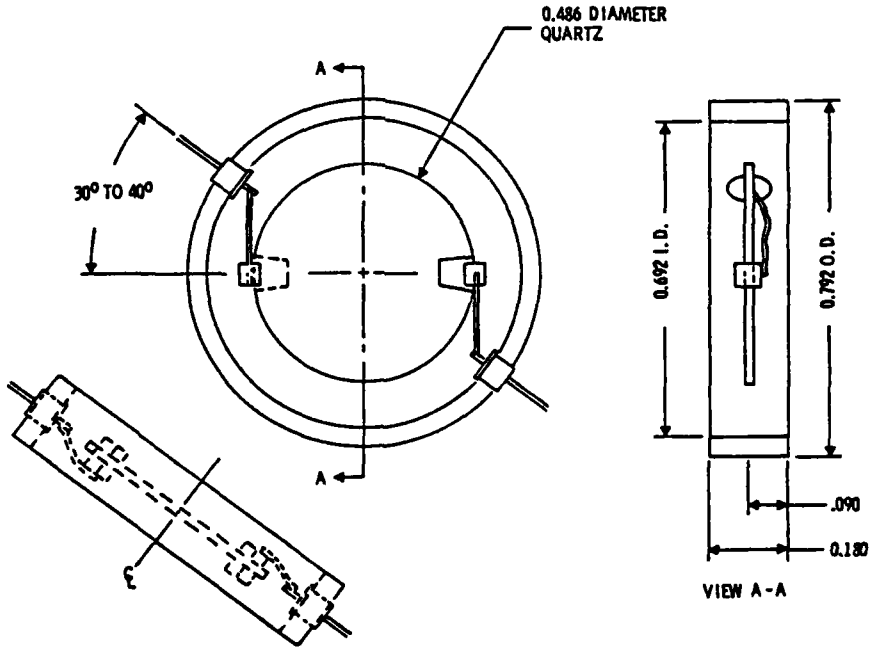

Figure 21. Mounting configuration.

The covers were soldered to the ring with a 96 percent tin, 4 percent silver solder (221°C), using a reflow technology. One of the covers had a small hole for evacuation and backfilling. The enclosure was outgassed at 5 x 10^{-6} torr for 40 hours at 150°C. It was then backfilled with nitrogen at about 10 torr. The hole was sealed by solder reflow (96 percent tin, 4 percent silver) using a remotely controlled soldering iron tip in a vacuum system. To prevent any solder from striking the crystal, a copper foil baffle had been previously welded over the hole on the inside of the cover. A fixture to seal five crystal enclosures in a single pump down was used.

5.1.5 Microcircuit enclosure. A special microcircuit enclosure, having radial leads and a particular thermal design, has been fabricated. The maximum dimension across the diagonal has been made equal to the maximum dimension of the ceramic crystal enclosure. A drawing for the microcircuit enclosure is shown in Figure 22.

5.1.6 Sealing the microcircuit enclosure. This enclosure was sealed in vacuum. The cover contained a hole and baffle similar to that of the crystal enclosure. The cover was soldered on, in air, using the 95 percent tin, 4 percent silver solder. The microcircuit enclosure was then placed in a vacuum chamber and outgassed at 5 x 10^{-6} torr for 40 hours at 150°C. The evacuation hole was then sealed in the same manner as the crystal enclosure.

5.1.7 Soldering the crystal and microcircuit enclosures together. The crystal and microcircuit enclosures are soldered together so that there will be good heat transfer from the heater to the crystal. The sides without the sealing holes are first tinned with solder. The enclosures are then held together, reheated until the solder flows, and then cooled. Because of the solder temperature problems discussed in paragraph 5.1.8, a special solder was employed for this purpose. This solder is 55

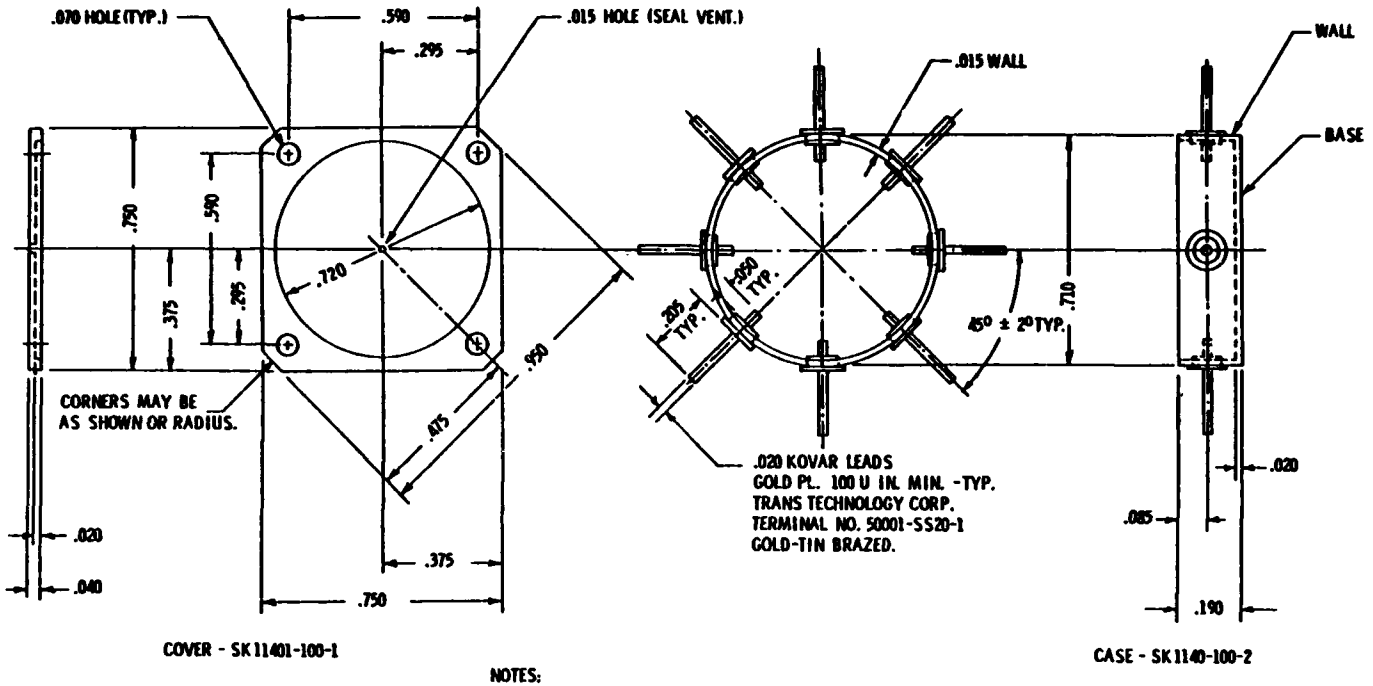

NOTES:

1. COVERS WILL BE SEALED TO CASES WITH 60-40 OR 63-37 SOLDER. AFTER SEALING, PACKAGE MUST BE CAPABLE OF PASSING HERMETIC SEAL TEST PER MIL-STD-883, METHOD 1014, TEST COND. A OR B, CALCULATED LEAK RATE = 1×10^{-8}.
2. CASES AND COVERS TO BE OFHC COPPER.
3. ALL METAL PARTS GOLD PLATED 100 U IN. THICK MIN.
4. ONE GLASS BEAD OF LEAD INSUL. TO BE A DISTINCTIVELY DIFFERENT COLOR.

Figure 22. Microcircuit enclosure.

percent tin, 45 percent lead. This is not a standard formulation; therefore, it was prepared in our laboratory from the pure elements. This solder has a solidus of 181°C and a liquidus of 205°C. At 185°C, this solder shows no flowing tendency even with added liquid flux.

5.1.8 Solder temperature problems. Improper selection of solders can lead to catastrophies. Such a catastrophe occurred when we originally chose the 60 percent tin, 40 percent lead solder (181°C eutectic) for joining the crystal enclosure to the microcircuit enclosure. When sealing the TMXO, this 181°C solder flowed, coating the microcircuit enclosure, and shorting out the oscillator. The TMXO was sealed with a 162°C eutectic, being heated to about 180°C to make the seal. The 181°C solder was changed as described in paragraph 5.1.7. The correct solders to use are indicated in Figure 23.

5.1.9 The pedestal. The thermal insulating pedestal is machined out of DuPont polyimide VESPEL-SP-1. Thermal resistance of this pedestal is 1,830°C/W. A drawing of the pedestal is shown in Figure 24.

5.1.10 Sealing the external package. Sealing the TMXO enclosure required special fixturing for vacuum sealing the stainless steel TMXO case. It consisted of the following:

(a) An upper oven to outgas the TMXO cap just prior to final sealing.

(b) A lower oven to outgas the TMXO header, pedestal, crystal package, and microcircuit package just prior to sealing. This lower oven will also supply the heat to seal the TMXO.

(c) A remote controlled mechanism, which lowers the TMXO cap from the upper oven to the lower oven. To ensure a better seal, it can also turn the cap during the solder reflow sealing.

(d) Several thermocouples to measure the temperature at various places.

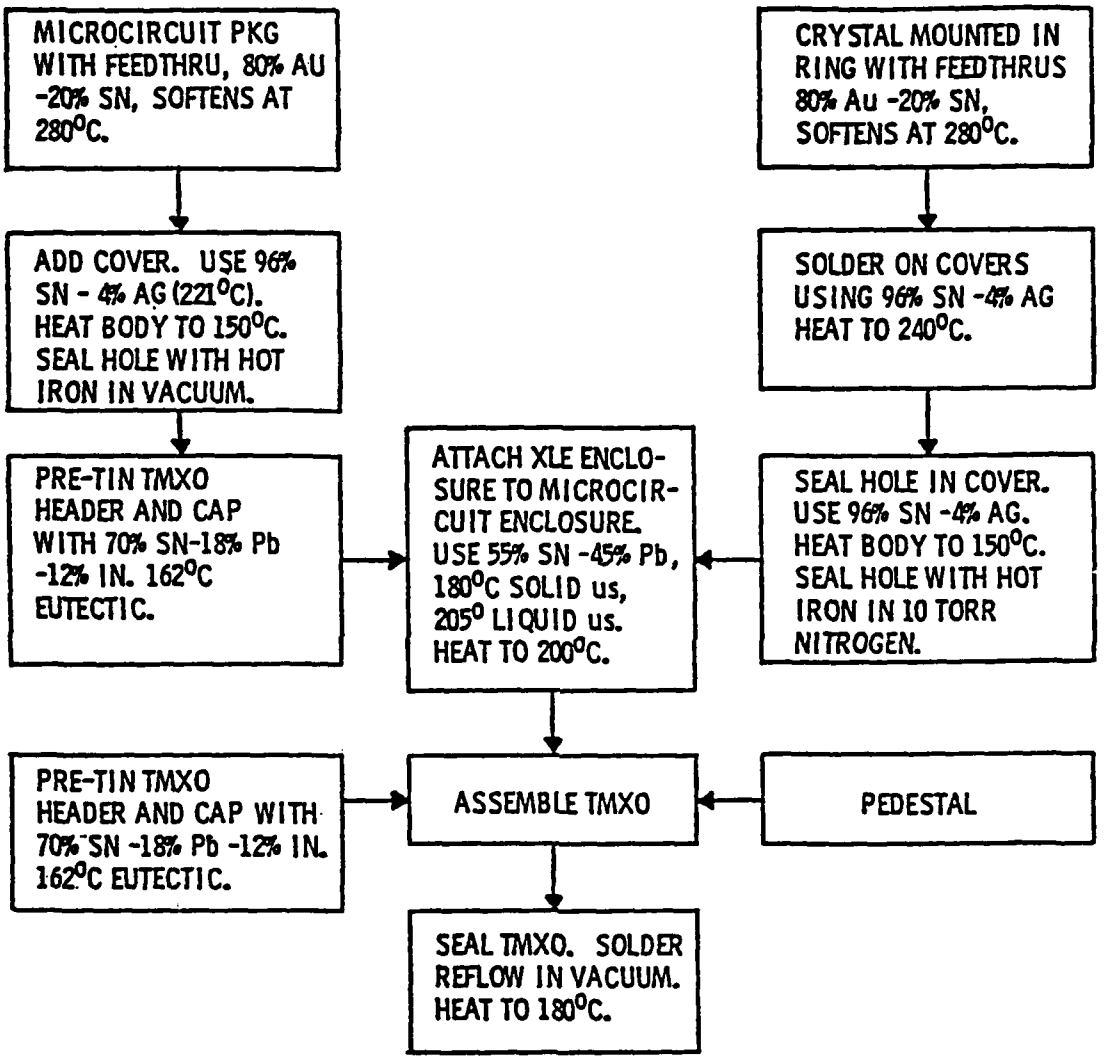

Figure 23. Solder flow chart.

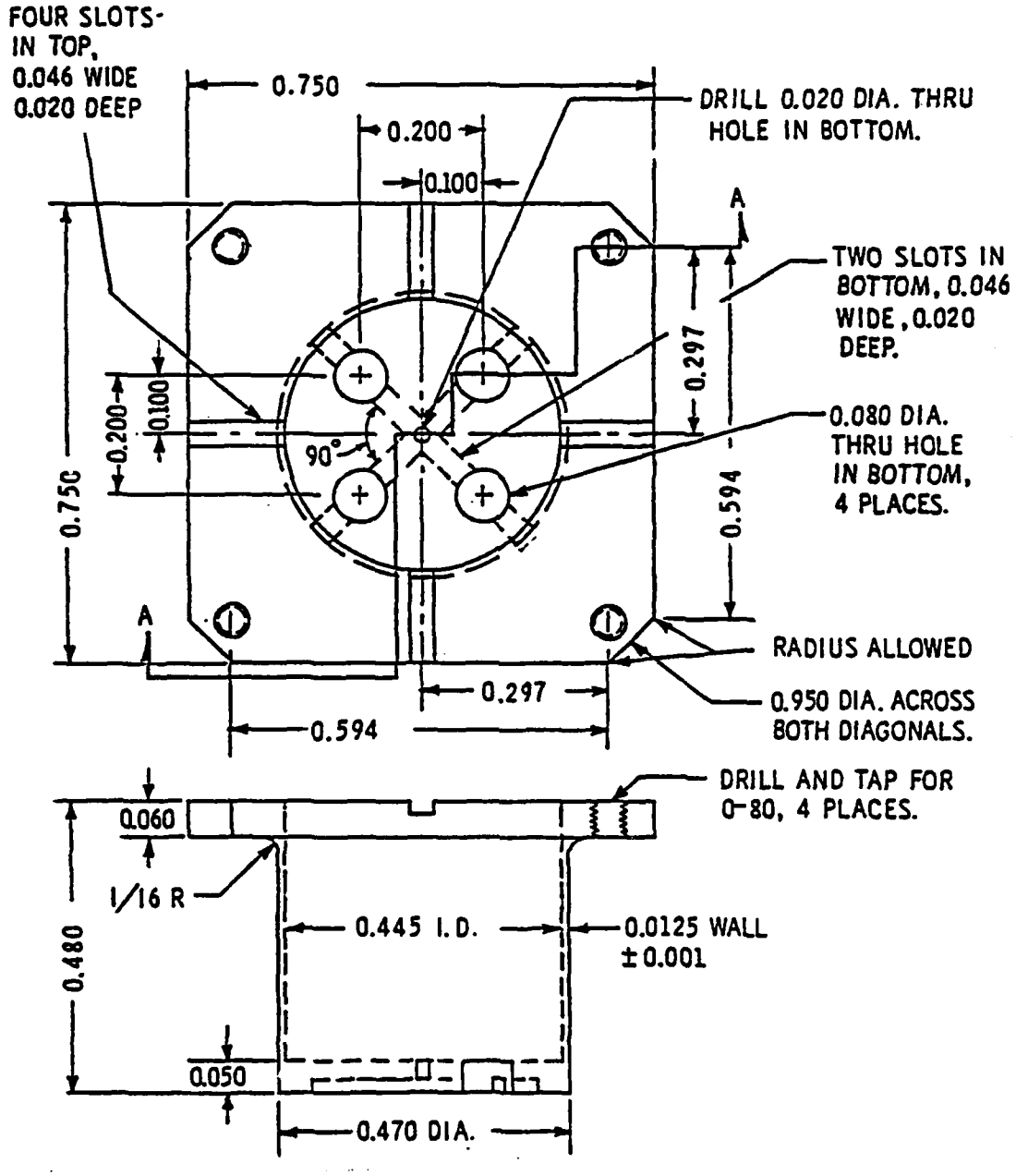

Figure 24. Pedestal for TMXO.

The header and cap are pretinned with the 162°C eutectic solder. The TMXO is then assembled, tested, and placed in the sealing fixtures in the vacuum chamber. The unit is tested under vacuum conditions and then shut off. The header assembly is outgassed in the lower oven at 150°C, and the cap is outgassed in the upper oven at 220°C. Both are at a pressure between 1×10^{-5} and 5×10^{-6} torr for 90 hours. After the 90 hours, the temperature of the header is raised to 175°C, the cap is lowered, and the seal is made. The temperature at the seal at this time is 180°C.

5.2 For phase 2.

5.2.1 Difference between phase 1 and phase 2. The three major mechanical differences between phase 1 and phase 2 were the crystal enclosure, the microcircuit package, and the addition of a thermally conductive heat spreading plate. The new crystal enclosure was ceramic and octagonal instead of circular and metallic, and is described in more detail in paragraph 5.2.2. The microcircuit enclosure was also changed from metal to ceramic (see paragraph 5.2.3). To enhance the spreading of heat from the microcircuit to the crystal, a copper plate was added between these two enclosures.

5.2.2 Crystal and crystal enclosure. The crystals in their enclosures were manufactured by GEND under a separate contract with ERADCOM. The enclosure consists of an octagonal shaped ceramic frame containing fired-in feedthroughs through four of its walls (see Figure 25). The ceramic cover for the enclosure are shown in Figure 26. To solder the crystal enclosure to the microcircuit enclosure, one side of the crystal enclosure had to be metallized. The other side of the crystal enclosure was also metallized to reduce radiation losses.

The metallization of the crystal enclosure consisted of thermally evaporating a thin film of chromium on the flat sides of the enclosure. The enclosure was then electroless nickel

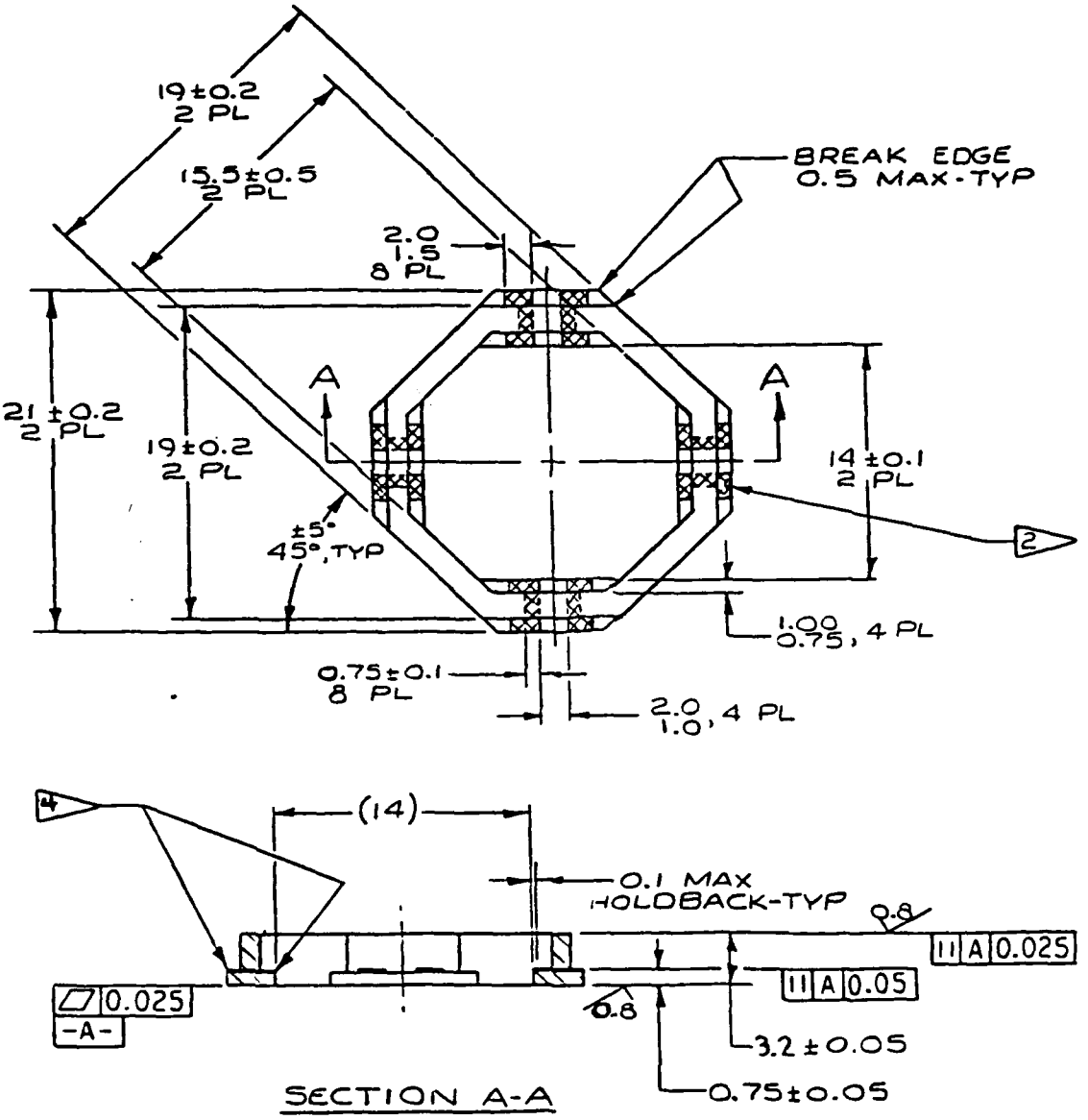

NOTES:

1. MATERIAL: 94% MINIMUM Al_2O_3 DENSE ALUMINA CERAMIC.
2. INDICATED AREA TO BE TUNGSTEN METALLIZED THRU FROM INSIDE TO OUTSIDE. CONFIGURATION OF FEEDTHRU PORTION OPTIONAL.
4. FOLLOWING FABRICATION AND PLATING. RESISTANCE OF FEEDTHRU TO BE LESS THAN .05 OHM.
5. UNLESS OTHERWISE SPECIFIED. ALL DIMENSIONS ARE IN MILLIMETRES.
6. ASSEMBLY SHALL BE LEAK CHECKED WITH EQUIPMENT CAPABLE OF DEJECTING LEAKS AS LOW AS 1×10^{-9} STD CC'S/SEC. ASSEMBLY SHALL SHOW NO INDICATION OF A LEAK.

Figure 25. Frame, crystal enclosure.

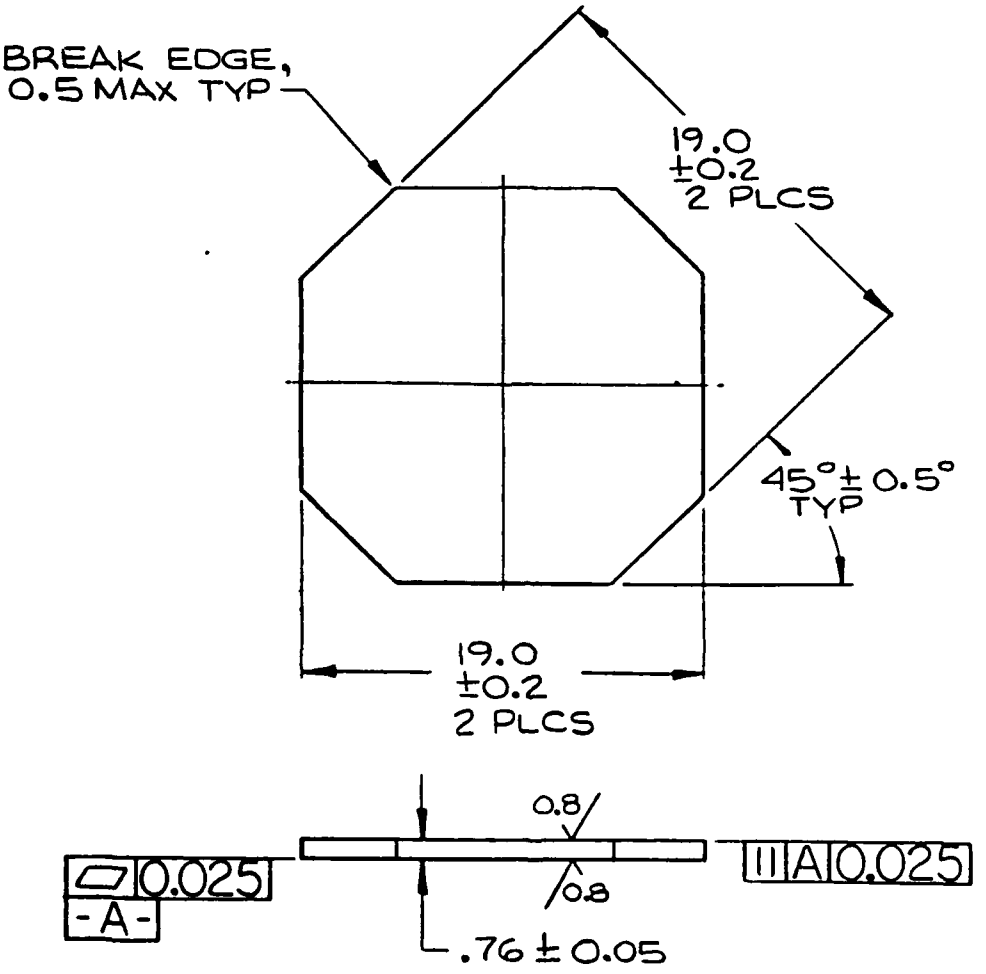

NOTES:

1. MATERIAL: 94% MINIMUM Al_2O_3 DENSE ALUMINA CERAMIC.
2. UNLESS OTHERWISE SPECIFIED. ALL DIMENSIONS ARE IN MILLIMETRES.

Figure 26. Cover, crystal enclosure.

plated, masking the enclosure sides and terminals. Crystal number 162 was tinned with 96 percent tin, 4 percent silver solder. The enclosure tinned very well.

The stability of crystal numbers 161, 162, 208, and 209 was remeasured after the metallization and compared with the stability before metallization. Stability measurements were made using a 10-second sampling time, and the frequency variation was recorded on strip chart, using the standard nonreactive test circuit. Comparison of the strip charts showed the following:

(a) Crystal number 161, stayed about the same.

(b) Crystal number 162, got a little better.

(c) Crystal number 208, stayed about the same.

(d) Crystal number 209, got a little worse.

The changes for better or worse were not large, less than 1 magnitude, that is, from 1×10^{-9} to 1×10^{-10} $\Delta F/F$.

TMXO serial number 209 was sealed at GEND and returned to Bendix. The unit was placed on a vibration table. The TMXO was turned on and the vibration table was vibrated in accordance with curve M, Method 514 of MIL-STD-810B. At 33 Hz, the TMXO failed, a large part had become loose inside the unit. The cover was carefully cut off, revealing that the crystal enclosure separated from the copper plate/microcircuit assembly. The attachment of the crystal enclosure was accomplished by the following steps:

(a) The crystal enclosure had a thin film of chromium vacuum deposited on the two flat ends.

(b) The ends were then electroless plated with nickel.

(c) The end which was to contact the microcircuit was then tinned with a soldering iron using 63/37 tin/lead solder.

(d) Both ends of the microcircuit, the copper plate (between the heater and the crystal) and the nickel plate (between the pedestal and the microcircuit) were tinned as in (c) above.

(e) The assembly was placed on a hot plate (at room temperature) in the following order: a 1/4 inch thick steel block, the nickel plate, microcircuit (oscillator down), copper plate, and crystal.

(f) The hot plate was turned on, and after several minutes the solder at the nickel plate reflowed. The tempera ture of the hot plate surface was maintained at 200°C, and 2 to 3 minutes later, the crystal enclosure/copper plate solder interface reflowed. The hot plate was turned off, and the assembly with the steel block was placed on a nonmetallic table.

In hindsight, the chromium/electroless nickel was a poor choice of metallization. Chromium oxidizes easily, forming a thin oxide layer to which the electroless nickel adheres poorly. Having the identical heater/oscillator microcircuit, the warmup with the new crystal can be compared with that of the old. The latter had a very slow warmup time, never overshooting, indicative of a poor thermal connection.

This problem of poor adhesion was solved by changing the metallization on the crystal enclosure from (a) vacuum deposited chromium, electroless nickel, 63/37 tin/lead solder to (b) sputtered chromium, sputtered copper, 63/37 tin/lead solder. TMXO number 209 was reassembled using crystal 227, which had the copper-chromium metallization. This TMXO was renumbered as 209/227. This unit was placed on the vibration table without its cover, and vibrated in accordance with curve M, Method 514 of MIL-STD-810B. The crystal unit remained adhered to the heater circuit during this environmental test, and afterwards the TMXO worked electrically.

5.2.3 Microcircuit enclosure. The microcircuit enclosure consists of two parts. Each part is a cup consisting of an octagonal wall and a flat bottom plate. The wall is similar to that described in the previous paragraph. The flat plate is an octagonal thick film substrate onto which parts are added to build a microcircuit. One cup contains the oscillator/amplifier circuit, while the other cup contains the heater/voltage regulator circuit.

Sealing the wall to the substrate plate was very difficult, and no satisfactory method to produce a hermetic seal was found.

Thermocompression bonding using a gold ring between the wall and the plate was unsuccessful. Low temperature brazing also did not work. High temperature brazing could not be used, as it would alter the thick film resistors already on the flat substrate plate. The maximum sealing temperature of this interface without damaging the resistors is about 600°C (see the thick film resistor stability data in section 4).

The sealing surfaces of all the ceramic microcircuit cups were electroless nickel plated, and then coated with solder. This was done prior to adding any microcircuit parts to the substrates. The solder is 96 percent tin, 4 percent silver, and melts at 220°C.

A soldering fixture for soldering the two ceramic cup shaped microcircuit halves was designed. The soldering was accomplished under vacuum, remotely controlled. The fixture consists of two parts. The bottom part holds one of the microcircuit halves and has eight axial heaters, one at each octagonal flat. The top part contains the other microcircuit half and is lowered into the bottom half for soldering.

5.2.4 Inside assembly techniques. The inside of the TMXO was assembled as shown in Figure 27. Electrical connections between the crystal and the circuit, and between the circuit and the header, are all welded wire. The kinds of wire used are:

(a) Between crystal and circuit: 0.005 inch diameter gold.

(b) Between circuit and header, power, and ground: 0.010 inch diameter nickel.

(c) Between circuit and header, all other connections: 0.0003 inch diameter palladium.

The [illegible]kel plate, soldered to the back of the oscillator circuit, had four mounting holes so that 0-80 screws could be screwed into the pedestal.

[illegible] Pedestal. The Vespel pedestal was redesigned. The [illegible] is shown as Figure 28. Changes included in this [illegible]

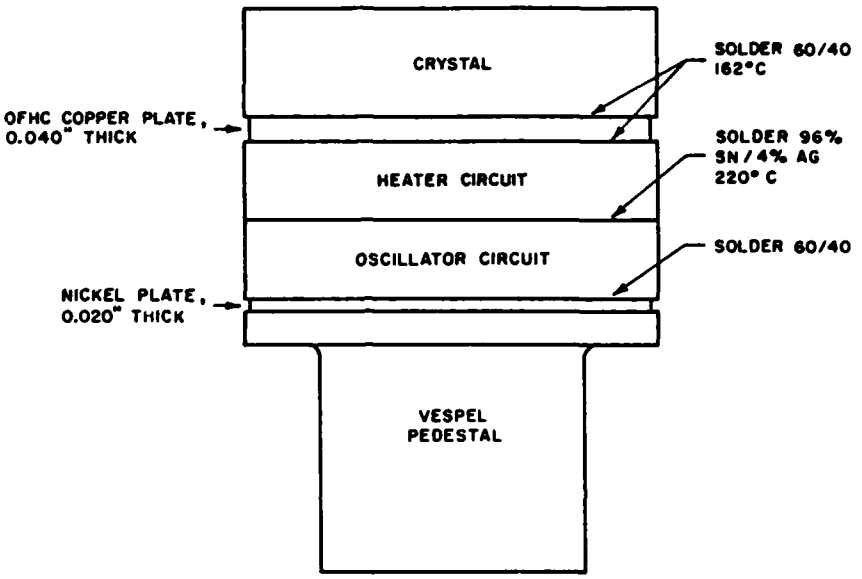

Figure 27. TMXO assembly through solder reflow.

(a) The four holes in the corners were moved out to accom modate the tolerance of the ceramic frame/substrate assembly.

(b) Two semicircular notches were put in one side of the pedestal to eliminate the interference due to the GEND header.

(c) To strengthen the pedestal, the radius was changed from 1/16 inch to 1/8 inch.

5.2.6 External package

Externally, the TMXO is a 1-1/4 inch diameter cylinder attached to a 1-1/4 inch square mounting header. Excluding the

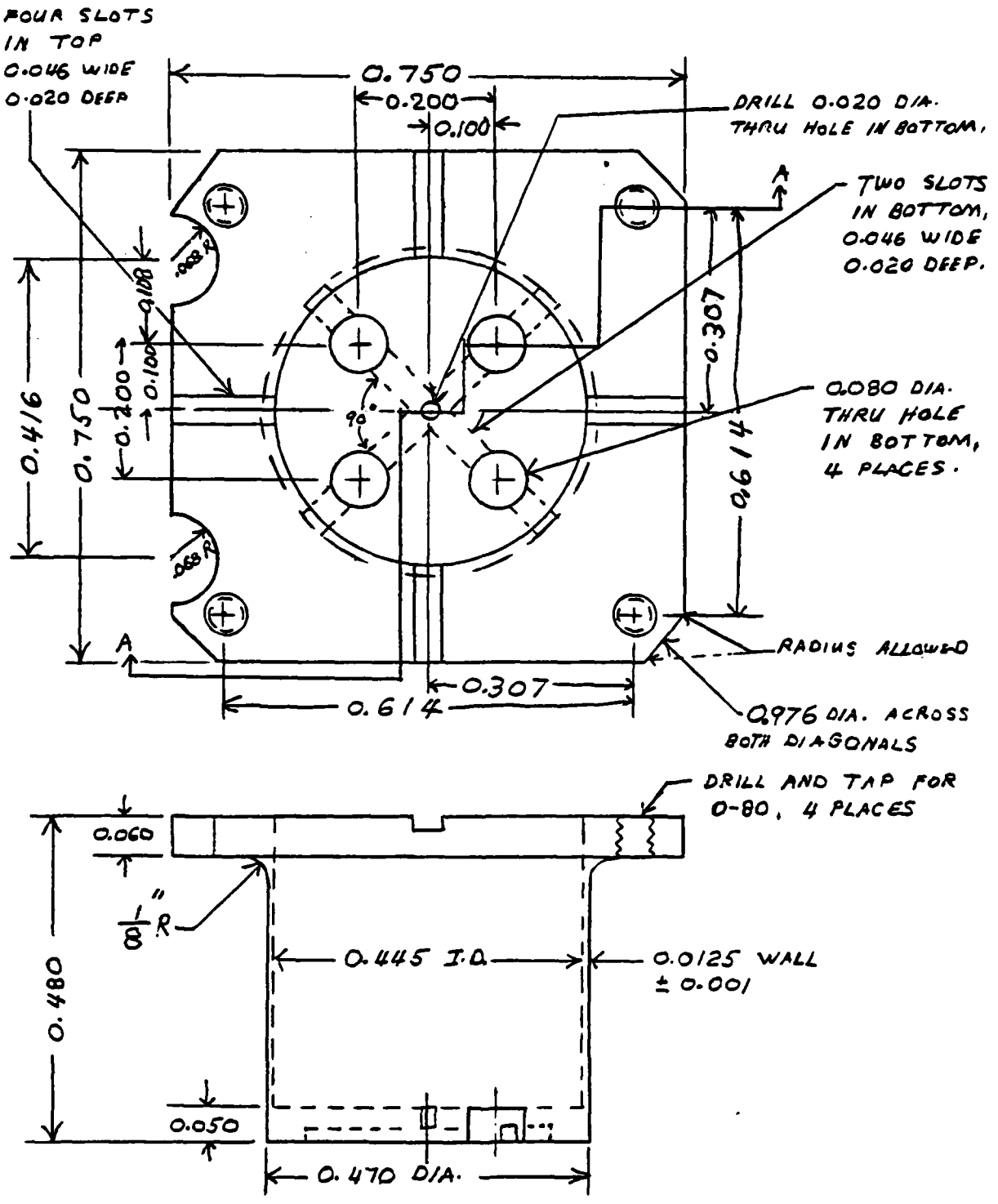

Figure 28. Pedestal.

pumping tubulation, the unit is 1-1/4 inches high. The header and cover are made out of kovar; the tubulation is copper. Figures 29 through 31 show details of the header. Figure 32 shows the bottom view electrical connections.

5.2.7 Sealing the external package. The cover with its tubulation was sealed to the header by electron beam welding. None of the sealed units leaked, and only one out of five welding operations damaged the electrical circuit.

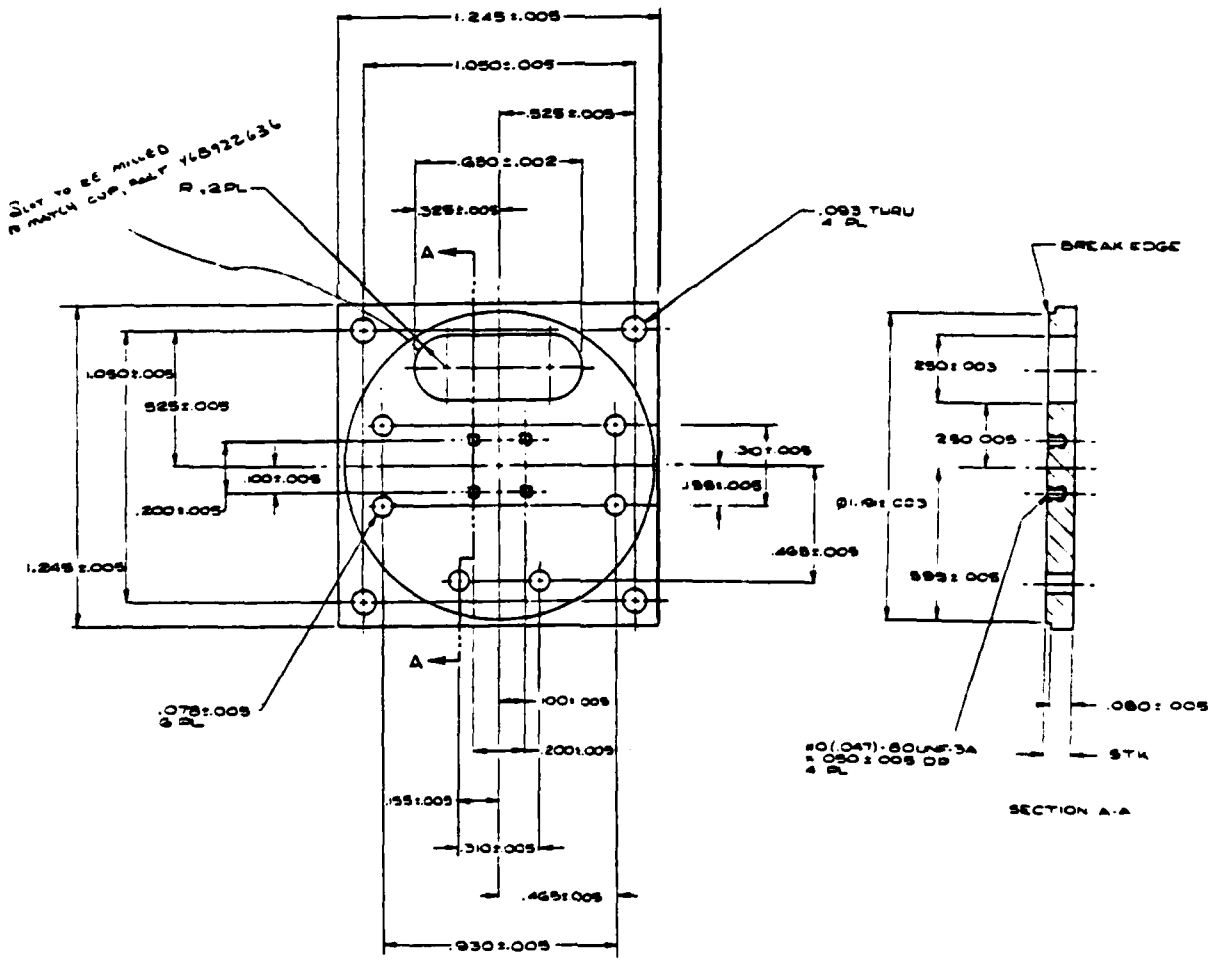

Figure 29. Header, TMXO.

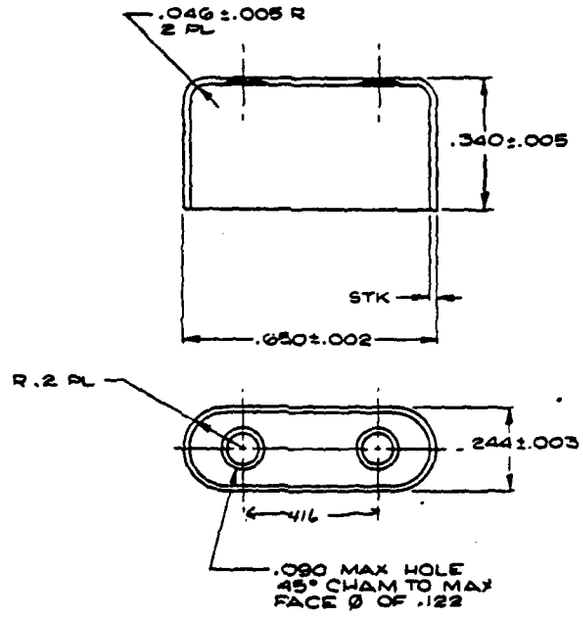

Figure 30. Cup for TMX0 header.

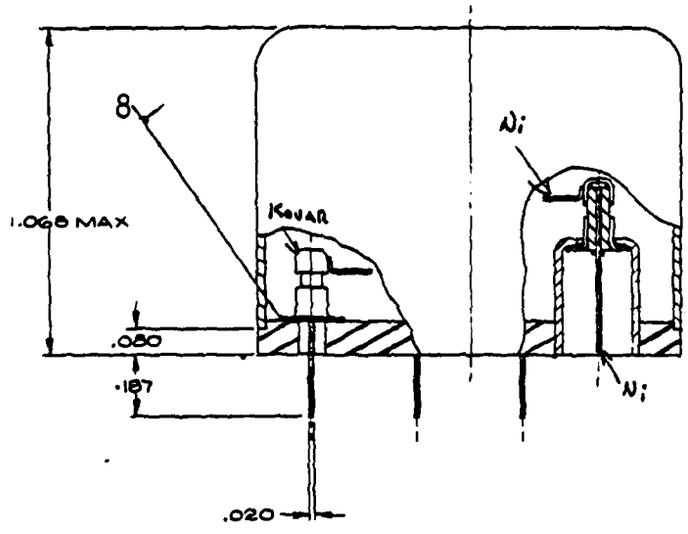

Figure 31. Header feedthrough details.

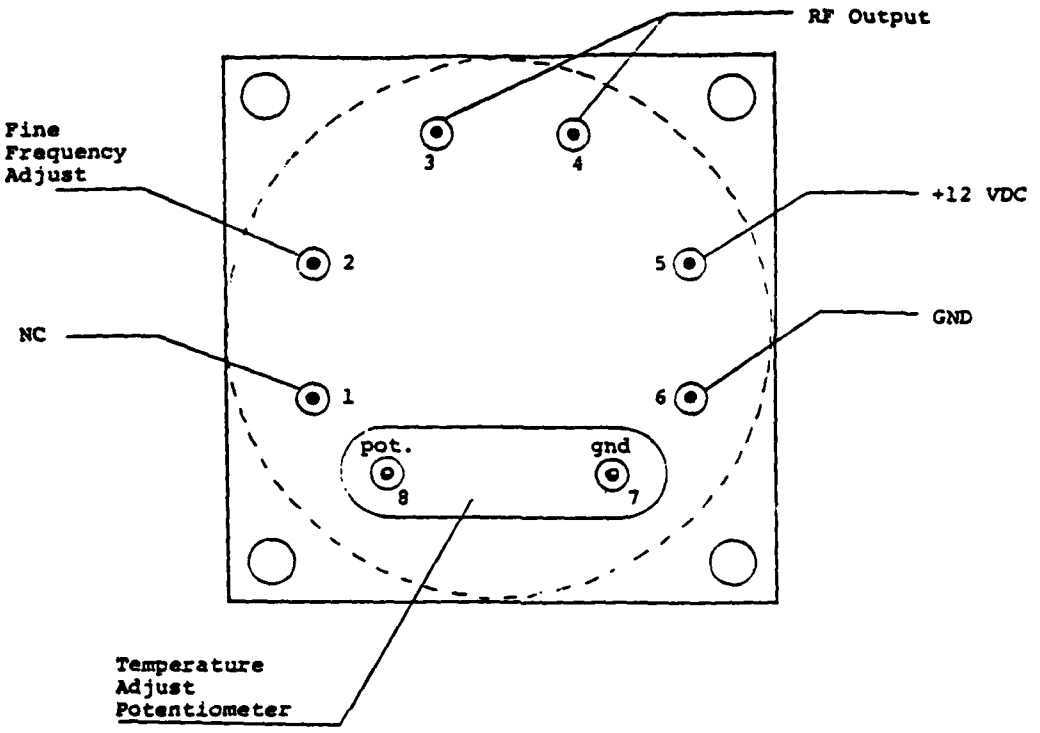

Figure 32. TMXO pinout, bottom view.

6. THE VACUUM PROBLEM

6.1 General. Maintaining a vacuum in the sealed TMXO has been a problem. To show no degradation in power or performance for a period of 1 year, the pressure inside the TMXO must remain below 5×10^{-4} torr. If the pressure increased to 1×10^{-3}, the performance would be adequate, except for a few percent increase in power.

The pressure increase in the TMXO is primarily due to outgassing inside or a leak in the TMXO package. A leak in the microcircuit or crystal enclosure is less of a problem, as the pressure inside these enclosures is 2 to 3 magnitudes below atmospheric pressure. Whatever the source of the residual gases, the getter welded in the TMXO cover will absorb some portion of

these gases. Our experiments indicate that the pumping speed of the getter is greater than 4×10^{-12} torr liter/s mg. The getter consists of 110 mg of active mass, for a pumping speed greater than $110 \times 4 \times 10^{-12} = 4.4 \times 10^{-10}$ torr liter/s.

Therefore, if the outgassing and leak rate can be kept below this level, the TMXO will maintain its vacuum.

6.2 Outgassing experiments. Being unable to maintain a good vacuum in the TMXO after sealing causes an increase in operating power. The problem is sometimes easily seen immediately after sealing by observing the value of the current into the TMXO. For example, before sealing, the current is about 14 mA. After sealing, the current rose in a couple of minutes to 20 mA, and in 2 hours to 60 mA.

In this particular phase 1 TMXO, the microcircuit and crystal enclosures had previously been exposed to three atmospheres of helium during the leak test procedure. The possibility existed that helium was leaking out of either the microcircuit or crystal enclosures, or both, when they were at their operating temperature of 89°C. To determine whether this helium was the cause of the pressure rise in the TMXO, the following experiment was performed. Both the crystal and microcircuit enclosures were opened and resealed under a vacuum of 5×10^{-6} torr. These units were not leak tested with helium. They were placed in the TMXO case and sealed. After sealing, the current rose as before, indicating that the helium was not the primary cause of the problem.

To systematically investigate the cause of the problem or to determine the relative contribution to the problem from each part of the TMXO, an experimental technique was initiated. The technique was to build a sensor which would indicate the pressure or thermal resistance of the gas inside the TMXO enclosure. Having such a sensor would enable investigating the parts of the TMXO separately. The sensor consisted of an O.F.H.C. copper plate, gold-plated, (or later a solid gold plate) onto which was soldered a heating resistor. A diode for measuring the temperature of the plate was eutectically bonded onto it. With a con-

stant 1 mA dc into the forward direction, the diode voltage was measured as a function of temperature. This gave an exact straight line relationship from 25°C to 100°C of 1.945 mV per °C. The typical diode drop is around 500 mV, and using a digital voltmeter, the measurement error is ±0.1 mV which equals ±0.05°C. A thermocouple was used to measure the temperature of the header.

Mounting the plate on the pedestal and supplying constant power to the resistor, the diode is used to measure the temperature of the plate. Knowing this temperature, the thermal resistance between the plate and header and the thermal resistance of the gas around the plate can be calculated for various experimental conditions.

The plate was mounted on a polyimide (Vespel SP-1) pedestal, both mounted in a TMXO header. Constant power was applied so that under high vacuum, the hot plate temperature was 89°C. A temperature pressure curve was run at this time. The TMXO cap (having a solder seal hole) was sealed to the header with a metal gasket. This assembly was leak tested to verify the gasket seal. The unit was placed in a vacuum chamber, pumped on for several hours and then sealed. Just after sealing, the temperature started to drop, indicating a pressure rise in the TMXO.

The above experiment indicates that the cause of the vacuum problem is related to the pedestal and/or the TMXO enclosure. The problem could be absorbed gases on the surface of all the materials.

To degass the TMXO just prior and during sealing, an oven was designed to heat the unit from the outside. The next experiment utilized this outgassing oven and a stainless steel pedestal (replacing the Vespel pedestal).

To enhance the sensitivity of the stainless steel pedestal, four 1/4-inch diameter holes were drilled in the side of the pedestal This raised its thermal resistance from 170° C/W to 340° C/W. The TMXO exclosure with this pedestal, and a 0.020-inch evacuation hole was outgassed at a pressure of 5×10^{-6} torr. The temperature at the top of the pedestal was 120°C, the outside of the enclosure being 100°C. The unit was sealed, the inside and

outside temperature being at 110°C. The temperature of the pedestal top was monitored as a function of time. The effective thermal resistance, the thermal resistance of the gas in the enclosure, and the pressure inside the enclosure was calculated for different times after sealing. Whereas previously, it took only 34 minutes for θ_g of the Vespel/TMXO, with no external outgassing oven, to reach a value or 1,100°C/W, the stainless steel pedestal/TMXO with the external outgassing took 160 hours to reach the same thermal resistance. Although this was an improvement of several magnitudes, it is not good enough for the TMXO requirement.

The stainless steel pedestal was removed from the TMXO enclosure. The evacuation hole in the TMXO cap was enlarged from 0.020-inch diameter ot 0.20-inch diameter. The cap, header, plug, and Vespel pedestal was cleaned and outgassed at 300°C for 6 hours at a pressure of 1×10^{-5} torr. The Vespel pedestal was then mounted in the TMXO enclosure, the pedestal and the enclosure inside not being touched by hand. The unit was outgassed and sealed in the same manner as in the stainless steel pedestal experiment. The maximum temperature reached was 160°C for the pedestal and 115°C for the outside of the enclosure. The case was sealed under this condition.

While still in the vacuum chamber, the sealing plug was then unsoldered. A different outgassing procedure was then initiated. The inside hot plate (on the Vespel) was turned off. The unit was heated from the outside to a temperature of 150°C. Both the pedestal and exclosure outside were at this temperature for about 6 hours. The outside degassing oven was turned off. When at 100°C, The unit was sealed. The hot plate inside was then turned on so the thermal resistance measurements could be taken.

Results of the outgassing/sealing experiments indicate the following:

(a) Degassing the TMXO enclosure at 150°C and sealing at 100°C is far superior to outgassing and sealing at 120°C having the inside hot plate on.

(b) The stainless steel pedestal outgasses much less than the Vespel. This is true, even though the Vespel was out gassed using the better procedure and with a larger evacuation hole.

(c) The degassing/sealing procedure needed appreciable improvement.

Additional experiments in sealing the TMXO enclosure, containing the stainless steel pedestal, were performed. No improvement over the previous experiments were obtained. After 3 to 4 days, the pressure in the TMXO enclosure leveled off to a value of about 2×10^{-2} torr, corresponding to a thermal resistance of the gas $900^{\circ}C/W$. In the Vespel case, the value is reached in hours instead of days.

These experiments indicate that the basic problem is not the Vespel, as was previously reported.

Knowing the pressure after 100 hours, one can calculate the outgassing rate.

$$\text{Outgassing Rate} = \frac{\Delta P \times \text{volume}}{\text{time}} = \frac{10^{-2} \text{ torr} \times 16 \text{ cm}^3}{100 \text{ hrs}}$$

$$= \frac{10^{-2} \text{ torr} \times 16 \times 10^{-3} \text{ liters}}{3.6 \times 10^{-5} \text{ s}}$$

$$= 4.45 \times 10^{-10} \frac{\text{torr liter}}{\text{s}}$$

Assuming an internal surface area of 45 cm^2, the outgassing rate per square cm is approximately 1×10^{-11} torr liter/second cm^2. In terms of standard cc atmospheres, this becomes 1.3×10^{-11} atmp. cc/sec cm^2. The literature* gives the following outgassing data with regard to stainless steel.

---

* P.A. Redhead, J.P. Hobson and E.V. Kornelson, "The Physical Basis of Ultrahigh Vacuum," Chapman and Hall (1968), pp 371-178.

Treatment	Outgassing Rate torr liter/sec cm^2
Vacuum baked at 570°K for 75 hours	1.5×10^{-12} at 20°C 3.9×10^{-11} at 105°C
Vacuum baked at 1270°K for 3 hours then at 630°K for 25 hours	1.3×10^{-14} at 20°C
One torr of hydrogen for 12 days, then pumped for 3 days at 300°C	5×10^{-12} at 20°C
Mechanically polished, degreased vacuum baked at 700°K for 4 hours	1×10^{-11} at 25°C
Mechanically polished, degreased, vacuum baked at 700°K for 16 hours	5×10^{-12} at 25°C
Mechanically polished, degreased, vacuum baked at 700°K for 450 hours	5×10^{-14} at 25°C
Machined part, vacuum brazed at 1300°K, vacuum baked at 700°K for 1 hour	2.5×10^{-12} at 25°C
Machined part, vacuum brazed at 1300°K, vacuum baked at 700°K for 4 hours	1.5×10^{-13} at 25°C

The above data indicate that a smaller outgassing rate than our present 1×10^{-11} torr liter/sec cm^2 can be achieved with the proper degassing treatment. The needed improvement is to extend the time to reach 10^{-2} torr from 100 hours to 10,000 hours. This translates to a desired net outgassing rate of 1×10^{-13} torr liter/sec cm^2.

The two glass-to-metal feedthroughs in the TMXO header have limited the outgassing temperature to 250°C (523°K). These feedthroughs were replaced with the ceramic type. The header being brazed at 1,300°K can then be vacuum baked at 750°K for 16 hours, resulting in an outgassing rate of less than 10^{-13}. The stainless steel cap also can be vacuum baked so as to get down to 10^{-13}. Because of the temperature limitations on the crystal and microcircuit enclosures, it is not known how good they can get.

Our present indication that the Vespel pedestal is all right has been supported by data from other companies who regularly use Kapton (a sheet form of polyamide) in vacuum applications. Instead of vacuum baking at 300°C for 6 hours, they vacuum bake at 350 to 400°C for several days.

A TMXO enclosure containing a stainless steel pedestal and a solid gold hot plate was outgassed and sealed. The header, containing two gold-tin soldered terminals, had a prebake outgas temperature of only 200°C. The other parts were outgassed at 400°C. Outgassing after assembly and immediately before sealing was for 38 hours at 150°C. The unit was allowed to cool to 92°C, and then the plug was soldered in the cap, sealing the unit.

The thermal resistance of this unit under vacuum was 350°C/W. At first glance, this small decrease would lead one to believe that the outgassing in this sealed unit is much less than that of the previous units. However, the heat loss due to convection is directly proportional to the area of the hot plate. The area of the solid gold plate was much less than the hot plate area in previous experiments. This accounts for the small decrease in the net thermal resistance. The thermal resistance of the air alone is very high (816°C/W). That is, if the pressure in the TMXO enclosure rose to atmospheric, the net thermal resistance would be 245°C/W. However, this unit was a little better than the others, probably due to the longer outgassing time at 150°C immediately before sealing.

The outgassing experiment described above was repeated; however, this time a continuous getter was added. The getter material was Ceralloy 400, manufactured by the Ronson Metals

Corporation. The purchased getter was in the form of a coated (both sides) 0.005 inch thick nickel foil. The coated strip was welded to the inside of the TMXO cap. The getter surface area was 11 cm^2.

As in the previous experiment, baking just prior to solder sealing was for 40 hours at 150°C. The solder seal was made after the TMXO was allowed to cool to between 90 and 100°C. The thermal resistance before sealing, but under a pumping vacuum of about 4×10^{-6}, was 350°C/W. Three hundred and fifty-six hours after sealing, the value was 346°C/W. The measurement error is about $\pm$5°C/W.

The outgassing rate inside the TMXO enclosure was previously calculated from experiments. This rate was 4.5×10^{-10} torr liter/s. The getter is keeping up with this rate, so that the pumping rate of the getter must be equal to or greater than $4.5 \times 10^{-10}/11 = 4 \times 10^{-11}$ torr liter/s cm^2. In terms of getter weight, there is from 10 to 20 mg/cm^2. Using 10 mg/cm^2, our getter had a weight of 110 mg. This gives a pumping rate of $4.5 \times 10^{-10}/110 = 4 \times 10^{-12}$ torr liter/s mg.

The length of time which the vacuum can be maintained can, at the present, only be calculated. Gettering capacity for this getter varies with the gas. The capacity for nitrogen is one of the lowest, having a value of 16×10^{-3} torr liter/mg. Assuming a pesimistic gettering capacity of 10^{-2} torr liter/mg, and having 110 mg available, gives a capacity inside the TMXO of 1.1 torr liters. If we divide this gettering capacity by the outgassing rate, 1.1 torr liters/4.5×10^{-10} torr liter/s, we arrive at a lifetime of 2.45×10^9 s. This corresponds to 77.5 years, a year having 3.15×10^7 seconds.

This calculation shows that the getter has sufficient capacity for an outgassing rate 10 times greater than that observed in the TMXO enclosure. This safety factor may be needed, as the pedestal, crystal, and microcircuit packages will certainly contribute additional outgassing.

The above vacuum-sealing-outgassing experiment, to evaluate the TMXO enclosure and getter, has been terminated after 800

hours. The unit exhibited no noticeable decrease in vacuum. This getter is doing an excellent job.

Experiments with the stainless steel pedestal in a stainless steel TMXO package have shown that the outgassing is below the getter's pumping speed (greater than 4.4×10^{-10} torr liter/s). The pedestal and cap was outgassed for 96 hours at 400°C. The header was outgassed at 200°C for 96 hours. Just prior to sealing, the assembly was outgassed 40 hours at 150°C.

A similar experiment with a Vespel pedestal resulted in a pressure rise in the TMXO package. A small leak in the TMXO package as well as insufficient outgassing of the pedestal was probably the cause. The pedestal had previously been outgassed as follows:

(a) 3 hours at 300°C in vacuum

(b) 24 hours at 350°C in air

(c) 40 hours at 400°C in vacuum.

Outgassing temperature of the microcircuit/crystal assembly is limited to 160°C because of construction materials.

6.3 Electropolishing. The outgassing of the TMXO enclosure is proportional to the enclosure's inside surface area. To decrease this surface area, a procedure was developed to electropolish the stainless steel enclosure. The chemical composition (by weights of the solution) was:

(a) 56 percent phosphoric acid

(b) 12 percent chromic acid

(c) 32 percent water.

The temperature of this solution is 100°C $\pm$5°C, and the current density is 2.5 $\pm$0.5 A/inch^2. The electropolishing time can vary from 2 to 10 minutes depending upon the shape of the cathode and the cathode to anode distance. The above process produces a very shiny surface.

6.4 Leaks in the TMXO package. The TMXO header contains eight metal/ceramic feedthroughs. This type of feedthrough did not leak when previously used. They had been vacuum brazed t

AD-A100 374 BENDIX CORP BALTIMORE MD COMMUNICATIONS DIV F/G 9/1
TACTICAL MINIATURE CRYSTAL OSCILLATOR.(U)
APR 81 H M GREENHOUSE, R L MCGILL, W FEFEL DAAB07-75-C-1327
UNCLASSIFIED BCD-FR-81-001 DELET-TR-75-1327-F NL

2 OF 2
AD A
100374

END
DATE FILMED
7-81
DTIC

hours. The unit exhibited no noticeable decrease in vacuum. This getter is doing an excellent job.

Experiments with the stainless steel pedestal in a stainless steel TMXO package have shown that the outgassing is below the getter's pumping speed (greater than 4.4×10^{-10} torr liter/s). The pedestal and cap was outgassed for 96 hours at 400°C. The header was outgassed at 200°C for 96 hours. Just prior to sealing, the assembly was outgassed 40 hours at 150°C.

A similar experiment with a Vespel pedestal resulted in a pressure rise in the TMXO package. A small leak in the TMXO package as well as insufficient outgassing of the pedestal was probably the cause. The pedestal had previously been outgassed as follows:

(a) 3 hours at 300°C in vacuum
(b) 24 hours at 350°C in air
(c) 40 hours at 400°C in vacuum.

Outgassing temperature of the microcircuit/crystal assembly is limited to 160°C because of construction materials.

6.3 Electropolishing. The outgassing of the TMXO enclosure is proportional to the enclosure's inside surface area. To decrease this surface area, a procedure was developed to electropolish the stainless steel enclosure. The chemical composition (by weights of the solution) was:

(a) 56 percent phosphoric acid
(b) 12 percent chromic acid
(c) 32 percent water.

The temperature of this solution is 100°C $\pm$5°C, and the current density is 2.5 $\pm$0.5 A/inch^2. The electropolishing time can vary from 2 to 10 minutes depending upon the shape of the cathode and the cathode to anode distance. The above process produces a very shiny surface.

6.4 Leaks in the TMXO package. The TMXO header contains eight metal/ceramic feedthroughs. This type of feedthrough did not leak when previously used. They had been vacuum brazed by

the ECOM laboratory. In the present program, the brazing was done by a commercial company, in an argon atmosphere.

All feedthroughs were leak tested prior to sending them and the headers out for brazing. When the brazed parts were returned, the header was leak tested. A small percentage of the feedthroughs had small leaks. The headers were then vacuum outgassed at 400°C for 100 hours. The small leaks became larger, and new small leaks were found.

Most of the leaks were at the ceramic-pin interface and were probably due to rapid cooling after brazing. Insufficient time did not allow procuring new feedthroughs and reprocessing the headers. The leaks were repaired using 80 percent gold, 20 percent tin solder (280°C). After this repair, a few small leaks (between 2×10^{-9} and 2×10^{-10} std cc/s) were found. These were eliminated by sealing with epoxy on the outside of the header. The possibility of the epoxy contributing to the outgassing inside the TMXO is almost nonexistent. The surface area of the epoxy exposed through such a small leak is infinitesimal. However, permeation through the epoxy could be a problem.

6.5 Procedure followed in the deliverable models, phase 1. The various solder temperatures used in the fabrication of the TMXO, followed the solder flow chart shown in Figure 21.

The outgassing schedules for the various parts and assemblies were as follows.

(a) TMXO cover: Outgassed at 1×10^{-5} torr at 480°C for 96 hours. Electropolish. Outgass at 1×10^{-5} torr at 400°C for 96 hours.

(b) TMXO header: Before feedthroughs, outgassed at 1×10^{-5} torr at 480°C for 96 hours. Electropolish. Braze in feedthroughs. Outgas at 1×10^{-5} torr at 400°C for 96 hours. Repair leaks with 80 percent gold, 20 percent tin solder. Complete repair with epoxy. Outgas 100 hours at 1×10^{-5} torr and 180°C.

(c) Vespel pedestal: Bake in air at 350°C for 48 hours. Outgas at 1×10^{-5} torr for 96 hours at 400°C.

(d) Microcircuit package (without the microcircuit): Outgas at 1 x 10^{-5} torr for 96 hours at 180°C.

(e) Crystal enclosure ring and covers: Outgas at 1 x 10^{-5} torr for 96 hours at 480°C.

(f) TMXO assembly just prior to sealing: Vacuum outgas at 1 x 10^{-5} torr at 150°C for 90 hours.

6.6 Procedure followed in the deliverable models, phase 2. The microcircuit's physical design for the phase 2 models was greatly different from the design of the phase 1 models (see paragraph 5.2 of this report). The inability to seal the microcircuit enclosure made any outgassing procedure futile. Special outgassing procedures were therefore not initiated, and the TMXOs were sealed with a tubulation so that the units could be dynamically pumped during evaluation.

7. PERFORMANCE OF DELIVERED MODELS, PHASE 1

7.1 General description of the models. The Tactical Miniature Crystal Oscillator (TMXO) models have been fabricated in accordance with the electrical schematic shown in Figure 1. The mechanical configuration can be seen in Figure 15. The electrical terminals are also indicated in this figure.

7.2 Test equipment.

7.2.1 Test setups. In the evaluation of the TMXO's, three test equipment setups have been used. These are identified as test setup numbers 1, 2, and 3 and are shown in Figures 33, 34, and 35. The particular test setup used to measure a particular performance parameter is specified under that particular performance parameter.

7.2.2 Test equipment calibration. Only calibrated test equipment has been used. Test equipment is calibrated and maintained in accordance with MIL-C-45662.

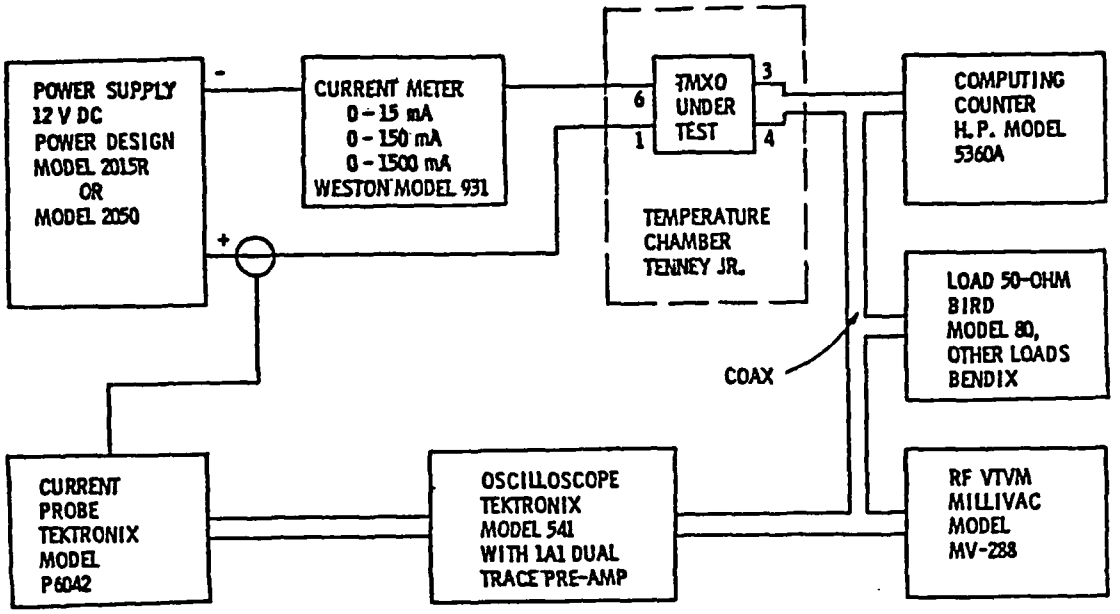

Figure 33. Test setup number 1.

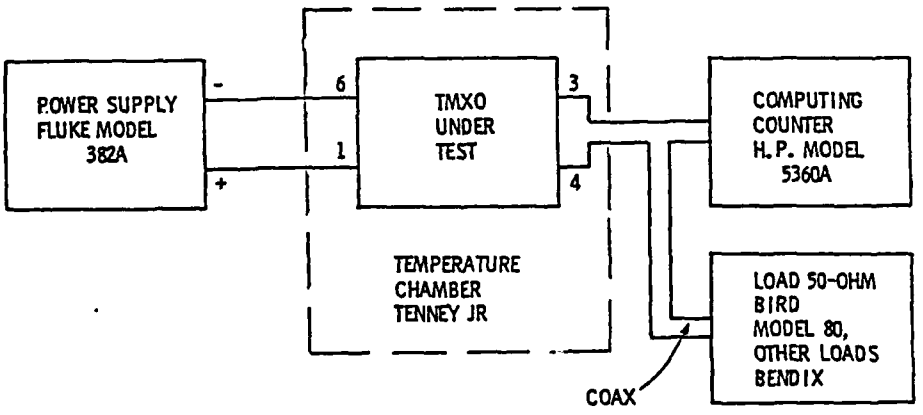

Figure 34. Test setup number 2.

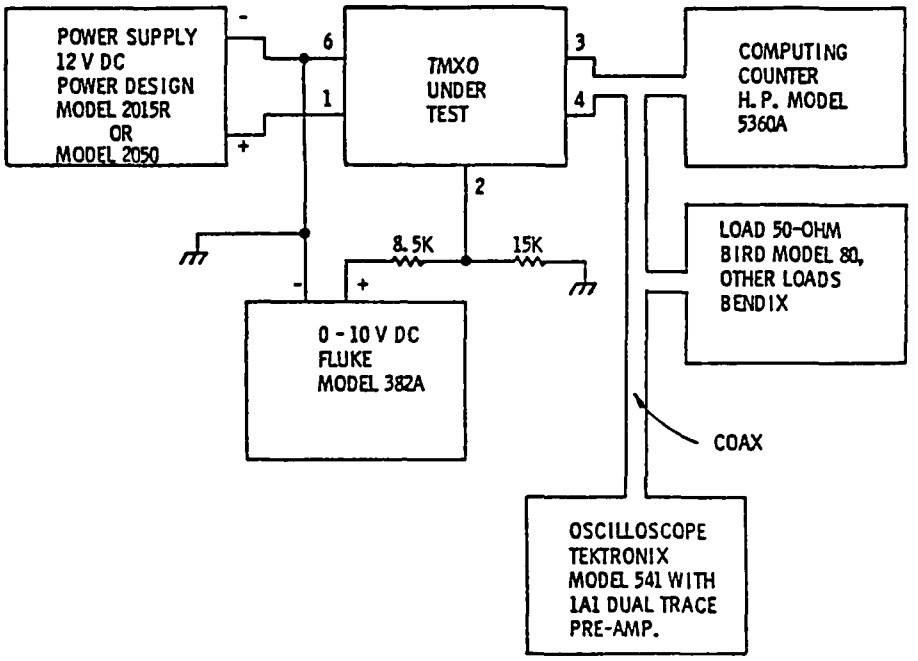

Figure 35. Test setup number 3.

7.3 Performance. Five engineering models were delivered. They were tested in accordance with the test setups shown in Figures 33, 34, and 35.

7.3.1 Setting the optimum crystal temperature. When testing the unsealed TMXO both in air and in vacuum, the temperature was set to a nominal 90°C by a fixed resistor connected remotely from the TMXO across terminals 8 and 7. After sealing, while still in the vacuum chamber, the TMXO was briefly tested in the same manner. After removal from the vacuum chamber, the optimum crystal temperature was set.

Experience has shown that it takes less time to set this critical temperature if a resistance decade box is first used, and then replacing it with the potentiometer. Using the potentiometer only is very difficult because the value of the potentiometer at any setting is not known. It is difficult to keep track of the number of turns, and its linearity is unknown. The

resistance decade box is connected across terminals 8 and 7, and set at 25 kΩ. In a temperature chamber at 25°C, the TMXO is turned on, and after a few minutes, the resistance is changed until the frequency is near its minimum value. Lower the temperature to -40°C, and set the resistance box so that the frequency is 2×10^{-8} higher than it was at room temperature. Return to room temperature and note the frequency. The -40°C to +25°C frequency change will probably be greater than 2×10^{-8} of the last -40°C reading. Repeat the -40°C to +25°C cycle. Change the temperature to +70°C and note the frequency. It should be greater than the room temperature value and be approximately equal to the -40°C value. If not, a resistance change at +70°C and at 25°C should be made. Set a potentiometer to the decaded resistance value and insert it in the base of the TMXO. Repeat the thermal cycling, going from +25°C, -54°C, +75°C, +25°C, setting the temperature to optimize the frequency/temperature curve. Only a $\pm$ half turn of the potentiometer should be required.

7.3.2 Operating power. The operating power depends upon the amount of vacuum in the TMXO. The power was calculated from the input current measurement using setup number 1. The input current is not a constant dc value, but is a current pulse whose amplitude, width, and period is a function of the ambient temperature. The setup shows the current being measured by a Weston milliampere meter and a Tektronix current probe. At times, a Triplett (dc milliamperes) was used in place of the Weston meter. Both of these meters give the correct result of the average current. There is an oscillation in the indicating needle due to the pulsing characteristic of the input current, but the average reading is the average current.

The validity of the dc meter reading was proved by the current measurement using the current probe. The average current was calculated from the pulse measurement using the following equation:

$$I_{avg} = \frac{\text{Pulse Amplitude (at 90\%)} \times \text{Pulse Width (at 50\%)}}{\text{Period}}$$

The operating powers for the models at various temperatures are:

TMXO No. 1

+25°C, 0.28 W	-54°C, 0.50 W
-40°C, 0.40 W	+75°C, 0.084 W

TMXO No. 2

+25°C, 0.56 W	+74°C, 0.17 W
-54°C, 1.20 W	

TMXO No. 3

+25°C, 0.44 W	-54°C, 0.90 W
-40°C, 0.75 W	+67°C, 0.20 W

TMXO No. 4	TMXO No. 5
25°C, 0.30 W	25°C, 1.0 W

TMXO Nos. 4 and 5 had no RF output, and only limited measurements were made on these units.

7.3.3 Peak power. This is the input power at turnon. It is limited by current limiting resistors in the TMXO. The duration of this peak power is a function of the ambient temperature, varying from a few seconds at +75°C to about 80 seconds at -54°C. The peak power is measured using test setup no. 1 and is:

TMXO No. 1	8.4 W	TMXO No. 4	9.0 W
TMXO No. 2	7.8 W	TMXO No. 5	9.0 W
TMXO No. 3	9.0 W		

7.3.4 Voltage control. A voltage source of 0 to 10 V dc, in conjunction with two resistors (85 kΩ and 15 kΩ), will result in a fine frequency adjustment. The test setup for this measurement is shown in Figure 35. The frequency range in response to this voltage control for the various models is as follows:

Model No. 1	3.2×10^{-7}	Model No. 4	No RF output
Model No. 2	3.2×10^{-7}	Model No. 5	No RF output
Model No. 3	2.9×10^{-7}		

The control voltage/frequency curve can be seen in Figure 36.

7.3.5 Fine frequency adjustment. The fine frequency adjustment is accomplished with a 10-turn 100 kΩ potentiometer. The center of the tuning range occurs at about 22 kΩ. The tuning range for the models was:

Model No. 1	4.4×10^{-7}	Model No. 4	No RF output
Model No. 2	4.4×10^{-7}	Model No. 5	No RF output
Model No. 3	4.0×10^{-7}		

The frequency could be set to better than $\pm 3 \times 10^{-10}$, which was the resolution of the test setup. This setup is shown in Figure 32.

7.3.6 Frequency/temperature stability (steady state). The steady state frequency/temperature characteristics, over an ambient temperature range of -55°C to +75°C, is plotted in Figures 37 through 39 for models 1, 2, and 3. No data are available for models 4 and 5, as they had no RF output. Model no. 1 had a good vacuum, and its frequency change over the temperature range was only $\pm 4 \times 10^{-9}$. Models 2 and 3 had poor vacuums, and their frequency change was $\pm 7 \times 10^{-8}$ and $\pm 1.05 \times 10^{-7}$, respectively. The test setup to make these measurements is shown in Figure 33.

7.3.7 Frequency/temperature stability (transient). The frequency should not be sensitive to transient temperatures. The maximum allowable frequency change is $\pm 1 \times 10^{-8}$ when subjected to a positive 10°C amplitude at a rate of 1°C/min, starting from -40°C, -5°C, +30°C, and +65°C. This parameter was measured for model 1 with the following results:

Starting Temperature	Temperature Ramp Rate	Maximum ΔF/F
-40°C	6.7°C/min	-2.8×10^{-9}
-5°C	6.7°C/min	-3.8×10^{-9}
+30°C	7°C/min	-5.2×10^{-9}
+65°C	4.4°C/min	-5.2×10^{-9}

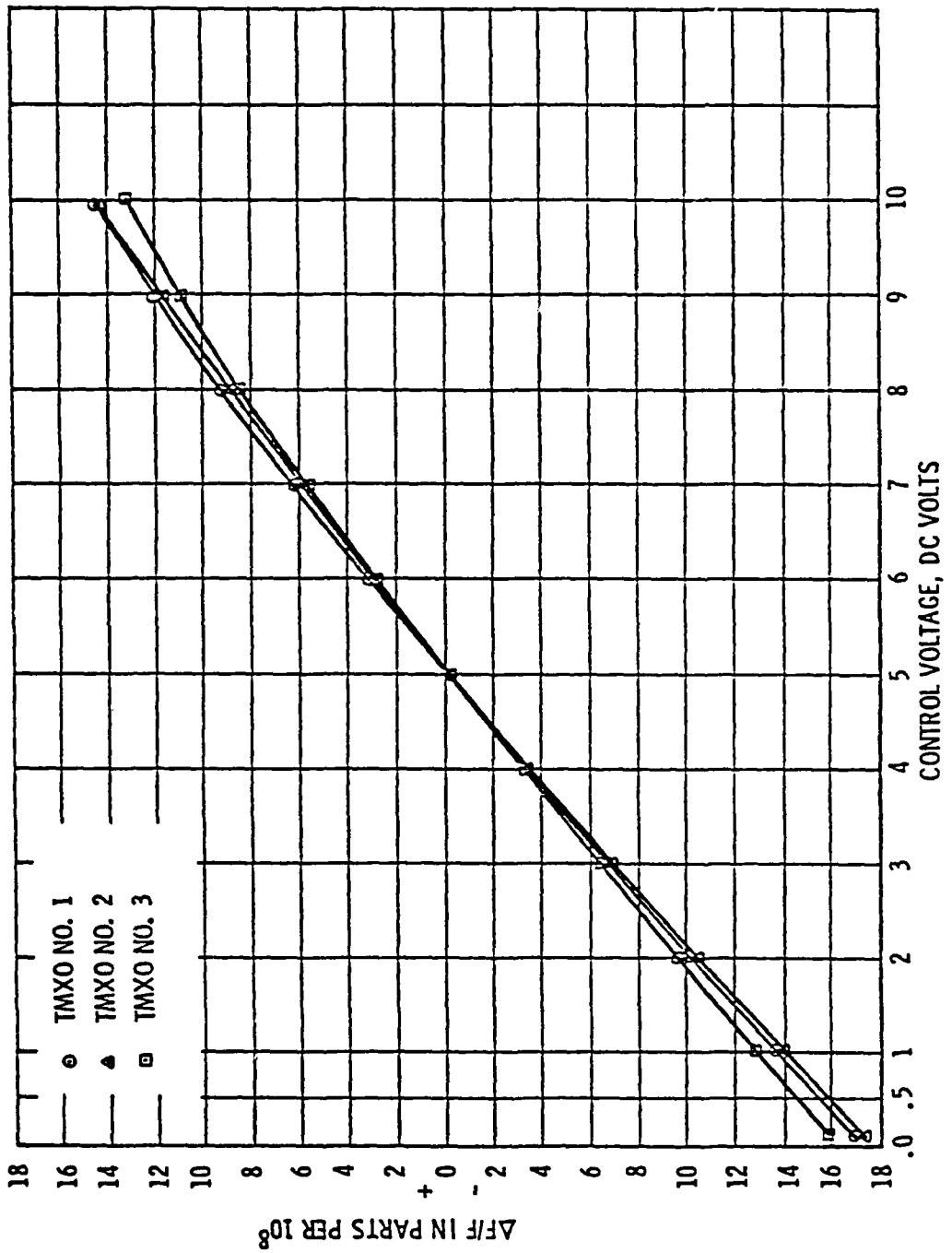

Figure 36. Control voltage versus freyuency.

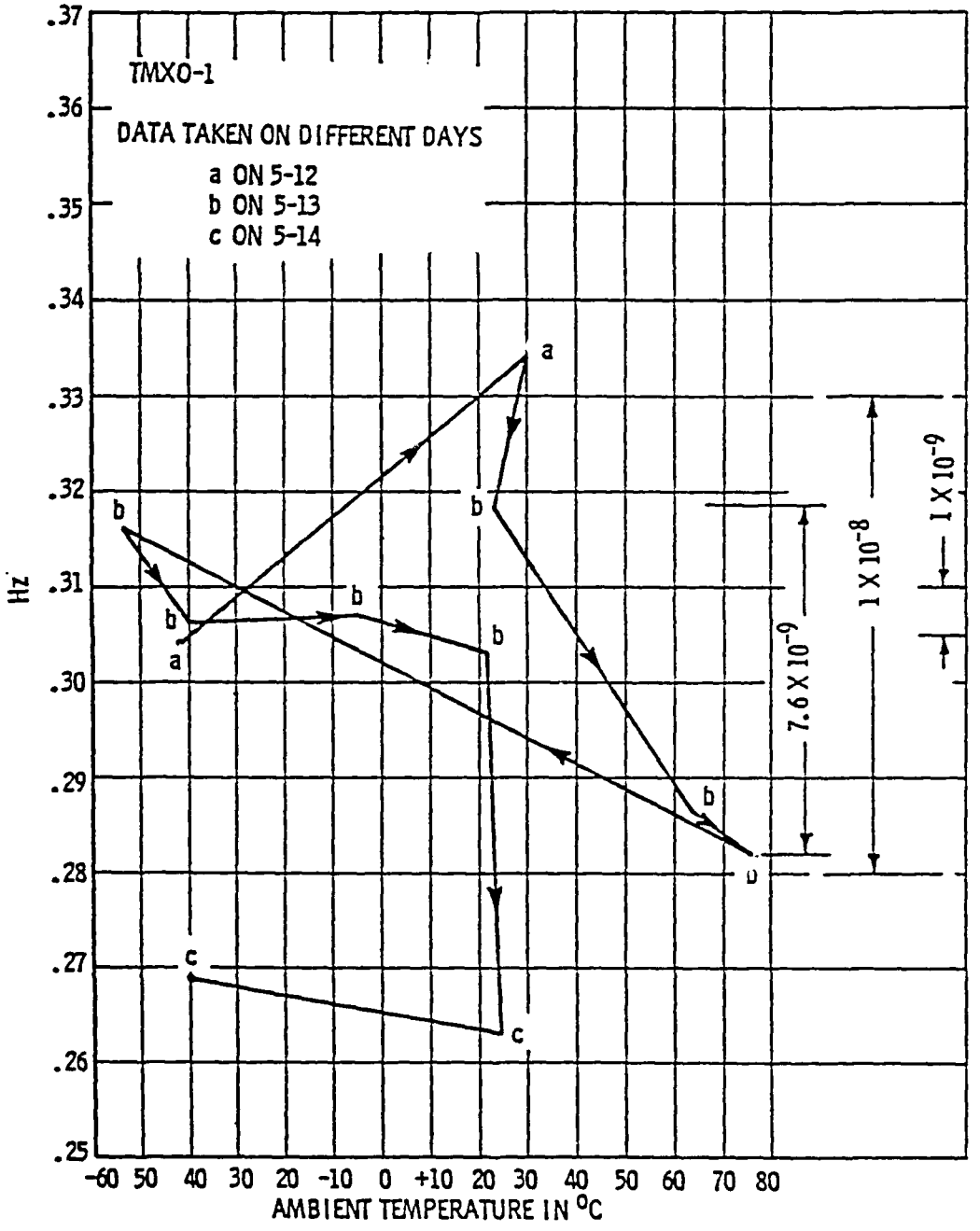

Figure 37. Frequency versus ambient temperature for TMXO number 1.

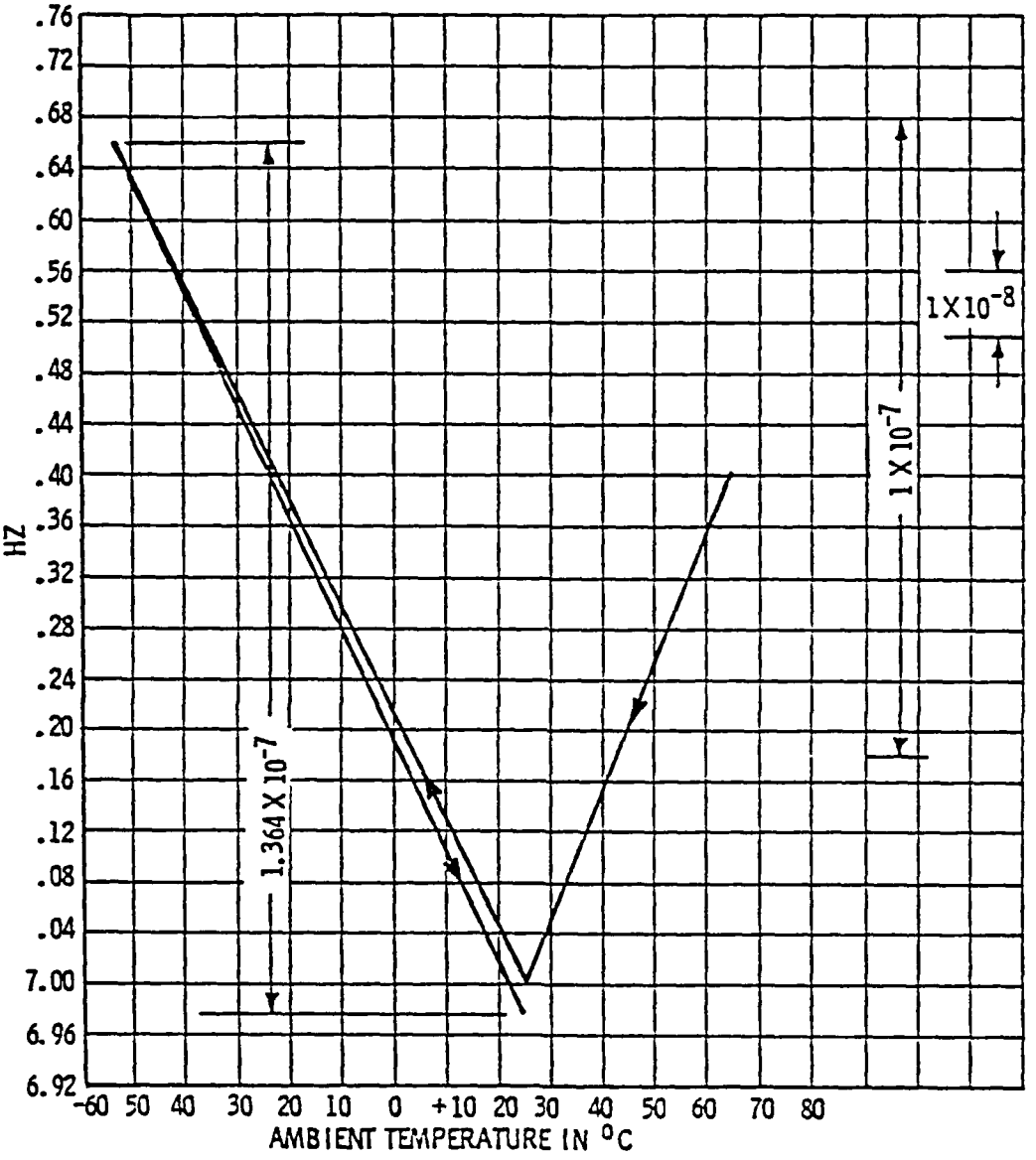

Figure 38. Frequency versus ambient temperature for TMXO number 2.

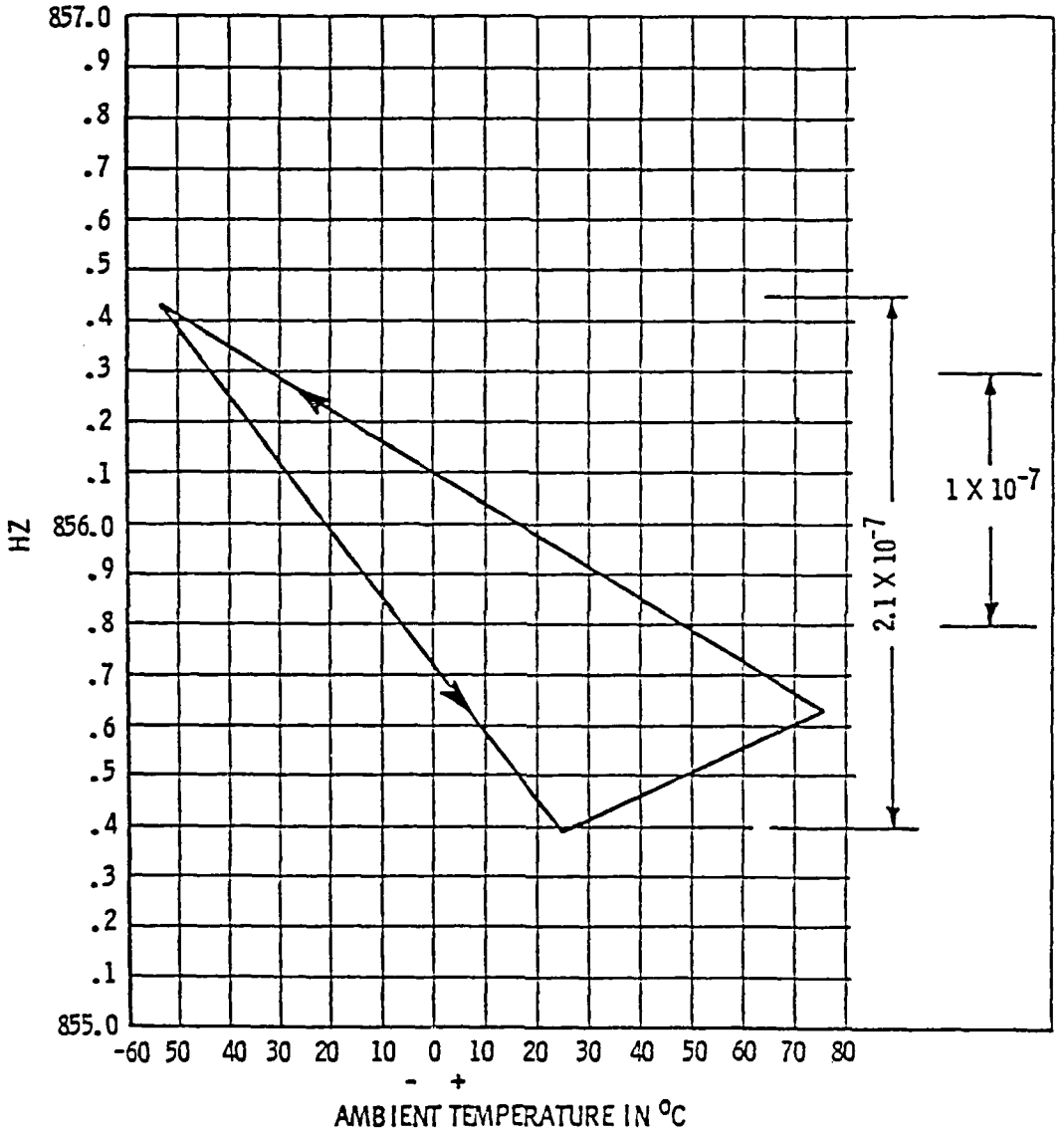

Figure 39. Frequency versus ambient temperature for TMXO number 3.

The test setup is shown in Figure 33.

7.3.8 Frequency/load stability. The change in frequency with a change in load was measured using the test setup shown in Figure 34. The measured values are given in the following table:

TMXO NO.	LOAD	ΔF/F
1	56Ω + 20°ϕ	-2.1×10^{-9}
1	56Ω - 20°ϕ	$+2.8 \times 10^{-9}$
1	44Ω + 20°ϕ	-1.2×10^{-9}
1	44Ω - 20°ϕ	$+2.0 \times 10^{-10}$
3	56Ω + 20°ϕ	-1.4×10^{-9}
3	56Ω - 20°ϕ	$+4.2 \times 10^{-9}$
3	44Ω + 20°ϕ	-1.4×10^{-9}
3	44Ω - 20°ϕ	$+3.6 \times 10^{-9}$

7.3.9 Frequency/power supply voltage stability. The change in frequency due to a change of ±5 percent in the power supply voltage was measured with the test setup shown in Figure 34. The measured data are tabulated below:

TMXO No.	Power Supply Voltage Change	ΔF/F
1	+5%	-3×10^{-9}
1	-5%	$+2 \times 10^{-9}$
3	+5%	$\pm 3 \times 10^{-10}$
3	-5%	-8×10^{-10}

7.3.10 Short term stability. The short term stability was measured using the test setup shown in Figure 34. Peak frequency deviation readings were taken on the computing counter having an error of $\pm 3 \times 10^{-10}$. The averaging time was 1 second, and readings were taken over a time period of 20 minutes. Results were as follows:

Model No. 1: Better than $\pm 3 \times 10^{-10}$ peak-to-peak, corresponding to an rms value of approximately better than $\pm 3 \times 10^{-11}$

Model No. 2: $\pm 2 \times 10^{-8}$ peak-to-peak corresponding to an rms value of approximately $\pm 2 \times 10^{-9}$

Model No. 3: $\pm 1.2 \times 10^{-9}$ peak-to-peak, corresponding to an rms value of approximately $\pm 1.2 \times 10^{-10}$

The high noise in models 2 and 3 was due to noise on the input pulse to the TMXO.

7.3.11 Frequency/attitude stability. Frequency/attitude stability is a measurement of the change in frequency when the orientation of the TMXO is changed relative to the ground. This measures the effect of the gravitational force on the TMXO frequency. Measurements were made on model no. 1. For a 90-degree change in attitude, the frequency deviation was less than $\pm 3 \times 10^{-10}$. For an attitude change of 180 degrees (Δ2G), the frequency deviation was 8×10^{-10} or 4×10^{-10}/G.

7.3.12 Stabilization time. From turnon, the time needed for the frequency to be within 1×10^{-8} of the final frequency was measured using the setup as shown in Figure 33. The warmup curves from various ambient temperatures are plotted in Figures 40, 41, and 42.

7.3.13 Frequency recovery at -40°C. The ability of the TMXO to return to the same frequency after being in the off condition is an important stability parameter. The TMXO was maintained at an ambient temperature of -40°C. It was then subjected to five on-off cycles, each off cycle being at least 30 minutes. The maximum frequency deviation was $\pm 5 \times 10^{-8}$. As in previous measurements on earlier TMXOs, this change in frequency seems to be crystal dependent. There also seems to be two superimposed effects. One is a slow continuous hysteresis phenomenon while the other is a step change.

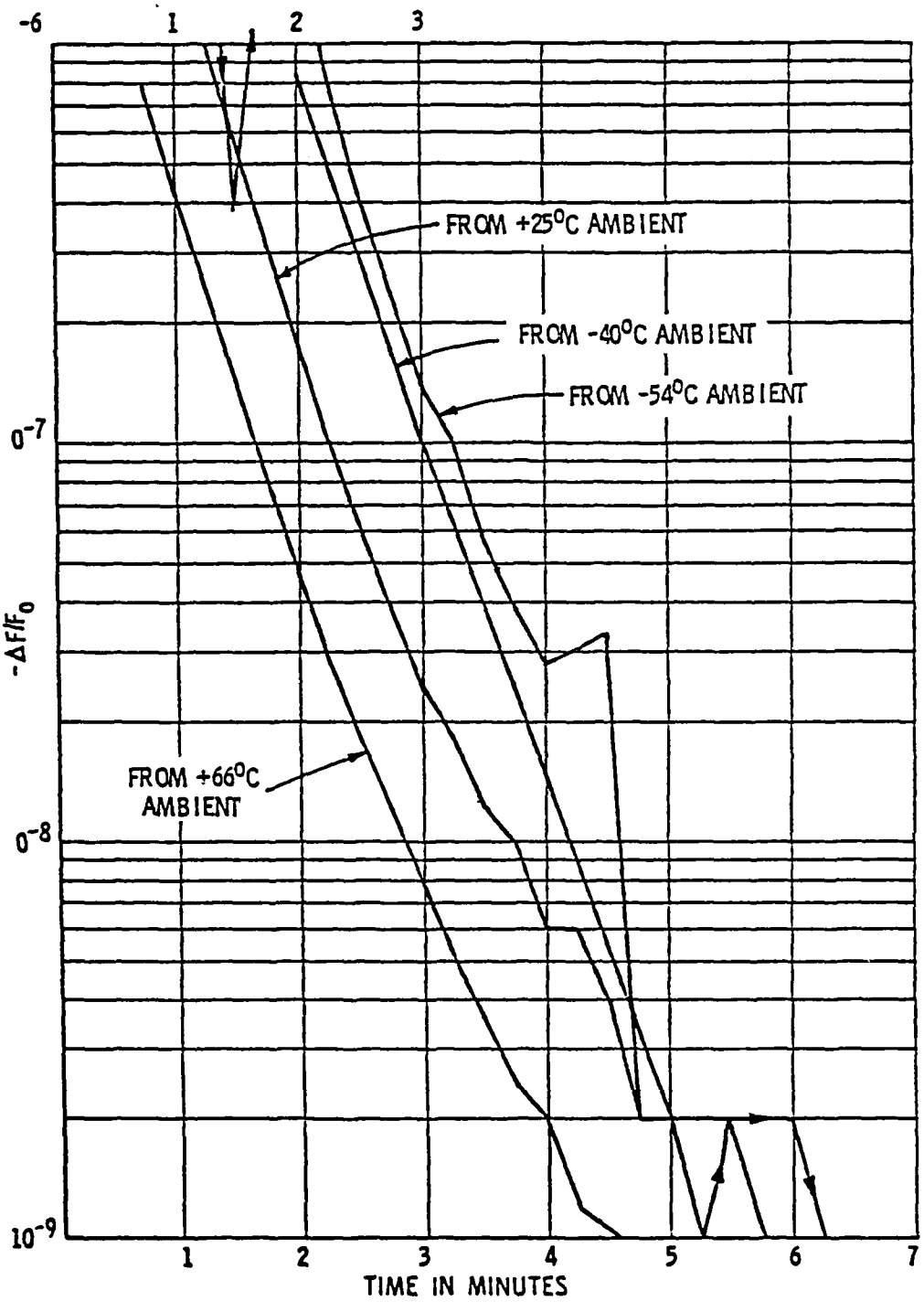

Figure 40. Warmup of TMXO number 1.

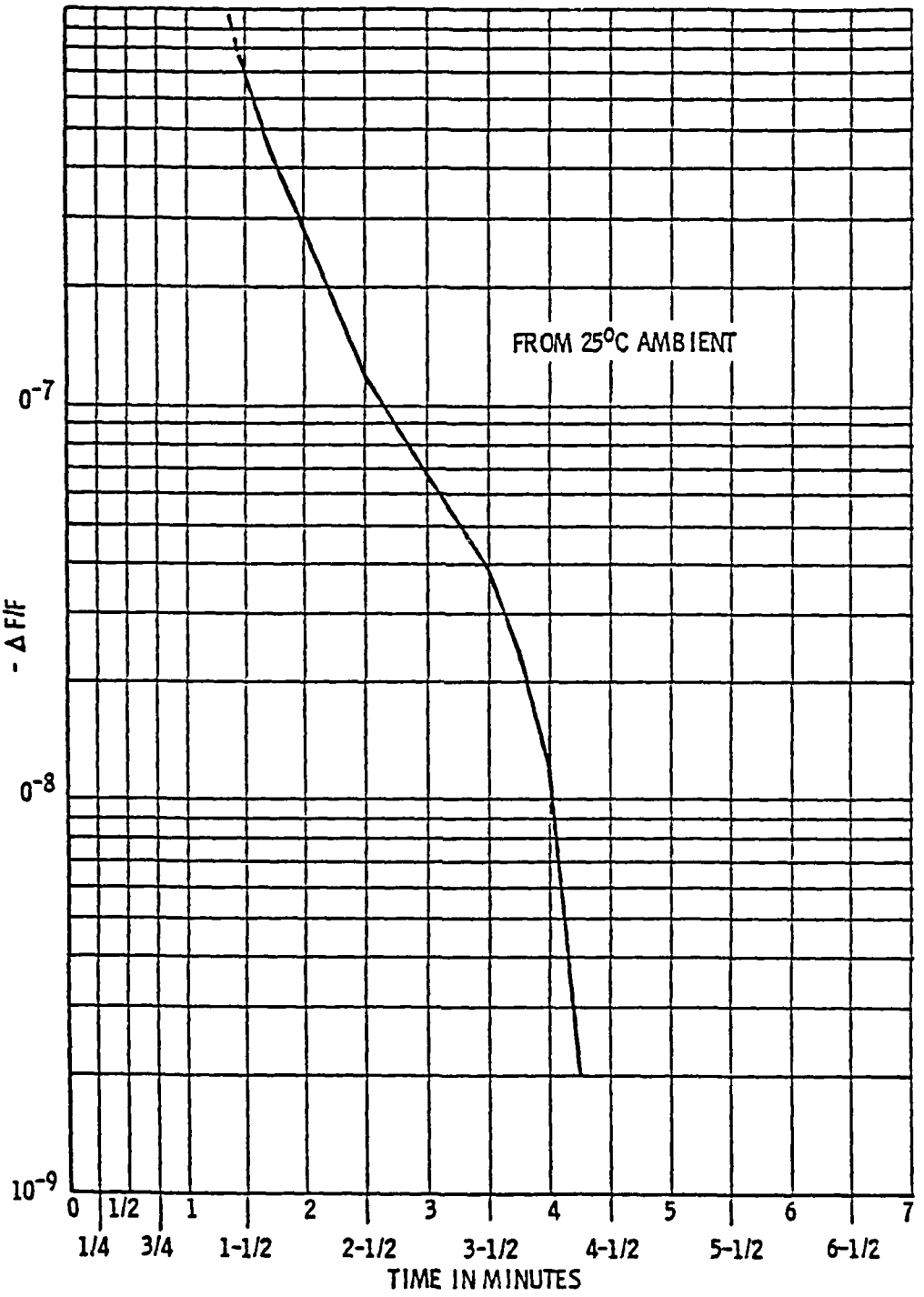

Figure 41. Warmup of TMXO number 2.

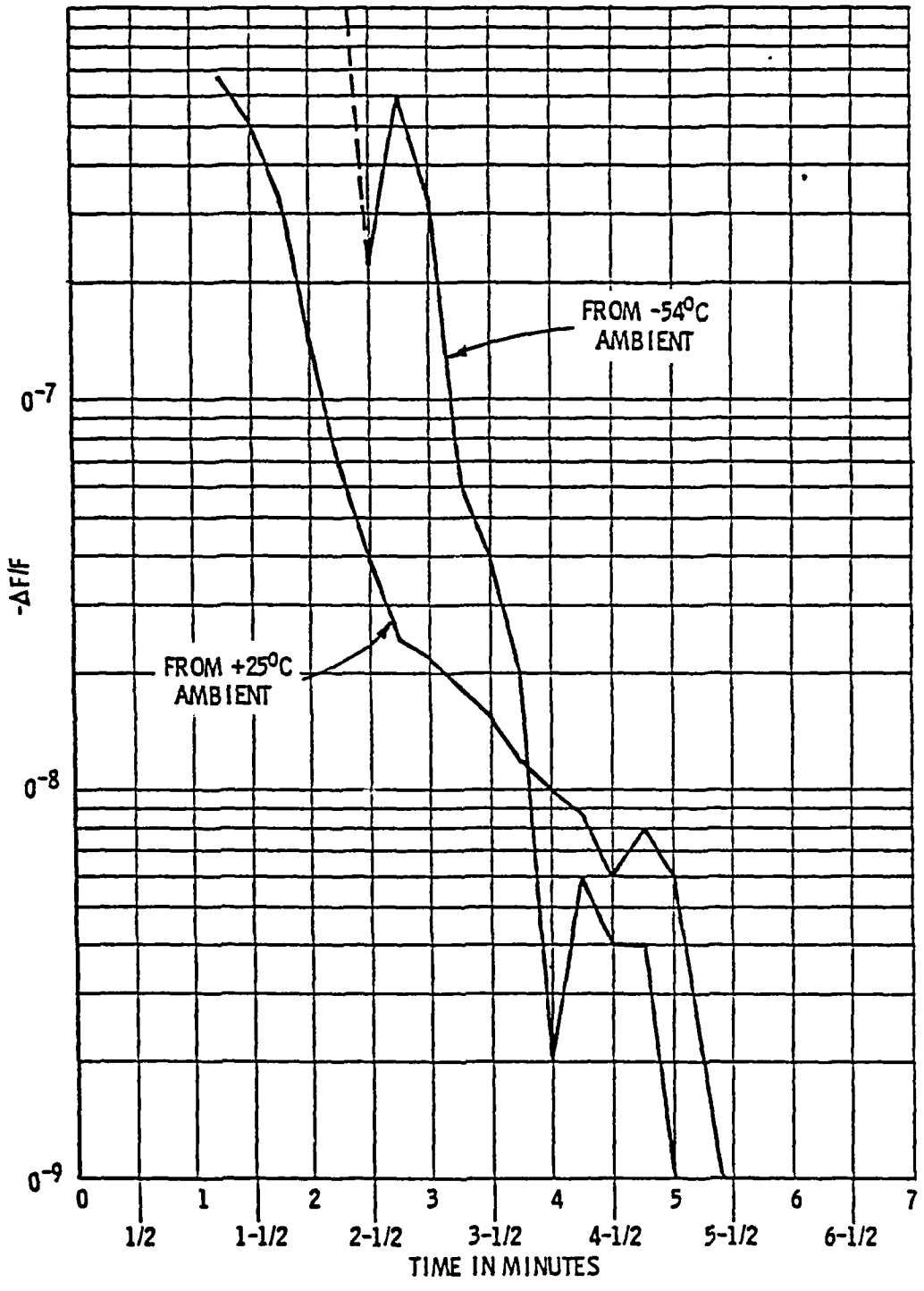

Figure 42. Warmup of TMXO number 3.

7.3.14 Output voltage. The minimum output voltage requirement of 0.125 volt rms into 50 ohms was easily satisfied. The values for the TMXO models ranged from 0.148 volt to 0.28 volt.

8. PERFORMANCE OF DELIVERED MODELS, PHASE 2

8.1 General physical description. The TMXOs are cylindrical in shape, having a diameter of 1-1/4 inches and a height of 1-1/4 inches (excluding the tubulation of the top). At the bottom is a 1-1/4 inch square mounting flange. Figure 32 shows a bottom view, identifying and numbering the connecting pins coming out the bottom.

The temperature adjusting potentiometer has been set for the vacuum environment, optimized for the ambient temperature range of -40°C to +70°C. The adjustment screw of this potentiometer was not cemented in place so that the temperature setting of the crystal could be changed. Proper adjustment of this screw, either for the vacuum or air environment, takes about 8 hours of elapsed time.

The three models are identified by numbers scratched into the bottom of the TMXO. The model numbers are 161-2, 162, and 195. All contain fundamental AT-cut quartz resonators in ceramic enclosures, manufactured by GEND. Model 161-2 contains GEND crystal number 161. Model 162 contains GEND crystal number 162. Model 195 contains GEND crystal number 195.

All measurements were conducted under a dynamic vacuum, except the measurement of frequency stability while being vibrated.

8.2 Operating power.

8.2.1 Requirements. After warmup, the maximum power input to the TMXO shall not exceed 250 milliwatts at any temperature between -40°C and +70°C.

8.2.2 Test setup. See Figures 43, 44, and 45.

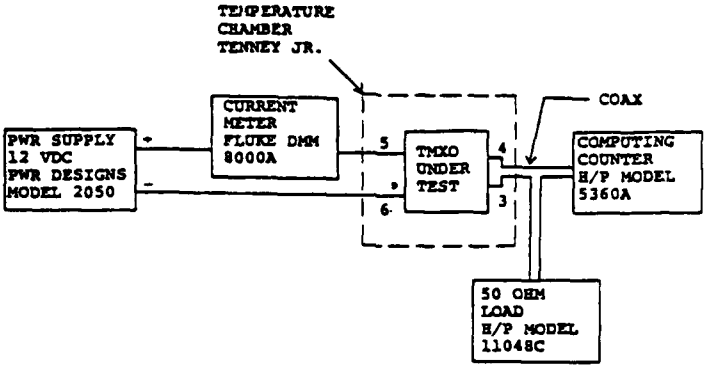

Figure 43. Test setup number 1, phase 2.

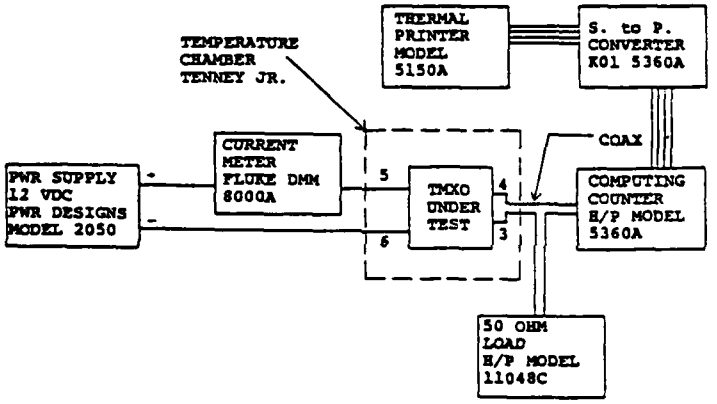

Figure 44. Test setup number 2, phase 2.

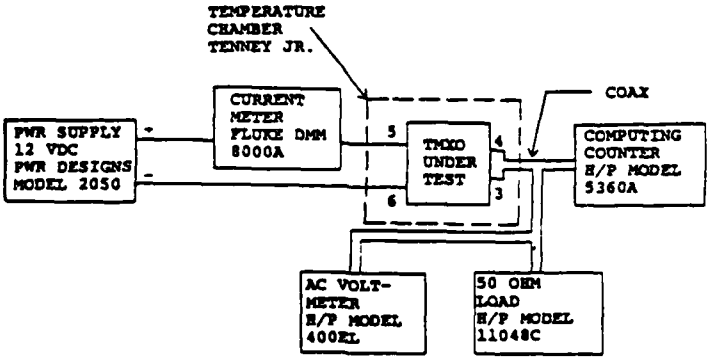

Figure 45. Test setup number 3, phase 2.

8.2.3 Performance.

	Ambient Temperature			UTP
Model No.	+70°C	+25°C	-40°C	°C
161-2	155 mW	280 mW	456 mW	90.6
162	144 mW	240 mW	384 mW	87.3
195	155 mW	282 mW	445 mW	88

8.3 Output voltage.

8.3.1 Requirement. A minimum of 0.125 volt rms at the 5.115 MHz output frequency shall be available across an external resistive load of 50 ohms.

8.3.2 Test setup. See Figure 45.

8.3.3 Performance.

Model Number	Output Voltage 25°C
161-2	0.209 V rms
162	0.167 V rms
195	0.240 V rms

8.4 Frequency recovery at -40°C.

8.4.1 Requirements. The output frequency of the TMXO after warmup during each turnon period for a five-cycle frequency recovery test shall remain within $\pm 3 \times 10^{-9}$ of the frequency measured on the first cycle. Each cycle shall consist of complete frequency stabilization during turnon, followed by complete thermal stabilization after power is removed.

8.4.2 Test setup. See Figure 44.

8.4.3 Performance.

MODEL 161-2

When Measured	Frequency (Hz)
At start	5115304.115
After first turn-off cycle	5115304.112
After second turn-off cycle	5115304.112
After third turn-off cycle	5115304.113
After fourth turn-off cycle	5115304.112
After fifth turn-off cycle	5115304.114

The maximum change from the starting frequency was $\Delta F/F = -5.9 \times 10^{-10} + 0$.

MODEL 162

When Measured	Frequency (Hz)
At start	5115190.081
After first turn-off cycle	5115190.084
After second turn-off cycle	5115190.066
After third turn-off cycle	5115190.061
After fourth turn-off cycle	5115190.085
After fifth turn-off cycle	5115190.084

The maximum change from the starting frequency was $\Delta F/F = +8 \times 10^{-10}, -4 \times 10^{-9}$.

MODEL 195

When Measured	Frequency (Hz)
At start	5115045.206
After first turn-off cycle	5115045.201
After second turn-off cycle	5115045.203
After third turn-off cycle	5115045.209
After fourth turn-off cycle	5115045.208
After fifth turn-off cycle	5115045.204

The maximum change from the starting frequency was $\Delta F/F = +5.0 \times 10^{-10}, -9.8 \times 10^{-10}$.

8.5 Frequency versus power supply voltage.

8.5.1 Requirement. The maximum permissible frequency deviation for a supply voltage variation of 12 V dc ±5 percent shall be $\pm 1 \times 10^{-9}$.

8.5.2 Test setup. See Figure 43, 44, or 45.

8.5.3 Performance.

Model No.	+5% V	-5% V
161-2	$\Delta F/F = +1.96 \times 10^{-10}$*	$\Delta F/F = +1.96 \times 10^{-10}$*
162	$\Delta F/F = +1 \times 10^{-9}$	$\Delta F/F = +8 \times 10^{-10}$
195	$\Delta F/F = -3.9 \times 10^{-10}$	$\Delta F/F = -1.96 \times 10^{-10}$*

* Measurement error is $\pm 1.96 \times 10^{-10}$

8.6 Frequency versus load.

8.6.1 Requirement. The maximum frequency deviation for a load variation of 50 ohms ±10 percent, ±20 degrees phase, shall be $\pm 1 \times 10^{-9}$.

8.6.2 Test setup. See Figure 43, 44, or 45, with additional loads of:

56 ohms - 20 degrees
56 ohms + 20 degrees
44 ohms - 20 degrees
44 ohms + 20 degrees

8.6.3 Performance.

	MODEL 161-2	
Load	Frequency (Hz)	$\Delta F/F$
50 ohms	5115303.813	--
56 ohms + 20 degrees	5115303.789	-4.7×10^{-9}
56 ohms - 20 degrees	5115303.800	-2.5×10^{-9}

44 ohms - 20 degrees	5115303.829	$+3.1 \times 10^{-9}$
44 ohms + 20 degrees	5115303.830	$+3.2 \times 10^{-9}$
50 ohms	5115303.813	--

MODEL 162

Load	Frequency (Hz)	ΔF/F
50 ohms	5115190.040	--
56 ohms - 20 degrees	5115190.006	-6.8×10^{-9}
56 ohms + 20 degrees	5115190.035	-1.0×10^{-9}
44 ohms - 20 degrees	5115190.070	$+6 \times 10^{-9}$
44 ohms + 20 degrees	5115190.085	$+9 \times 10^{-9}$

MODEL 195

Load	Frequency (Hz)	ΔF/F
50 ohms	5115044.969	--
56 ohms - 20 degrees	5115045.021	$+1.0 \times 10^{-8}$
56 ohms + 20 degrees	5115044.960	-1.8×10^{-9}
44 ohms - 20 degrees	5115045.029	$+1.2 \times 10^{-8}$
44 ohms + 20 degrees	5115044.939	-5.9×10^{-9}

8.7 Short/medium term stability.

8.7.1 Requirement. The maximum rms frequency deviation shall be $\pm 1 \times 10^{-11}$ for averaging times ranging from 1 second to 20 minutes, under conditions of input voltage and ambient temperature controlled to ±1 millivolt and $\pm 0.1^{\circ}C$, respectively.

8.7.2 Test setup. See Figure 44. Sampling time per measurement was 1 second. Allan Variance measured for 100 pairs. Readings taken for 20 minutes (10 sets). The average of these 10 sets, AV_{avg}, was then calculated.

8.7.3 Performance.

Model	AV_{avg} ΔF/F
161-2	1.44×10^{-10}
162	5.5×10^{-10}
195	2.59×10^{-10}

8.8 Frequency versus attitude.

8.8.1 Requirement. The maximum frequency change of the TMXO for a 90° $\pm 5^{\circ}$ attitude change in any axis shall be less than $\pm 5 \times 10^{-10}$.

8.8.2 Test setup. See Figure 43, 44, or 45.

8.8.3 Performance.

	MODEL 161-2	
Position	Frequency (Hz)	ΔF/F
Horizontal	5115302.685	--
Vertical	5115302.717	$+6.26 \times 10^{-9}$
Horizontal	5115302.685	-6.26×10^{-9}

8.9 Frequency versus temperature.

8.9.1 Requirement. The maximum permissible frequency deviation over the temperature range of $-54^{\circ}C$ to $+75^{\circ}C$ shall be $\pm 1 \times 10^{-8}$.

8.9.2 Test setup. See Figure 43, 44, or 45.

8.9.3 Performance.

Model No.	Ambient Temperature	Frequency (Hz)	Comment
161-2	$+25^{\circ}C$	5115303.830	See Figure 46
161-2	$-40^{\circ}C$	5115303.991	See Figure 46
161-2	$+70^{\circ}C$	5115303.990	See Figure 46

The maximum frequency deviation, from $-40^{\circ}C$ to $+70^{\circ}C$, was $\pm 1.5 \times 10^{-7}$.

162	$+25^{\circ}C$	5115189.950	See Figure 47
162	$-40^{\circ}C$	5115190.157	See Figure 47
162	$+70^{\circ}C$	5115190.185	See Figure 47

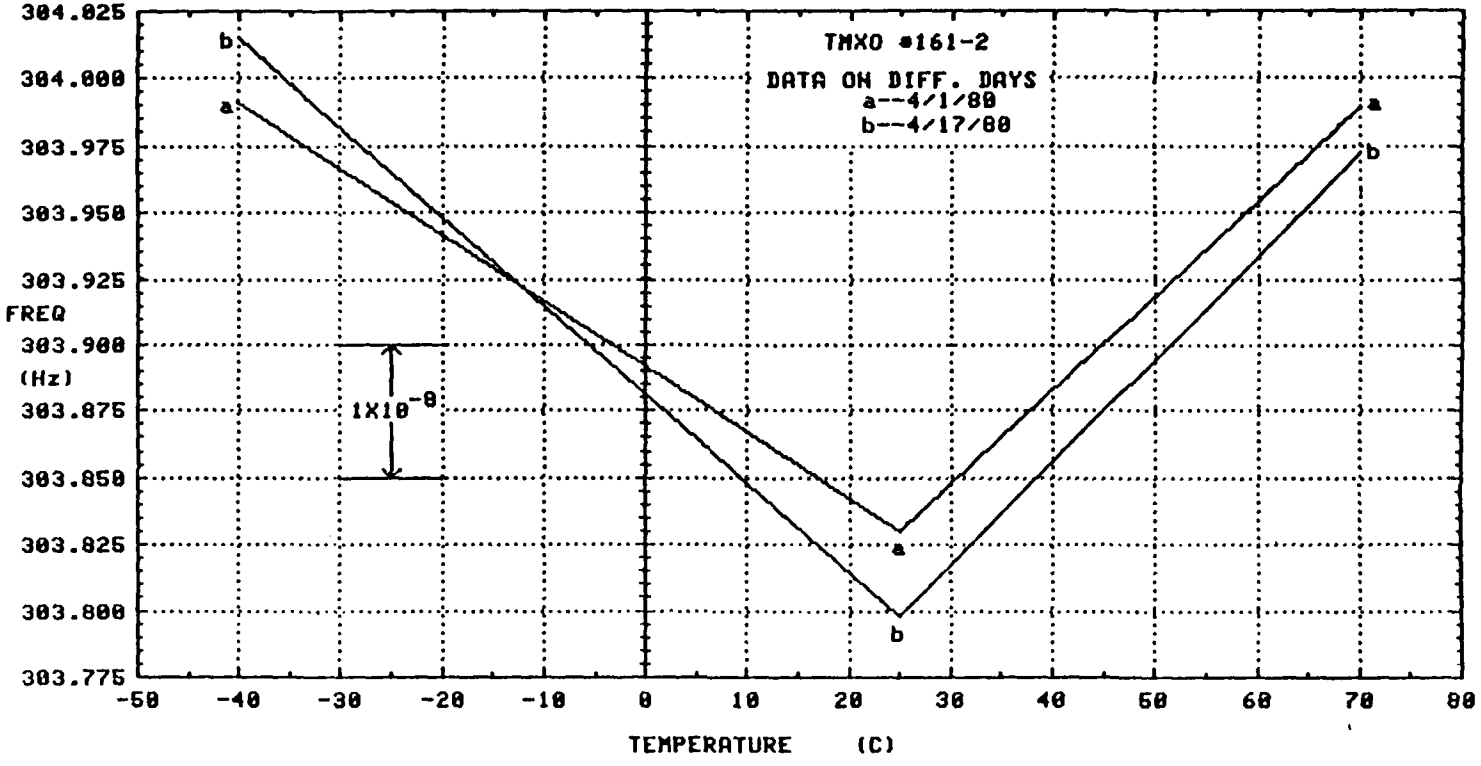

Figure 46. Frequency versus temperature for TMXO number 161-2.

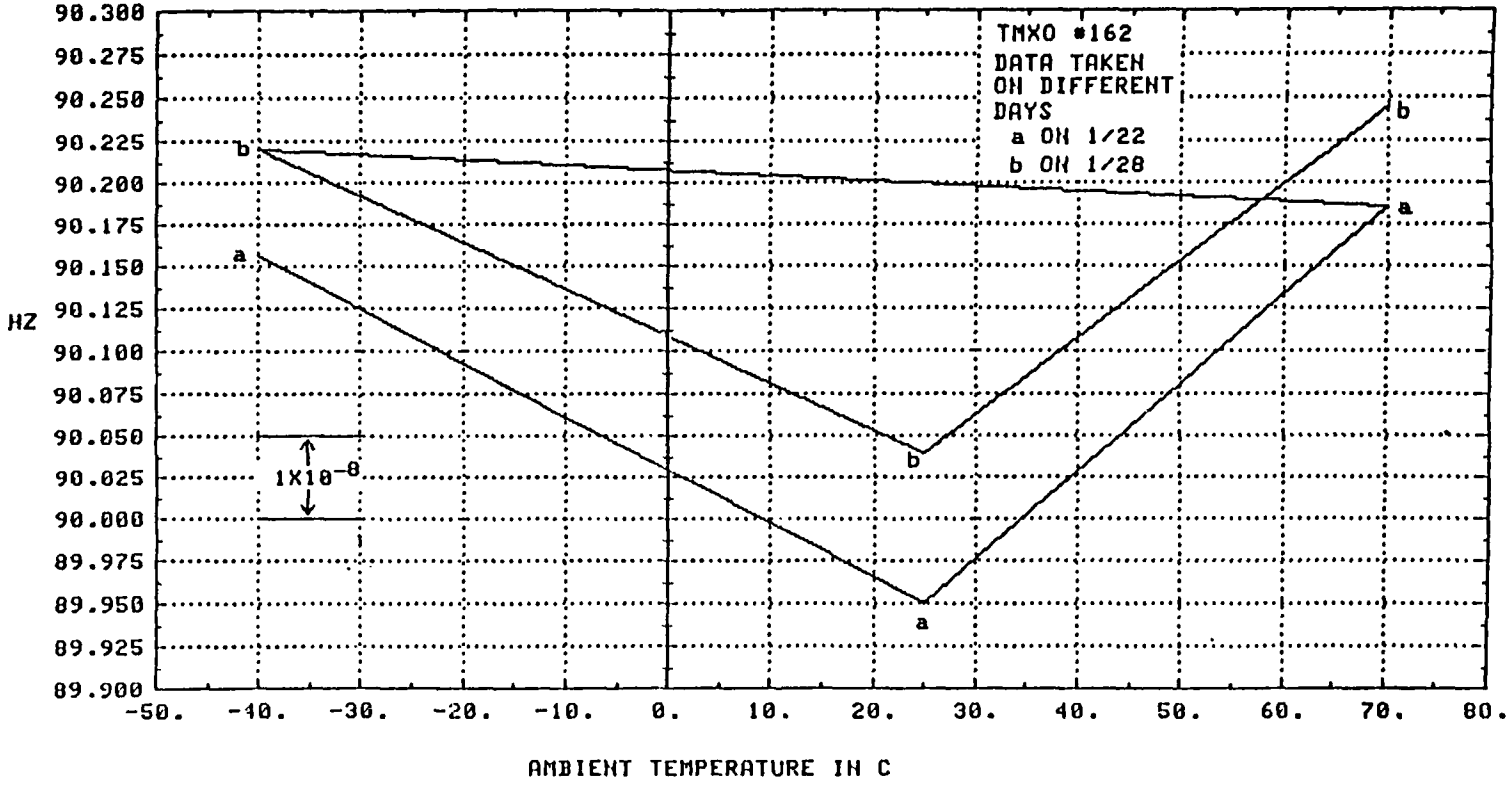

Figure 47. Frequency versus temperature for TMXO number 162.

The maximum frequency deviation, from -40°C to +70°C, was $\pm 2.4 \times 10^{-7}$.

195	+25°C	5115044.939
195	-40°C	5115045.194
195	+70°C	5115045.190

The maximum frequency deviation, from -40°C to +70°C, was $\pm 2.5 \times 10^{-7}$.

8.10 Warmup/stabilization time.

8.10.1 Requirement.

(a) Peak warmup power not to exceeed 10 watts at any operating ambient temperature.

(b) Following the application of power, the frequency of the TMXO shall be within $\pm 1 \times 10^{-8}$ of the final frequency in 3 minutes.

8.10.2 Test setup. See Figure 44.

8.10.3 Performance.

Model No.	Ambient Temperature	Peak Power	Time to Be Within $\pm 1 \times 10^{-8}$ of F_o
161-2*	+25°C	9.2 W	7 minutes
161-2	+25°C	8.2 W	11 minutes
161-2	+70°C	4.8 W	10 minutes
161-2	-40°C	8.3 W	11 minutes

*Not evacuated.

More detailed information concerning the warmup characteristics of model 161-2 is shown in Figures 48 through 54.

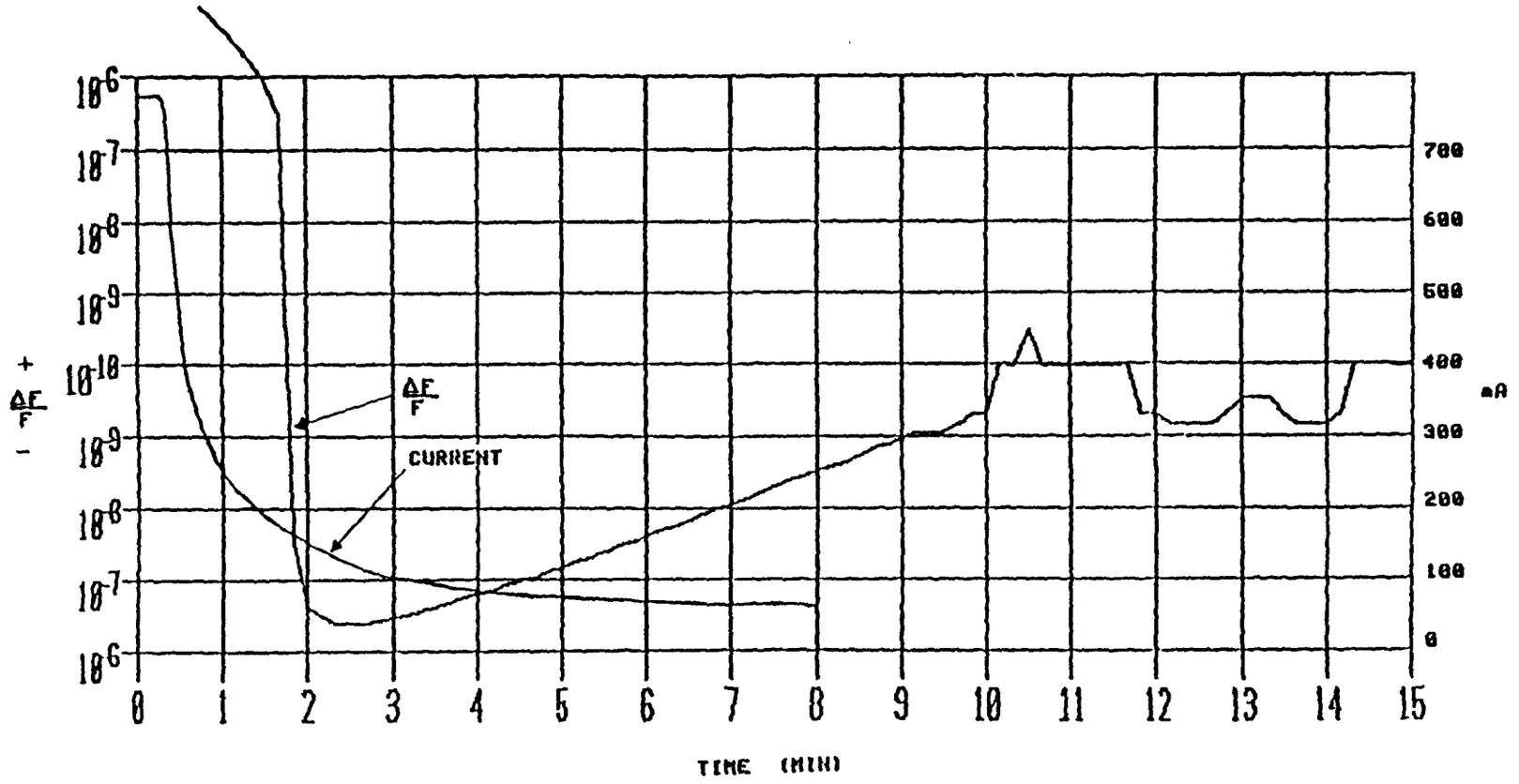

Figure 48. Warmup, 25°C, unevacuated, TMXO number 161-2.

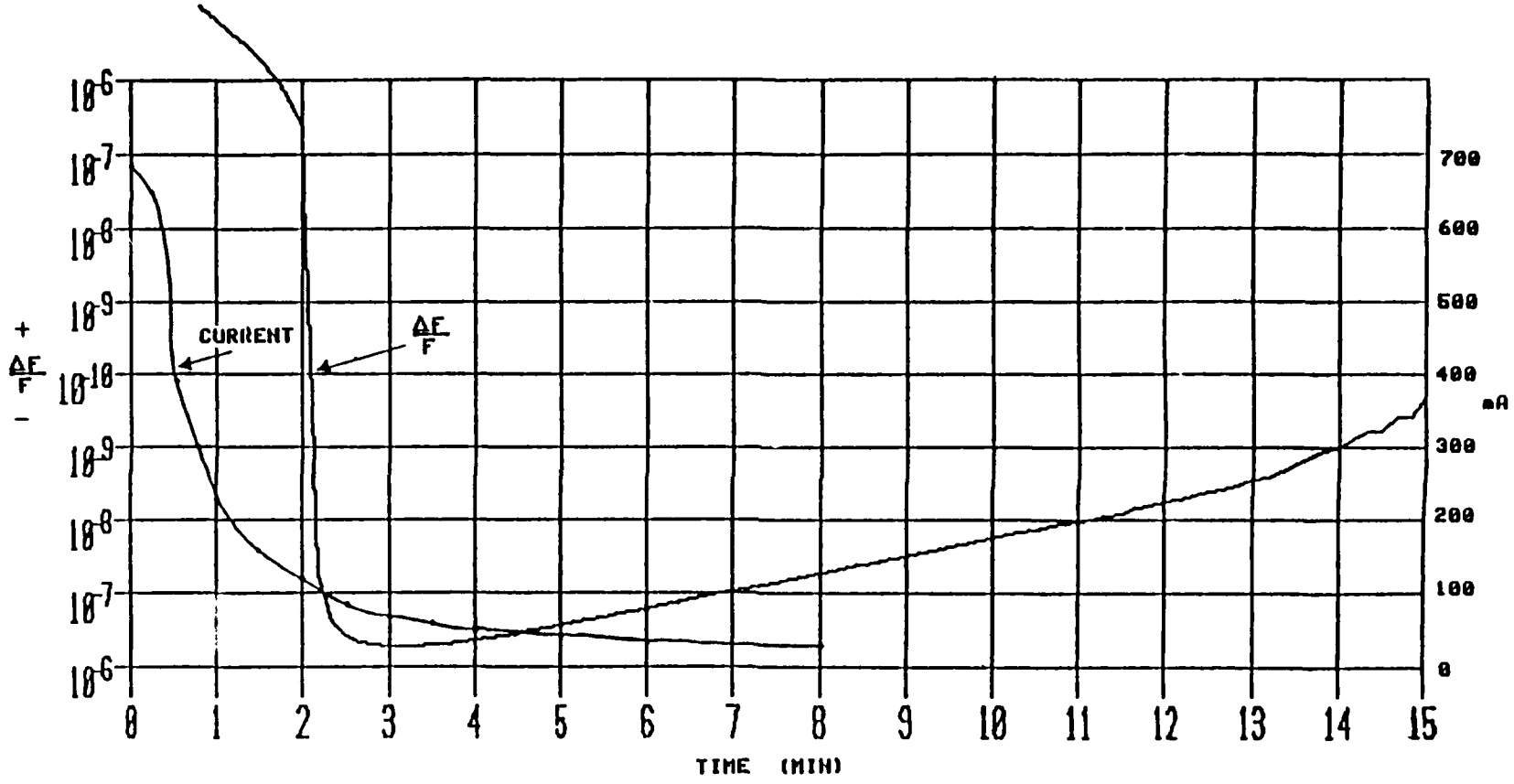

Figure 49. Warmup, 25°C, evacuated, TMXO number 161-2.

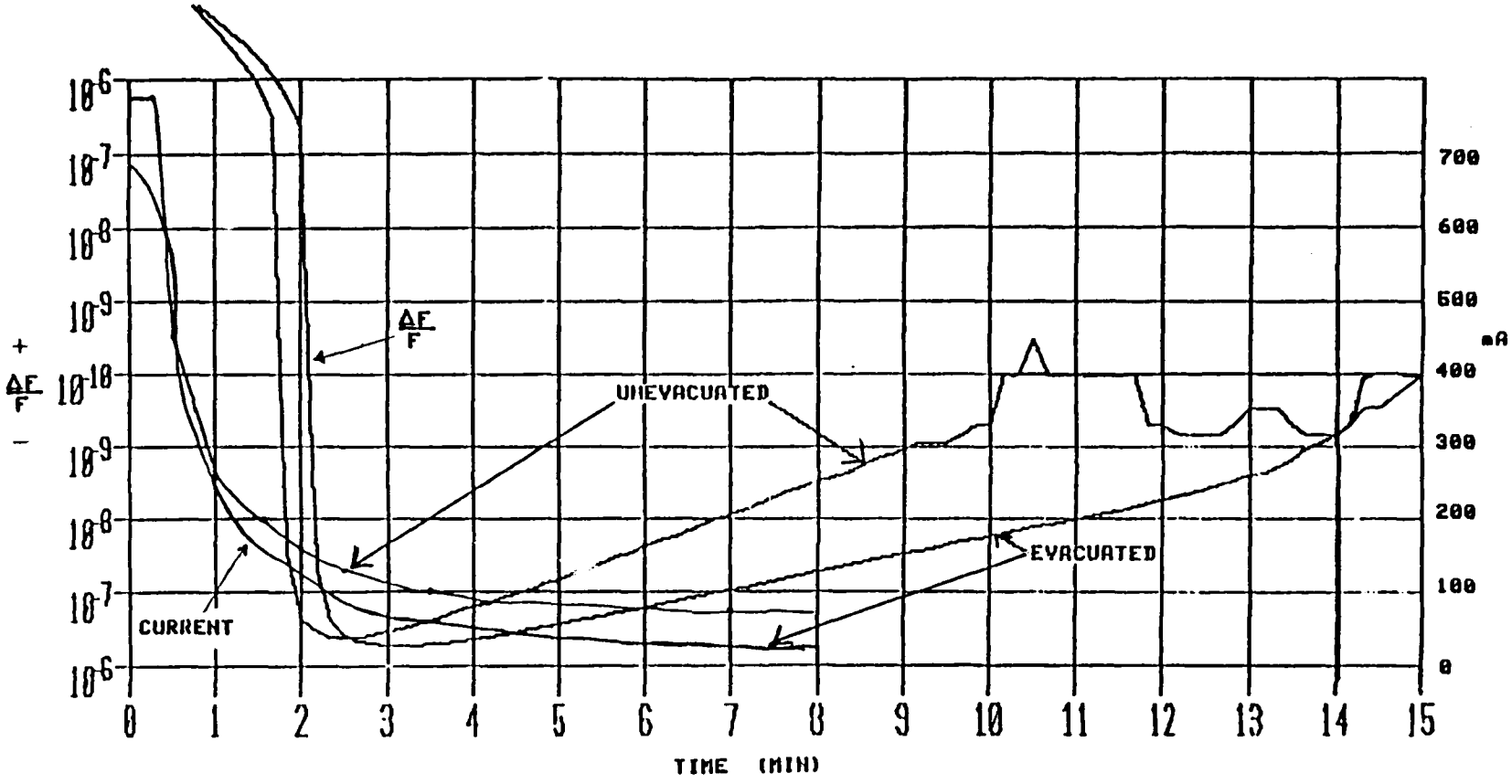

Figure 50. Warmup, 25°C, evacuated and unevacuated, TMXO number 161-2.

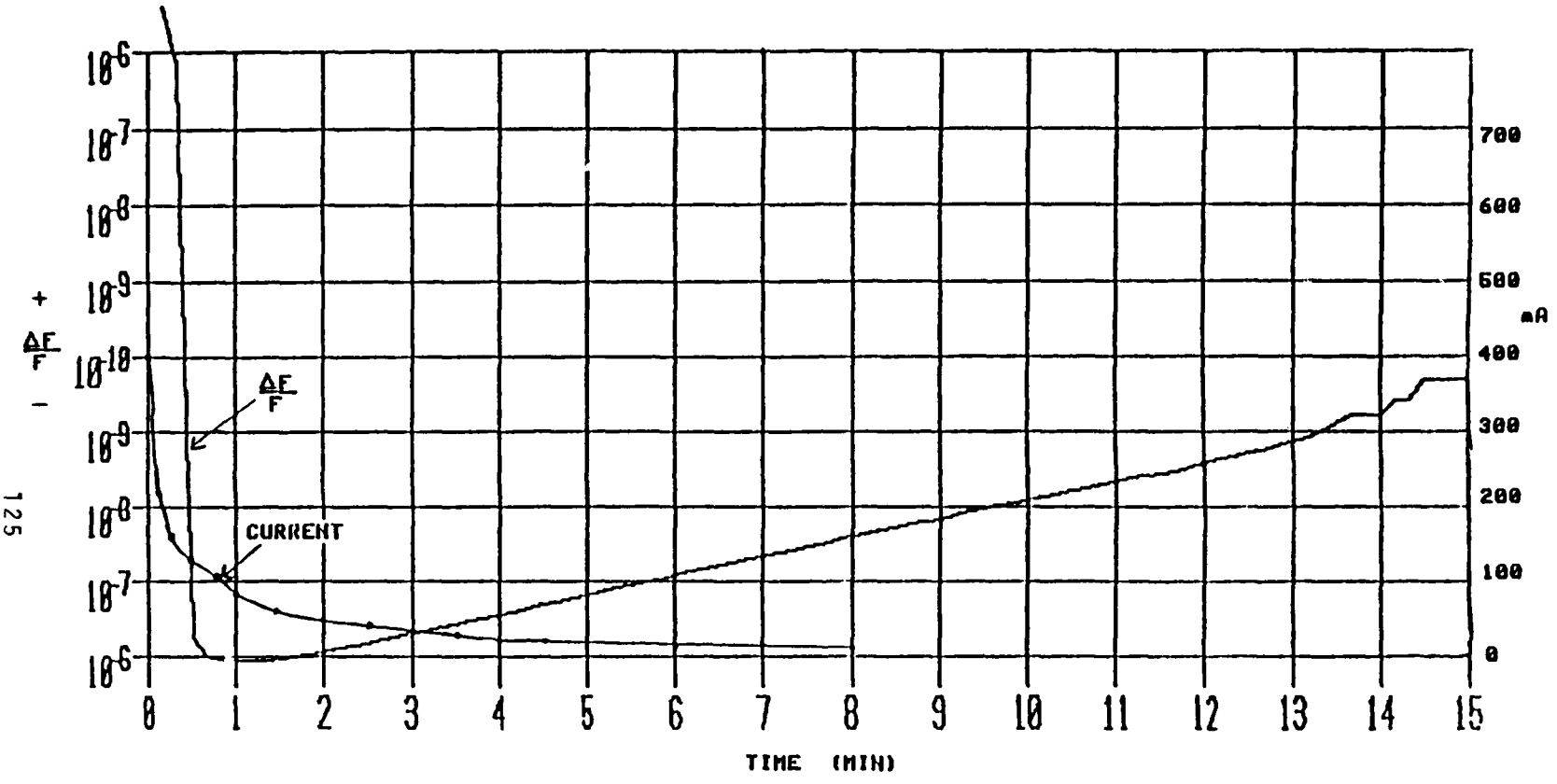

Figure 51. Warmup, 70°C, evacuated, TMXO number 161-2.

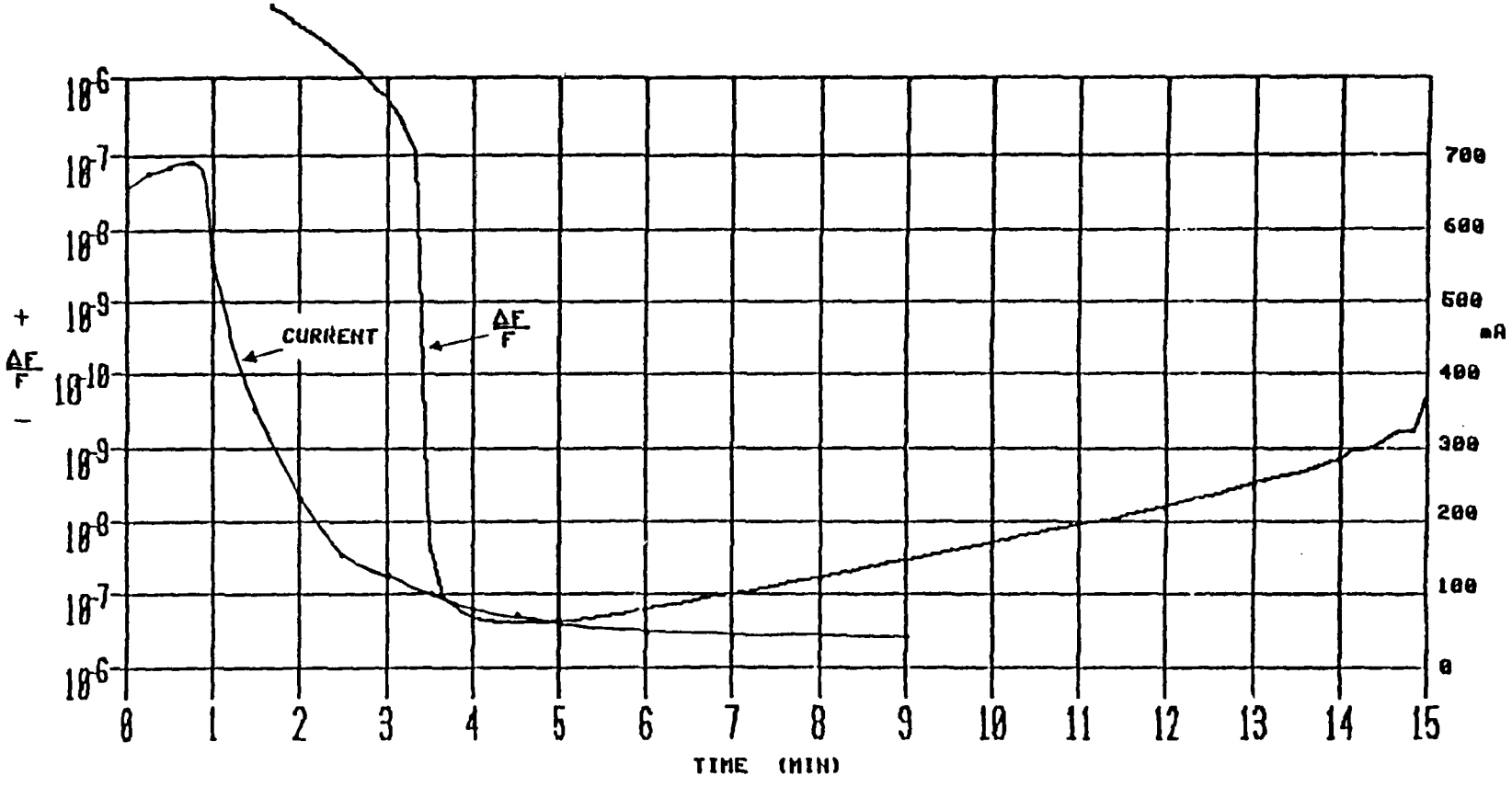

Figure 52. Warmup, -40°C, evacuated, TMXO number 161-2.

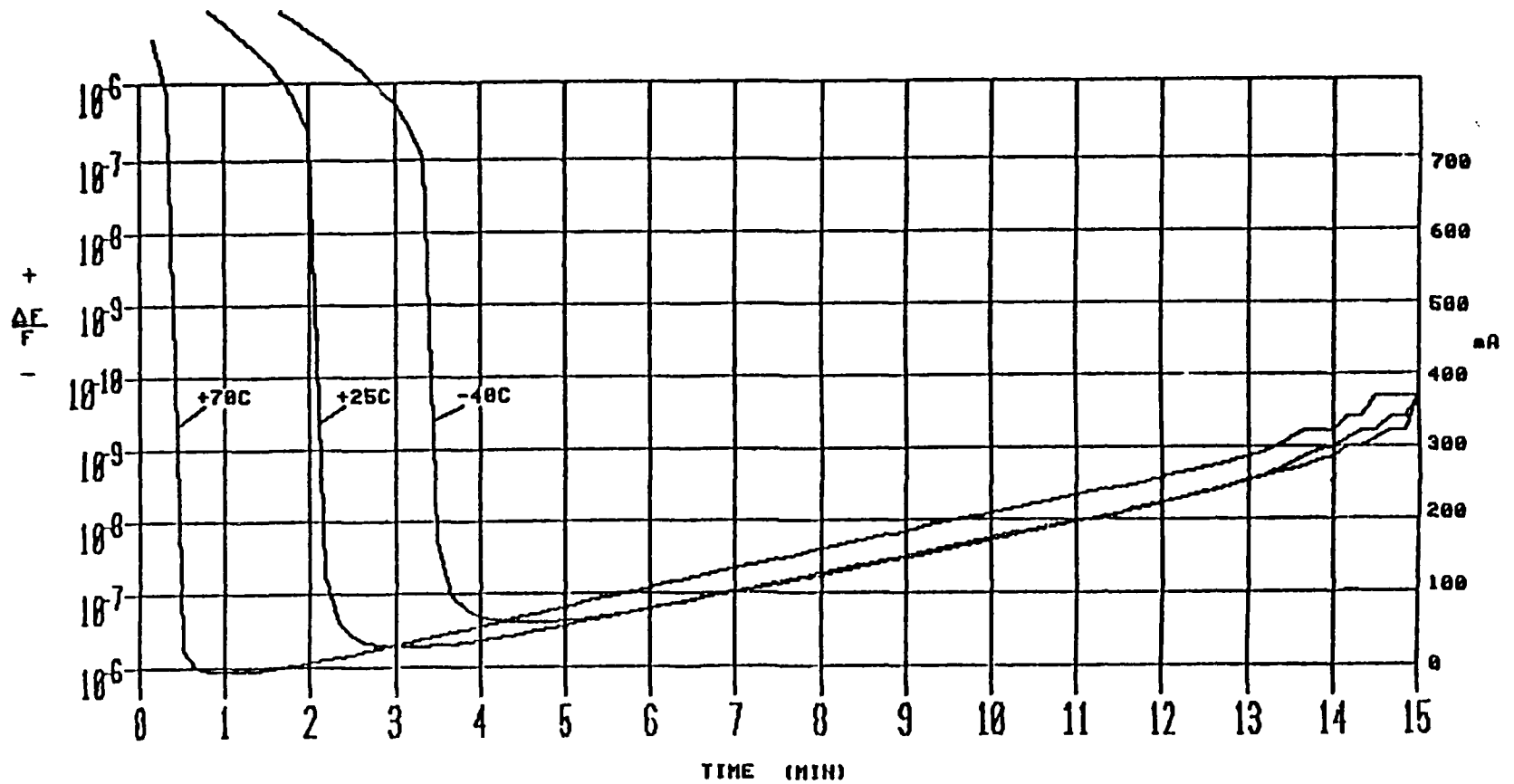

Figure 53. Warmup, +70°C, +25°C, -40°C, evacuated, TMXO number 161-2.

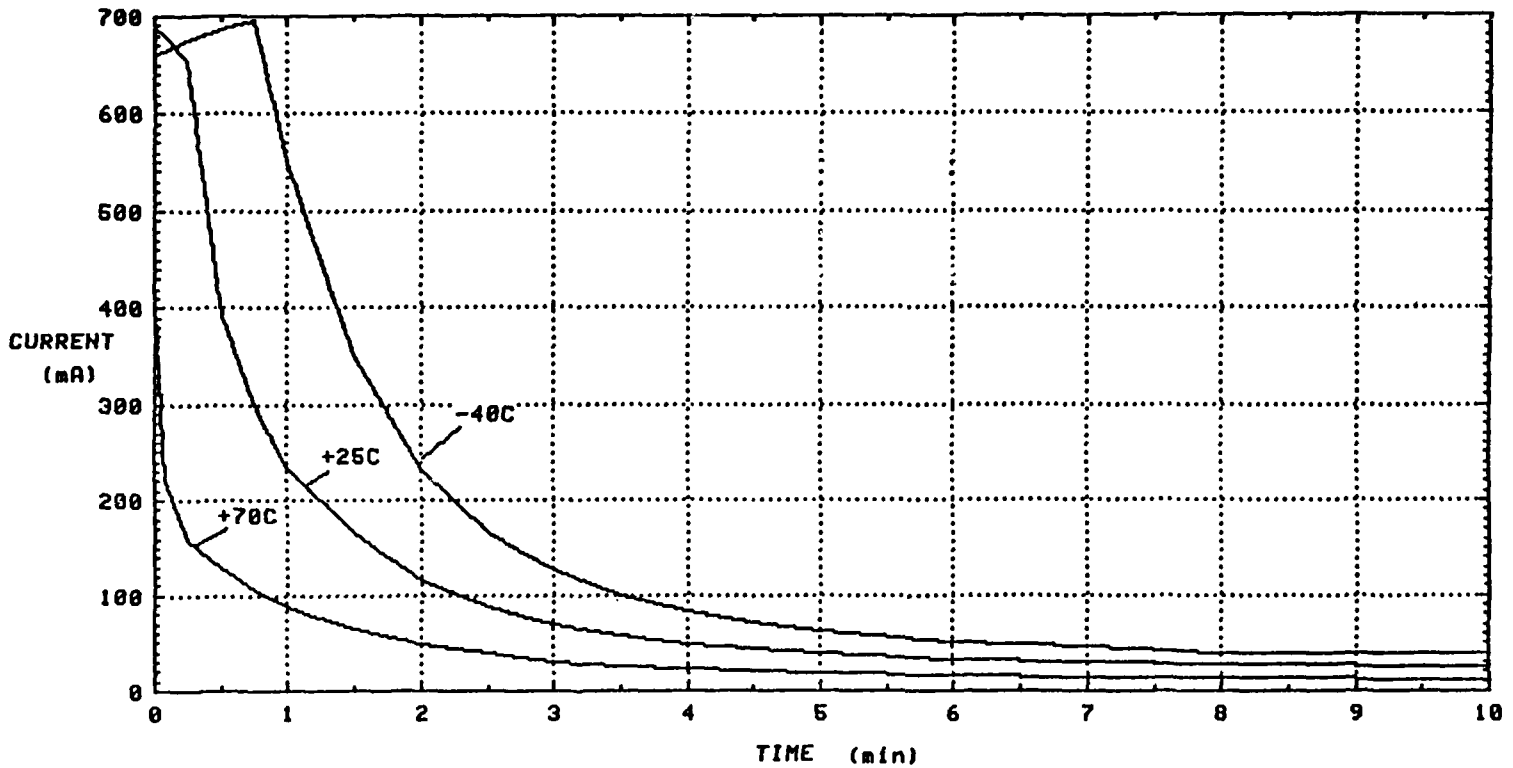

Figure 54. Warmup current, +70°C, +25°C, -40°C, evacuated, TMXO number 161-2.

Model No.	Ambient Temperature	Peak Power	Time to Be Within $\pm 1 \times 10^{-8}$ of F_o
162	+25°C	--	11 minutes
162	+70°C	--	8.5 minutes
162	-40°C	11.3 W	10 minutes

For more details concerning the warmup characteristics of model 162, see Figure 55.

Model No.	Ambient Temperature	Peak Power	Time to Be Within $\pm 1 \times 10^{-8}$ of F_o
195	+25°C	7.9 W	11 minutes
195	+70°C	2.0 W	9.5 minutes
195	-40°C	8.5 W	11 minutes

More detailed information concerning the warmup characteristics of model 195 is shown in Figures 56 through 60.

9. CONCLUSIONS

This TMXO program is directed at exploratory development of a high performance frequency source. The TMXO requirements allow a frequency variation of $\pm 2 \times 10^{-8}$ for all specified conditions simultaneously, as well as being compatible with other requirements. The other requirements have to do with size, power, and warmup characteristics.

The frequency deviation budget is as follows:

	Parameter	Allowed Frequency Deviation
(a)	Ambient Temperature, -54°C to +75°C	$\pm 1 \times 10^{-8}$
(b)	Change in Power Supply Voltage	$\pm 1 \times 10^{-9}$
(c)	Change in Load	$\pm 1 \times 10^{-9}$
(d)	Acceleration, 1 g	5×10^{-10}
(e)	Vibration	$\pm 1 \times 10^{-9}$

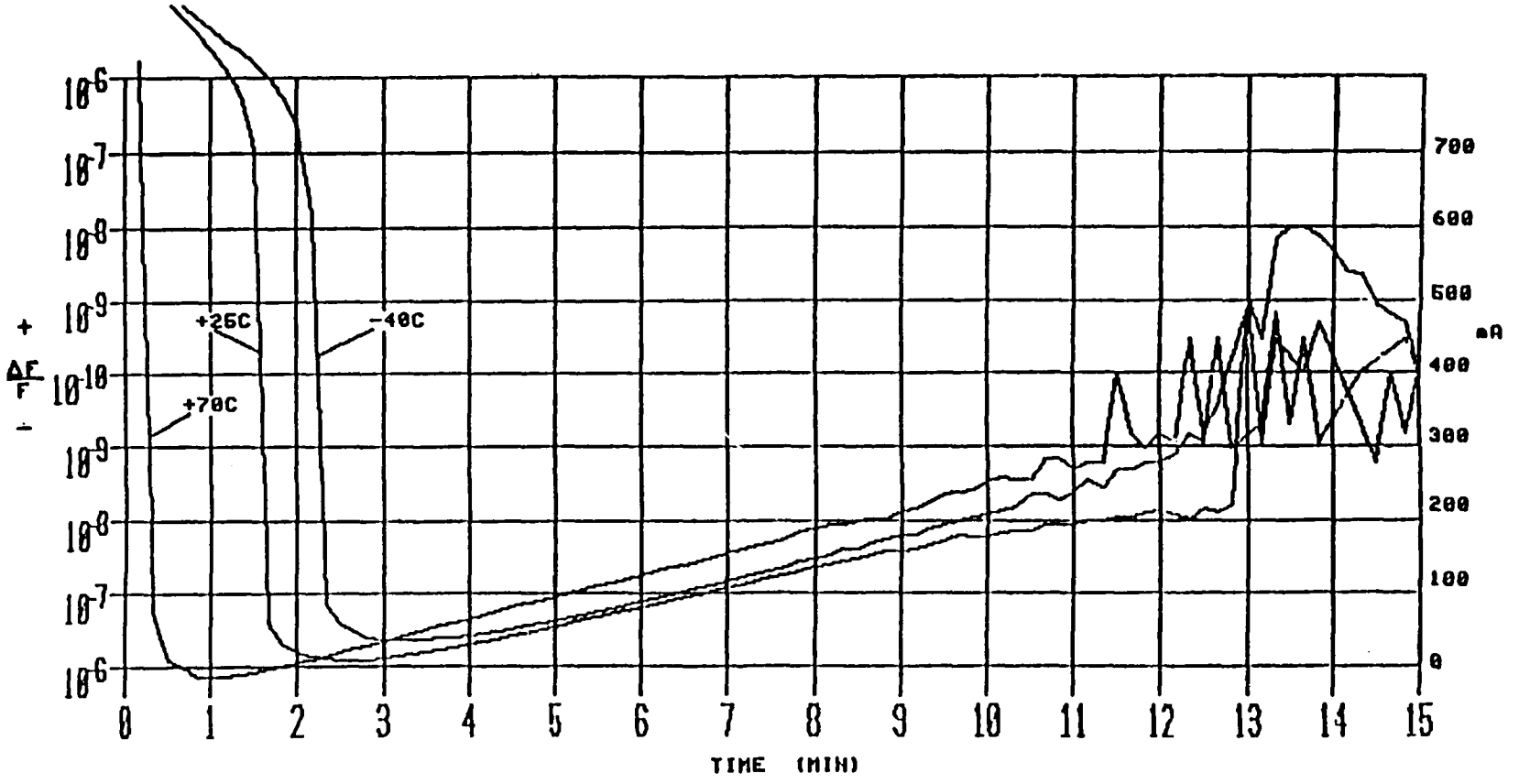

Figure 55. Warmup, evacuated, +25°C, +70°C, -40°C, TMXO number 162.

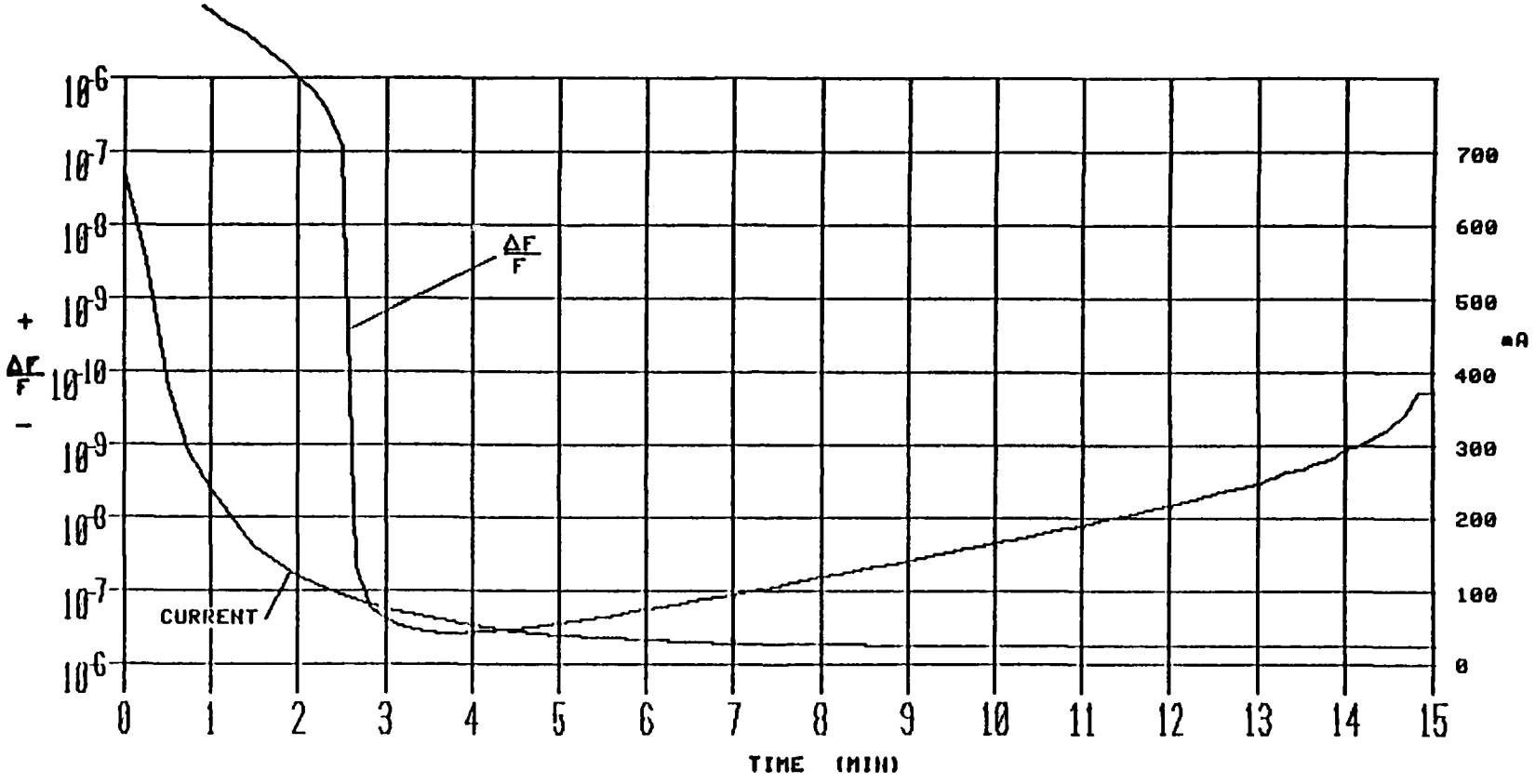

Figure 56. Warmup, evacuated, +25°C, TMXO number 195.

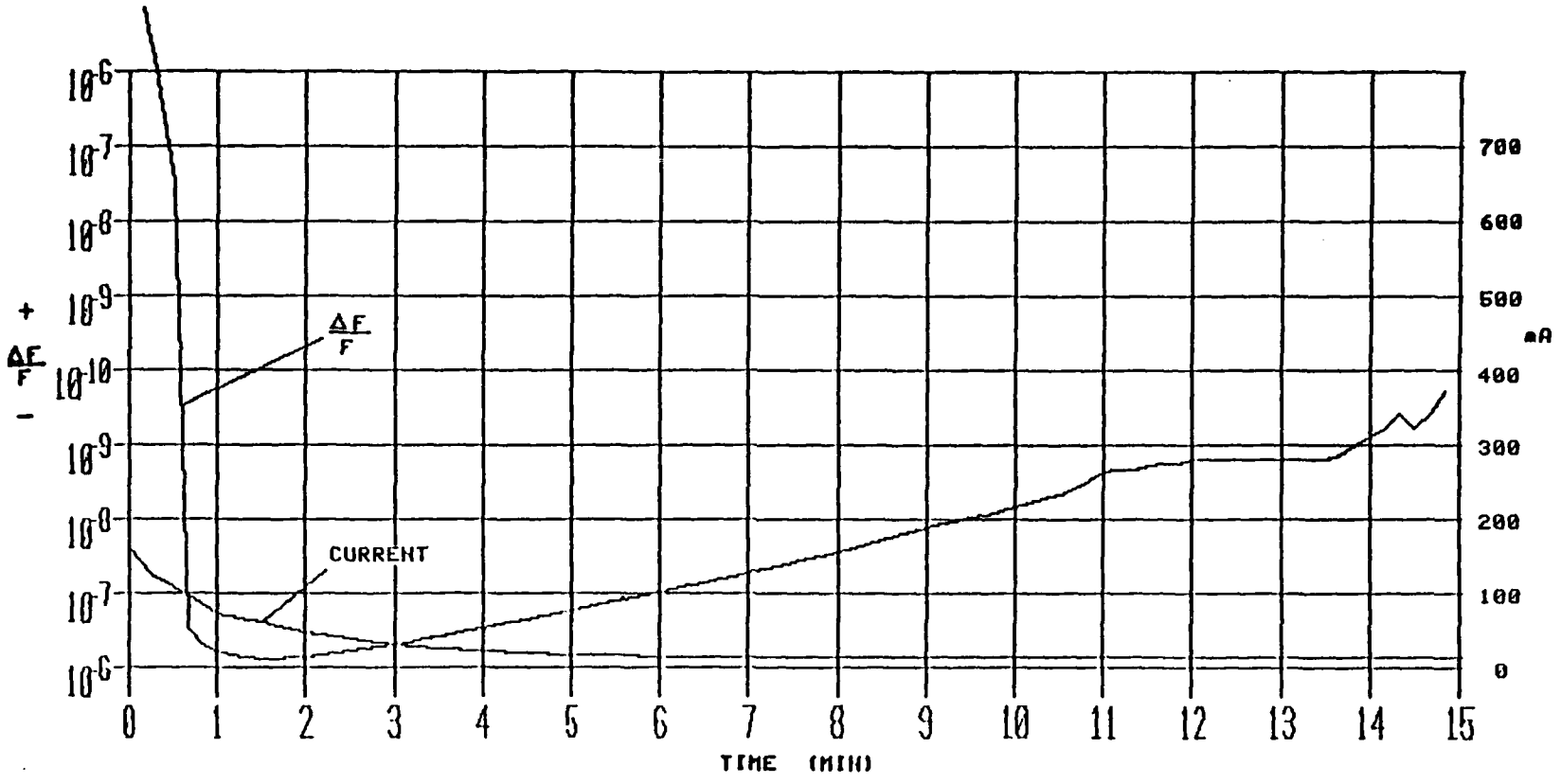

Figure 57. Warmup, evacuated, +70°C, TMXO number 195.

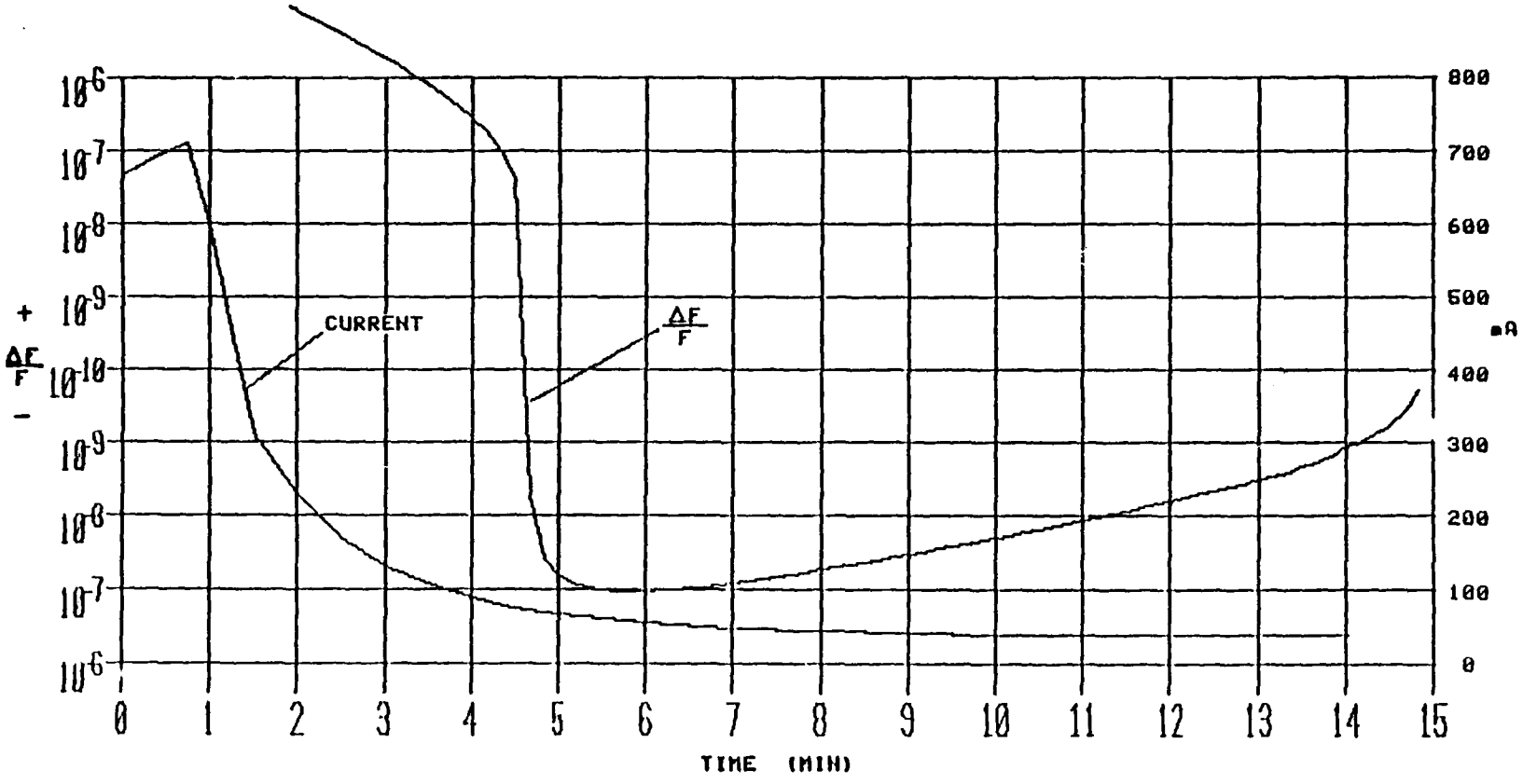

Figure 58. Warmup, evacuated, -40°C, TMXO number 195.

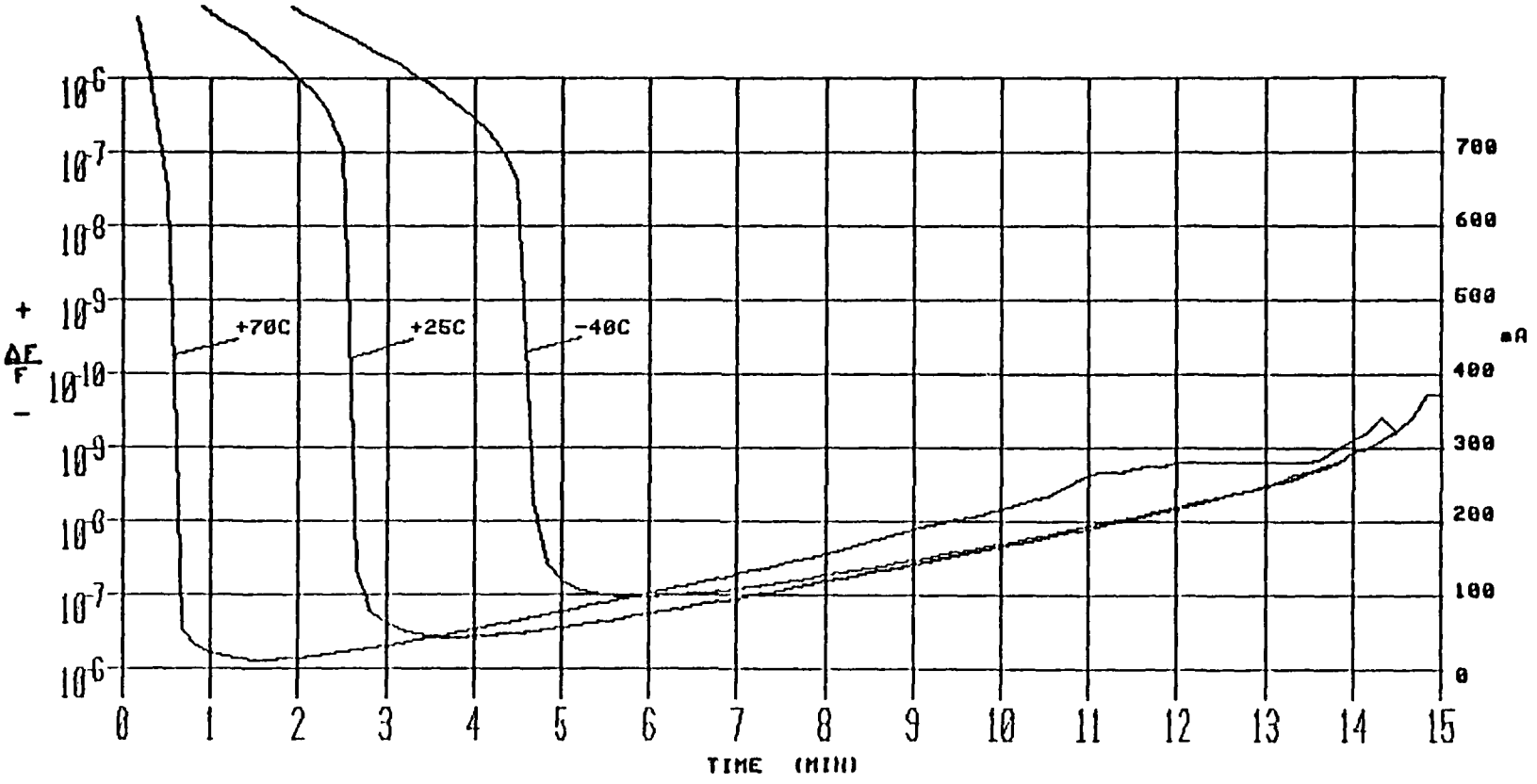

Figure 59. Warmup, evacuated, -40°C, +25°C, +70°C, TMXO number 195.

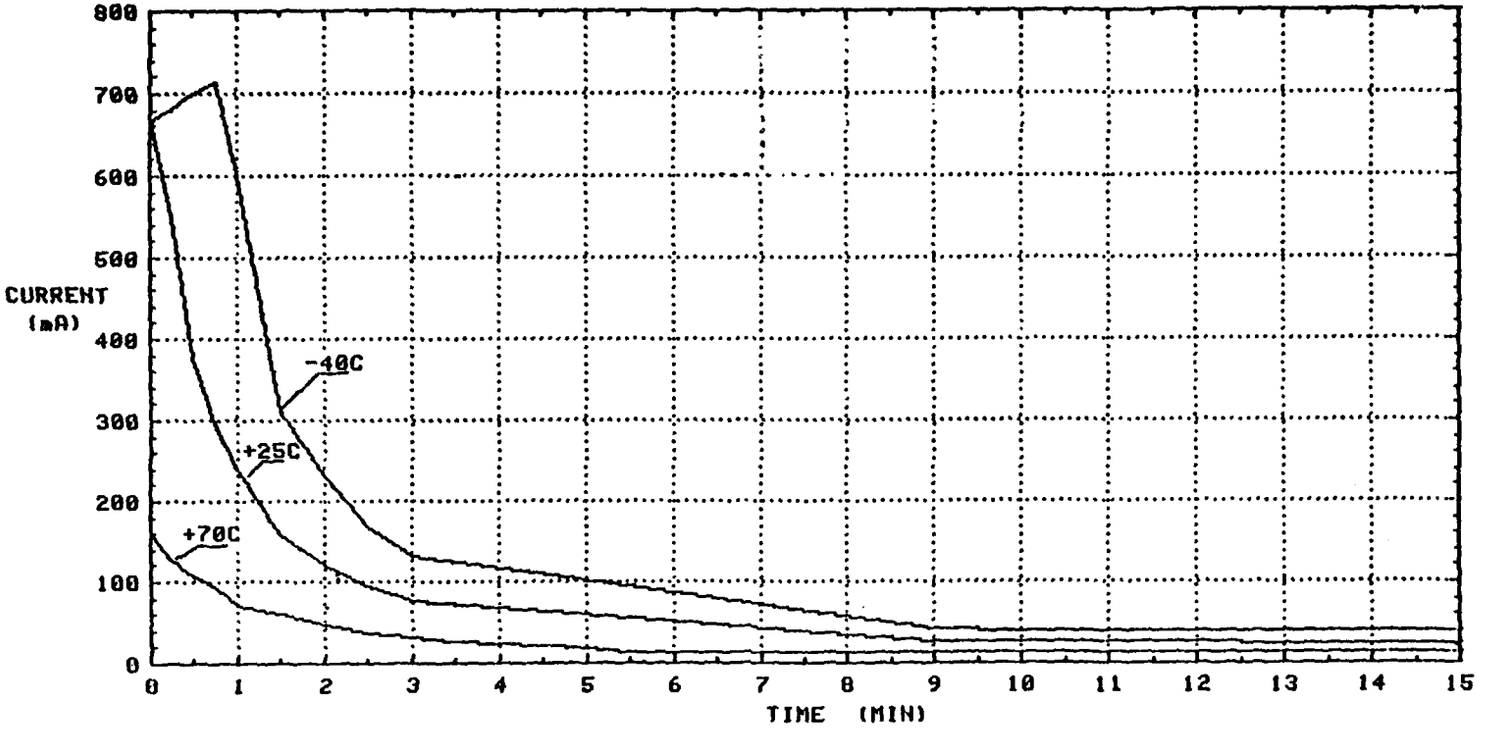

Figure 60. warmup current, evacuated, -40°C, +25°C, +70°C, TMXO number 195.

(f)	Mechanical Shock	$\pm 1 \times 10^{-9}$
(g)	Attitude	$\pm 5 \times 10^{-10}$
(h)	Altitude	1×10^{-9}
(i)	Frequency Recovery	$\pm 3 \times 10^{-9}$
(j)	Aging	2×10^{-10}/wk

The above parameters can be divided into groups:

Group Parameter	Allowed Frequency Deviation
Ambient Temperature -54°C to +75°C	$\pm 1 \times 10^{-8}$
Electrical Environment (b and c)	$\pm 2 \times 10^{-9}$
Mechanical Environment (d,e,f,g, and h)	$\pm 4 \times 10^{-9}$
Frequency Recovery	$\pm 3 \times 10^{-9}$
Aging	2×10^{-10}/wk

Model number 1 of phase 1 had the best vacuum and the best TMXO characteristics. Assuming a TMXO with a good vacuum, the following performance deficiencies (relative to the above group parameters) still existed at the end of phase 1. Frequency deviation due to the electrical environment is $\pm 6 \times 10^{-9}$. Frequency recovery deviation is $\pm 5 \times 10^{-8}$. Frequency changes due to aging were 2 orders of magnitude greater than required. The frequency/temperature requirement was easily met.

Several problems remained, some were major, while others can be considered minor. The major problems were vacuum, frequency recovery, quality of the crystal, and more reliable construction.

Model number 1 had a sufficient vacuum, permitting excellent frequency/temperature characteristics both under steady state and transient conditions. However, the vacuum was not as good as expected, resulting in an operating power at -54°C of 0.5 watt instead of the expected value of 0.3 watt. Although the 0.5 watt may be suitable for most TMXO applications, the other models were not that good. The primary cause of the poor vacuum was leaks through the seals in the outer case. Better construction techniques were needed in fabricating the outer case. Secondary

causes of the poor vacuum may be some leakage from the crystal and/or microcircuit enclosures.

The phase 1 TMXO models were constructed using the "chip and wire" technology and with crystals assembled in our laboratory. Several failures were experienced due to these nonproduction-like techniques. The new crystal enclosure should eliminate any crystal failures. Employing the thick film hybrid technology for the microcircuit would greatly increase the reliability of the TMXO.

Several minor problems exist, one old, and some new. The old problem was the change in frequency with load and voltage. The frequency variation was $\pm 3 \times 10^{-9}$ for either load or supply voltage. The circuit needed to be modified to give better isolation.

During phase 2, some circuit changes were made to eliminate the noise on the input power line and to increase the isolation. The noise on the input was eliminated and stability to power supply changes was improved. No improvement was made with regard to stability with change in load. With the new developmental ceramic enclosed crystal, a major improvement was achieved with regard to frequency recovery, the value now being within the design goal. The TMXO with the new crystal exhibited a degraded frequency/temperature performmance. This is because of a "Frequency/Applied Power Anomaly." The following paragraphs describe this anomaly.

The upper turn point (UTP) of an AT-cut crystal is defined as the temperature above $0^{\circ}C$ at which the temperature coefficient of frequency passes through zero. Also at this temperature the frequency is a minimum. A more descriptive name for this position would perhaps be the upper turn temperature (UTT).

The frequency/applied power anomaly is exhibited as a change in frequency at the UTT when the power to the TMXO is changed. This can happen in two ways:

(a) By changing the ambient temperature.

(b) By changing the heat transfer inside the TMXO, e.g., from vacuum to air.

The values for the frequency/power factor for these two conditions are not equal, probably because the heat transfer is different for equal applied powers.

Some measurements of this effect were measured on two of the models, and the frequency/power factor calculated

$$F/P = \frac{\text{Min. Freq. at } T1^{\circ} - \text{Min. Freq. at } T2^{\circ}}{\text{Power at } T1^{\circ} - \text{Power at } T2^{\circ}}$$

MODEL 161-2

Ambient Temperature	Frequency at UTT (Hz)	Power	Frequency Not At UTT
+70°C	--	.16 W	511530.3.990*
+25°C	5115303.747	.28 W	5115303.830*
-40°C	--	.46 W	5225303.991*
+25°C (air)	5115304.080	.96 W	--
+70°C (air)	--	.44 W	5115305.540**
+70°C (air)	5115303.687	.32 W	--

MODEL 195

Ambient Temperature	Frequency at UTT (Hz)	Power	Frequency Not At UTT
+70°C			5115045.190*
+25°C			5115044 939*
-40°C			5115045.194*
+25°C (air)	5115044.530	1.07 W	--
+70°C	--	?	5115049.378**
+70°C	5115044.675	.36 W	--

* Temperature set for optimum frequency versus ambient temperature characteristic.

** Frequency when the temperature was set to give the minimum frequency at 25°C ambient.

For model 161-2:

$$F/P\ (25^{\circ} \text{ air to } 70^{\circ} \text{ air}) = \frac{(4.080 - 3.687)\ \text{Hz}}{.96\ \text{W} - .32\ \text{W}}$$

$F/P = + .61$ Hz/W

$$F/P\ (25^{\circ}\ \text{air to}\ 25^{\circ}\ \text{vacuum}) = \frac{(4.080 - 3.747)\ \text{Hz}}{.96\ \text{W} - .28\ \text{W}}$$

$F/P = + .34$ Hz/W

For model 195:

$$F/P\ (25^{\circ}\ \text{air to}\ 70^{\circ}\ \text{air}) = \frac{(4.530 - 4.675)\ \text{Hz}}{1.07\text{W} - .36\text{W}} = \frac{-.145\ \text{Hz}}{.71\text{W}}$$

$F/P = - .20$ Hz/W.

This variability of frequency with power is probably due to thermal stress resulting from unsymmetrical heat flow from the heater through the crystal enclosure into the resonator. Additional crystal/crystal thermal interface development can solve this problem. The vacuum problem has been solved by using improved processing techniques and a new getter, as demonstrated by the more recent TMXO program under contract DAAB07-78-C-2990. The phase 2 microcircuit enclosure is inadequate in that it is not easily hermetically sealed. A new concept in the design of this enclosure is required. The remaining problems are currently being addressed under the referenced contract and are discussed in reports DELET-TR-78-2990-1, December 1979 and DELET-TR-78-2990-2, August 1980.

DISTRIBUTION

101 Defense Technical Information Center
ATTN: DTIC-TCA
Cameron Station (Bldg 5)
012 Alexandria, VA 22314

203 GIDEP Engineering & Support Dept.
TE Section
P.O. Box 398
001 Norco, CA 91760

205 Director
Naval Research Laboratory
ATTN: CODE 2627
Washington, DC 20375

301 Rome Air Development Center
ATTN: Documents Library (TILD)
001 Griffiss AFB, NY 13441

437 Deputy for Science & Technology Office,
Asst. Sec Army (R&D)
001 Washington, DC 20310

438 HQDA (DAMA-ARZ-D/Dr. F. D. Verderame)
001 Washington, DC 20310

482 Director
JS Army Materiel Systems Analysis Actv.
ATTN: DRXSY-T
001 Aberdeen Proving Ground, MD 21005

563 Commander, DARCOM
ATTN: DRCDE
5001 Eisenhower Avenue
001 Alexandria, VA 22333

564 Cdr, US Army Signals Warfare Lab
ATTN: DELSW-OS
Vint Hill Farms Station
001 Warrenton, VA 22186

579 Cdr, PM Concept Analysis Centers
ATTN: DRCPM-CAC
Arlington Hall Station
001 Arlington, VA 22212

602 Cdr, Night Vision & Electro-Optics
ERADCOM
ATTN: DELNV-D
001 Fort Belvoir, VA 22060

603 Cdr, Atmospheric Sciences Lab
ERADCOM
ATTN: DELAS-SY-S
001 White Sands Missile Range, NM 88002

607 Cdr, Harry Diamond Laboratories
ATTN: DELHD-CO, TD (In Turn)
2800 Powder Mill Road
001 Adelphi, MD 20783

609 Cdr, ERADCOM
ATTN: DRDEL-CG, CD, CS (In Turn)
2800 Powder Mill Road
001 Adelphi, MD 20783

612 Cdr, ERADCOM
ATTN: DRDEL-CT
2800 Powder Mill Road
001 Adelphi, MD 20783

680 Commander
US Army Electronics R&D Command
000 Fort Monmouth, NJ 07703
1 DELEW-D
1 DELET-DD
1 DELSD-L (Tech Library)
2 DELSD-L-S (STINFO)
36 Originating Office (DELET-MQ-O)
1 DELEW-V (J. KEEN)
1 DELCS-I (D. LONGINOTTI)
1 DELET-MQ (J. VIG)
1 DELET-MQ-R (R. FILLER)
1 DELTO (E. WESTHOVEN)

DISTRIBUTION (Continued)

681 Commander US Army Communications R&D Command
000 Fort Monmouth, NJ 07703
1 USMC-LNO
3 DRCO-COM-RN-3 (R. Whitman)
1 DRCPM-GARS-TM (R. Rugarber)
2 DRCPM-SC (O. Gutzmann)
1 DRDCO-COM-RF-2 (T.J. Klein)

Hewlett-Packard Lab
1501 Page Mill Road
Palo Alto, CA 94304
001 ATTN: Dr. Leonard S. Cutler
001 ATTN: Mr. Donald L. Hammond

Bell Telephone Labs, Inc.
Allentown, PA
001 ATTN: Mr. Warren L. Smith

Cincinnati Electronics Corp.
2630 Glendale Milford
Cincinnati, OH 45241
001 ATTN: Mr. Jerry Middendorf

McDonnell Douglas
P.O. Box 423
St. Charles, MO 63301
001 ATTN: Mr. Gerald Rogers

Sandia Laboratories
P.O. Box 969
Livermore, CA 94550
001 ATTN: Tech Library (RPT)

Conic Corp.
9020 Balboa Avenue
San Diego, CA 92123
001 ATTN: Mr. Martin Gold

Frequency Electronics, Inc.
3 Delaware Drive
New Hyde Park, NY 11040
001 ATTN: Mr. Martin Bloch

IBM
Bldg 905A, Dept. M94
Owego, NY 13827
001 ATTN: Mr. G. Ver Wys

Harris Electronics
Systems Division
Mail Stop I-1470
P.O. Box 37
Melbourne, FL 32901
001 ATTN: Mr. W. McGann

McDonnell Douglas
Astronautics Co.
5301 Boise Ave.
Huntington Beach, CA 92647
001 ATTN: A3-135 Library Services

Hughes Aircraft Co.
Missile Systems Division
Mail Station B-90
Canoga Park, CA 91304
001 ATTN: Mr. C. French

SAMSO-YEE
Headquarters
Space & Missile System Organization
P.O. Box 92960
Worldway Postal Center
Los Angeles, CA 90005
001 ATTN: Lt. Col. Goldtrap
001 ATTN: Mr. John Deewall
001 ATTN: Col. Henderson
001 ATTN: Lt. Karl Kovach

Northern Illinois Univ.
I & T Dept
Dekalb, IL 60115
001 ATTN: D. E. Newell

RADC/ETS
Hanscom AFB, MA 01731
001 ATTN: A. Kahan

JHU/Applied Physics Lab
John Hopkins Road
Laurel, MD 20810
001 ATTN: J. R. Norton
001 ATTN: L. J. Reuger

DISTRIBUTION (Continued)

ITT Aerospace/Optical Div
3700 East Pontiac
Ft. Wayne, IN 46803
001 ATTN: Mr. James Chen

Hughes Aircraft Company
500 Superior Ave.
Newport Beach, CA 92663
001 ATTN: H. E. Dillon

Rockwell International
Government Avionics Div
400 Collins Avenue
Cedar Rapids, IA 52406
001 ATTN: Mr. Bill Howard

Magnavox Advanced Products
Division
2829 Maricopa Street
Torrence, CA 90503
001 ATTN: Mr. David L. Hessick

Boeing Aerospace Corp.
P.O. Box 3999,
Mail Stop 8805
Seattle, WA 98124
001 ATTN: Mr. Jim W. Bieber

Stanford
Telecommunications Inc.
1195 Bordeau Drive
Sunnyvale, CA 94086
001 ATTN: Mr. Julius Ville

Savoy Electronics
P.O. Box 5727
Ft. Lauderdale, FL 33310
001 ATTN: Mr. Eugene Lussier

HDQ, TCATA
Fort Hood, TX 76544
001 ATTN: ATCAT-IA-I
(Mr. J. Austin)

ASD/XRQ-NIS
Wright Patterson AFB,
OH 45433
001 ATTN: Cpt. Michael
Gaydeski

RADC/ESE
Hanscom AFB
Bedford, MA 01731
001 ATTN: Dr. Nicholas Yannoni

Naval Research Lab
4355 Overlook Avenue
Washington, DC 20375
001 ATTN: Mr. David Philips,
Code 7524

General Electric Neutron
Devices
P.O. Box 11508
St. Petersburg, FL 33733
001 ATTN: Mr. Robert Ney

Mitre Corp.
P.O. Box 208
Bedford, MA 01730
001 ATTN: Mr. Gene O'Sullivan-
MS E035
001 ATTN: Mr. Donald Newman-
MSG100
001 ATTN: Mr. Peter Bratt-
MSB050

MIT, Lincoln Lab
P.O. Box 73
Lexington, MA 02173
001 ATTN: Mr. Richard Bush

F&T Standards Section,
227-04
NBS
325 Broadway
Boulder, CO 80302
001 ATTN: Dr. Samuel P. Stein

Rockwell International
Collins Tele, Prod. Div.
855 35th Street, N.E.
Cedar Rapids, IA 52406
001 ATTN: Mr. Marvin Frerking

Raytheon Company
Technology Development
Laboratory
528 Boston Post Road
Sudbury, MA 01776
001 ATTN: Mr. Arnie Pulver

DISTRIBUTION (Continued)

Hewlett-Packard
5301 Stevens Creek Blvd
Santa Clara, CA 95050
001 ATTN: Mr. John A. Kusters

705 Advisory Group on Electron Devices
201 Varick Street, 9th Fl.
002 New York City, NY 10014

Greenray
840 West Church Road
Mechanicsburg, PA 17055
001 ATTN: Mr. G. Kurzenknabe

Sentry Manufacturing Co.
Crystal Park
Chickasha, OK 73018
001 ATTN: Mr. Don R. Abel

Austron, Inc.
1915 Kramer Lane
Austin TX 78758
001 ATTN: Mr. George Price
001 ATTN: Mr. Bob Ellis

McCoy Electronics Co.
Chestnut & Watts
Mt. Holly Springs, PA 17065
001 ATTN: Mr. Walter D. Galla

Spectrum Technology, Inc.
Goleta, CA 93101
001 ATTN: Mr. Harry Gruen

Bulova Watch Co.
61-20 Woodside Avenue
Woodside, NY 11377
001 ATTN: Mr. Phil Duckett

NASA Goddard Space Flight Center
Greenbelt, MD 20771
001 ATTN: Mr. Bernard Trudell, Code 480
001 ATTN: Mr. Andrew R. Chi, Code 810

Westinghouse Electric Corp.
P.O. Box 746
Baltimore, MD 21203
001 ATTN: Mr. Dan Healy, III, MS 378

Harris Corp.
Government Systems Group Operation
P.O. Box 37,
Melbourne, FL 32901
001 ATTN: Mr. David Leigh

Frequency & Time Systems
182 Conant Street
Danvers, MA 01923
001 ATTN: Dr. Hellmut Hellwig

Tracor, Inc.
6500 Tracor Lane
Austin, TX 78721
001 ATTN: Mr. Robert Hanks
001 ATTN: Mr. Wm. F. Donnell

MIT, Lincoln Lab
244 Wood Street
Lexington, MA 02173
001 ATTN: L. Laughlin (Library)

C. S. Draper Labs
555 Technology Square
Cambridge, MA 02139
001 ATTN: Mr. Bob Coppeta

EG&G
35 Congress Street
Salem, MA 01970
001 ATTN: Mr. W. J. Riley

Motorola Inc.
Communications Systems Div.
2553 North Eddington Street
Franklin Park, IL 60131
001 ATTN: Mr. Roger Steele
001 ATTN: Dr. Dennis Reifel

Proteon Associates, Inc.
24 Crescent Street
Waltham, MA 02154
001 ATTN: Mr. Howard C. Salven

Vectron Laboratories, Inc.
166 Glover Avenue
Norwalk, CT 06850
001 ATTN: Mr. Alfred Camhi

Magnavox Company
1313 Production Road
Ft. Wayne, IN 46808
001 ATTN: Mr. Jim Keating

CTS Knights, Inc.
400 Reiman Avenue
Sandwich, IL 60548
001 ATTN: Mr. Donald Schroeder

Efratom California, Inc.
18851 Bardeen Avenue
001 Irvine, CA 92715

Quartztek Inc.
P.O. Box 14738
Phoenix, AZ 85063
001 ATTN: Mr. Daryl Kemper

Ovenaire Division
Walter Kidde & Company
706 Forrest Street
001 Charlottesville, VA 22901

Piezo Crystal Company
100 K Street
001 Carlisle, PA 17013

Raytheon Company
Industrial Components Div.
465 Centre Street
Quincy, MA 02169
001 ATTN: Michel Zilberstein

END

DATE
FILMED

7-81

DTIC